INSTITUTE OF GRADUATE STUDIES

DEPARTMENT OF PHARMACOGNOSY

ISOLATION AND CHARACTERIZATION OF SECONDARY METABOLITES FROM THE RHIZOMES OF *RHAPONTICUM ACAULE* (L) DC. A TRADITIONAL LIBYAN MEDICINAL PLANT

Ph.D. THESIS

MHMUOD ALI ZUGHDANI

NICOSIA-2021

NEAR EAST UNIVERSITY
INSTITUTE OF GRADUATE STUDIES
DEPARTMENT OF PHARMACOGNOSY

ISOLATION AND CHARACTERIZATION OF SECONDARY METABOLITES FROM THE RHIZOMES OF *RHAPONTICUM ACAULE* (L) DC. A TRADITIONAL LIBYAN MEDICINAL PLANT

Ph.D. THESIS

MHMUOD ZUGHDANI

SUPERVISOR
Prof. Dr. İhsan ÇALIŞ

CO-ADVISOR
Assist. Prof. Dr. Güner EKİZ

NICOSIA- 2021

APPROVAL

We certify that we have read the thesis submitted by MHMUOD ALI ZUGHDANI titled **"ISOLATION AND CHARACTERIZATION OF SECONDARY METABOLITES FROM THE RHIZOMES OF *RHAPONTICUM ACAULE* (L) DC. TRADITIONAL LIBYAN MEDICINAL PLANT"**

And that in our combined opinion it is fully adequate, in scope and in quality, as a thesis for the degree of (Ph.D.) in Pharmacognosy.

Examining Committee Name-Surname Signature

Head of the Committee: ……

Committee Member*: …….

Supervisor: ……

……..

Approved by the Institute of Graduate Studies

…../11/2021

Prof. Dr. Kemal Hüsnü Can Başer

Head of the Institute

Declaration

I hereby declare that all information, documents, analysis, and results in this thesis have been collected and presented according to the academic rules and ethical guidelines of Institute of Graduate Studies, Near East University. I also declare that as required by these rules and conduct, I have fully cited and referenced information and data that are not original to this study.

Mhmuod Zughdani

26/ 11/ 2021

ACKNOWLEDGMENTS

In the name of **Allah**, most gracious, most merciful. All praise and glory to Allah (SWT) for the strengths and his blessing in completing research work and this thesis. I gratefully acknowledged the Libyan Government for the PhD scholarship.

My deep appreciation goes to my thesis **Supervisor Prof. Dr. Ihsan ÇALIŞ** (Dean of Faculty of Pharmacy), whose gave me a lot of their expertise and research insight. He gave me a lot of his time and helped me go through the hard way with constant encouragement and influential discussions. I am deeply grateful to his valuable guidance and advices and for providing an amiable working environment. It would have never been possible for me to complete this work without his incredible support and encouragement. I would also like to extend my gratitude to my **Co-Supervisor, Assist. Prof. Dr. Güner EKİZ** for her suggestions, guidance, encouragement during the write-up and through the edition of the present dissertation as well as the publication. I owe a great debt of gratitude respect, and heartfelt thanks to **Prof. Dr. K. Hüsnü Can Başer** for his generous support throughout the duration of the study. Thanks are extended to **Dr. Azmi HANOĞLU** (Near East University, TRNC) for his kind of help and assistance all the time. Many thanks go to **Karar Shukur** (Eastern Mediterranean University, TRNC) for his help to run UV and FTIR measurements. I would like to thank **Prof. Mohamed Abu Hadra**, for the identification of the plant material used in my experiments. I would also like to thank **Anzarul Haque** for 1D and 2D NMR measurements and **Ayman Salkini** for HRMS (Prince Sattam Bin Abdul Aziz University, Saudi Arabia). I would like to thank **Prof. Dr. Anthony Linden** (University of Zurich Department of Chemistry) for all crystal structure determination.

Finally, I may not be in a position to thank each and every one, I extend a vote of appreciation to all persons who in one way or another made my studies a success.

Mhmuod Zughdani

DEDICATION

I wish to dedicate this thesis to

My beloved late father Ali (May Allah have mercy on him)

who taught me not to give up

My wonderful mother Amina

For her endless love, continued support, and encouragement all time.

My wife (Rabia)

who has been a constant source of support and encouragement during the challenges of life.

My lovely daughters

They are four flowers in my life (Mimouna, Roufida, Rihana & Massra)

My sisters

(Hussnia & Fathia**)**

My brothers

(Mohamed, Ramadan & Abdualhati**)**

I do not forget to send a bunch of thanks and gratitude

For my teachers and friends.

ABSTRACT

This study comprises a Ph.D. work entitled: “Isolation and Analytical Characterization of Phytochemicals from Selected Libyan Indigenous Medicinal Plants”. Based on information on its traditional medicinal uses and the literature survey, *Rhaponticum acaule* has been selected. *Rhaponticum acaule* (L.) DC., is an endemic plant growing in Libya and other countries in Southern part of the Mediterranean basin. The work comprises of collecting underground parts (roots and rhizomes), drying, extraction, isolation, and identification of phytochemicals constituents. In addition to two known ecdysteroids, 20-hydroxyecdysone and turkesterone, three previously undescribed stigmastane-type ecdysteroids were isolated from the underground parts of *Rhaponticum acaule* (L.) DC. by chromatographic techniques (CC, VLC, MPLC). The structures of the compounds were established by chemical (acetylation) and spectroscopic methods including UV, IR, HRMS, 1D-NMR: ^{1}H-NMR, ^{13}C-NMR, DEPT-135. and 2D-NMR: COSY, NOESY, HSQC, HMBC. Two compounds were isolated as an isomeric mixture and each of them was purified and converted to the corresponding acetylated derivative. Based on all the evidence, the structures of three undescribed stigmastane-type ecdysteroids were established as 2β,3β,11α,20β,22α,24,28-heptahydroxy-6-oxo-stigmast-7-en-25,29-lactone, and the cyclic 22,29-hemiacetals 22R and 22S stigmast-7-en-29- al,2β,3β,11α,20α,22,28-hexahydroxy-6-oxo, and the trivial names acaulesterone and rhapocasterones A and B are suggested, respectively. The structures and absolute configurations of 20-hydroxyecdysone and cyclic-22,29- hemiacetal-22R-stigmast-7-en-29-al,2β,3β,11α,20α,22,28-hexahydroxy-6-oxo were confirmed by X-ray crystal structure analyses of their acetyl derivatives. In addition, the major chemical constituents of oil of hydrodistillated rhizomes were determined as Aplotaxene (=1,8,11,14-heptadecatetraene) (34.6%) and carvacrol (11.1%), respectively.

TABLE OF CONTENTS

LIST OF TABLES

LIST OF FIGURES

LIST OF SPECTRA

LIST OF ABBREVIATIONS

$[\alpha]^{20}D$	specific rotation
ax	axial
C18	octadecylsilyl
CD_3OD	Deuterated methanol
^{13}C NMR	Carbon Nuclear Magnetic Resonance
COSY	correlation spectroscopy
d	doublet
δ	chemical shift
DEPT	distortionless enhancement by polarization transfer
eq	equatorial
EtOAc	ethyl acetate
FID	free induction decay
GCMS	gas chromatography – mass spectrometry
HMBC	heteronuclear multiple bond correlation
HMQC	heteronuclear multiple quantum correlation
HRMS	high-resolution mass spectrometry
IR	infrared
J	coupling constant
m	multiplet
M+	molecular ion
MHz	megahertz
mp	melting point
MPLC	medium pressure liquid chromatography
MS	mass spectrometry
m/z	mass-to-charge ratio
NMR	nuclear magnetic resonance
NOESY	nuclear Overhauser effect spectroscopy (2D)

ppm	parts per million
q	quartet
RA-6Ac1	Pentaacetyl-Rhacaulesterone B
RA-6Ac2	Pentaacetyl-Rhacaulesterone A
S	singlet
T	triplet
TLC	thin-layer chromatography
UV	ultraviolet
VLC	vacuum liquid chromatography

CHAPTER 1

1. INTRODUCTION

Throughout all of history, natural products and traditional medicines are of great importance. Natural products are the main source of possible therapeutic agents worldwide and earliest people noticed and recognized the great miscellany of plants available to them and they have relied on plants for basic needs such as shelter, food, stimulants for endurance, hunger suppression, clothing, poisons for hunting and on the top of that as the main source for treatments for various ailments and diseases (Ramawat & Mérillon, 2008). Every plant is identified by its own different therapeutic properties due to the presence of different bioactive molecules. The best-known and most illustrative examples of successful drug discovery from plants is Morphine, which is discovered as an analgesic agent from *Papaver somniferum* L., Penicillin: an important antibacterial agent isolated from *Penicillium rubrum* Soop., (Bennett & Chung, 2001), Salicylic acid: an anti-inflammatory agent in *Salix purpurea* L.,(Mahdi et al., 2006), Quinine: the anti-malarial drug obtained from *Cinchona officinalis* L., (Achan, et al., 2011), Digoxin: used as a drug for congestive heart failure from *Digitalis lanata* Ehrh., (Rastogi et al., 2016). In additional Camptothecin from *Camptotheca acuminata* Decne., has been approved as a promising anticancer drug (Cragg & Newman, 2013).

Nowadays, plants can still serve as the starting point in generating scientific knowledge useful for the conservation of cultural and biological diversity. Besides that, plants as a source of standardized preparations or detected pure compounds, provide an unconfined way for drug discoveries due to the unmatched availability of chemical diversity (Cis et al., 2006).The knowledge of traditional medicinal plants and the long history of ethnomedical applications has presented much essential guidance in modern research to clarify active compounds and discovery of new drugs. Based on this consideration, researchers reported many plants to have the same or a similar therapeutic purpose as their original ethnomedical use (Fabricant & Farnsworth, 2001).

The United Nations World Health Organization reports that as many as 3.5 billion people in the world, use Traditional Medicine for primary health care. Meanwhile, despite the higher plants form over 250,000 species available on earth, nonetheless, only 20% were investigated so far for their active compounds and 10%

have been screened for their biological activity (Srivastava et al., 2019). Synchronously, the intricacy of plant chemical ingredients and the gain of a satisfactory quantity of highly pure compounds remains a big challenge for the process of identification and complete structural elucidation of new natural genera. Libya is a country in North Africa. It has an area of 1760000 square kilometers. It has a flora of 2088 species belonging to 844 genera and 145 families and the dominant family is Asteraceae with 240 species of 97 genera (Abuhadra& Essokne, 2017). The dominant climate influences come from the Mediterranean Sea and the Sahara Desert (**Figure 1.1**). There are three areas of high biodiversity in Libya that account for >75% of the species diversity: Jabal Nafosa; Jabal Tibesti, and Jabal Alakhdar area located in the province of Cyrenaica (Gawhari A et al.,2018).

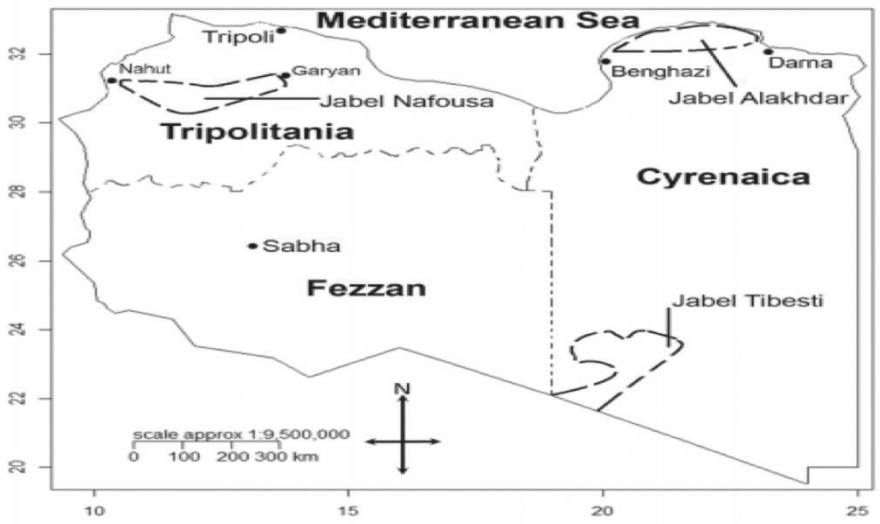

Figure 1. 1. The three major areas of biodiversity in Libya: Jabel Al Akhdar, Jebel Nafusa and Jabel Tibesti.

Reviewing of the literature studies for some species of genus *Rhaponticum* uncover many biological and phytochemical interests of *R. carthemoids*, *R. uniflorium*, *R. repens*. Intriguingly, nothing was documented concerning the study of *R. acaule* especially the underground part (rhizomes). So, it is of interest to investigate the active constituents for this plant. Therefore, the project was hypothesized that *R. acaule* used in traditional medicine in North Africa, contains secondary metabolites that might be scientifically isolated and documented and based on the existing ethnomedical and

literature information on biological activity and phytochemical analysis of plant; roots were selected to be evaluated.

The major aims of this thesis include to examine the volatile component of the underground part of *R. acaule* and meanwhile, provide a detailed report on the phytochemical composition of compounds isolated from the roots, emphasizing the ecdysteroids. Thus, it will be possible to compare the ecdysteroid profile of this plant with that of *R. carthamoides* and *R. uniflorum* used in different countries. Overall, this study gives an overview of the value of *R. acaule*.

CHAPTER 2

2. LITERATURE REVIEW

2.1. Asteraceae Family

Asteraceae, also called Compositae, is an important family of flowering plants and considered as the largest of all the families of Angiosperms, based on a large number of species Asteraceae family has more than 23,600 currently accepted species, spread across 1620 genera and 12 subfamilies (Funk et al., 2009). The majority of plant members representing this family are herbaceous in nature, but a significant number are also shrubs, vines, and trees. This family is well marked in its characteristics and cannot be confused with any other. It can be easily recognized from a distance by their characteristic "daisy-like" flower heads (Elpel, 2004). Aggregation of flowers called receptacle which is referred to as the banner of family Asteraceae (Tadesse, 2014).

2.2. Chemical Characteristics of the Family Asteraceae

The most characteristic compounds identified from species belonging to the Asteraceae family are the polyfructanes, methylated flavanols and flavones, sesquiterpene lactones such as parthenolide, triterpene and Polyacetylenic compounds. Fatty oils in the seeds are common constituents of many species. Essential oils and diterpenoids are also widely distributed, while cyanogenic glycosides, alkaloids, coumarins, amides, and various types of phenolic constituents display much more limited distribution (Heinrich et al ., 2017).

2.3. The Genus *Rhaponticum*

The genus *Rhaponticum* L. is one of the genera of the Asteraceae family and one of the representative genera within the tribe Cardueae Cass. and the subtribe Centaureinae (Bruno et al., 2013). The genus *Rhaponticum* is represented worldwide by about 25 species all over the world distributed mostly in, Eastern and middle of Asia, mountains of Siberian, Mongolia, Eastern Australia, and one in North Africa (Özbek et al., 2017). The nomenclature of the *Rhaponticum* genus is confusing due to many species of the genera are synonymous (Kokoska & Janovska, 2009a). The names *Rhaponticum* Vail (*Rhaponticum* Ludw, *Rhaponticum* Hill), *Leuzea* DC., *and*

Stemmacantha Cass., are used in floristic reports and in writing covering the studies of this genus (Greuter, 2003). It is worth noting that, there is an increasing global interest in the study of *Rhaponticum* genus as shown by the many studies conducted on the species in recent decades.

2.3.1. Species of The Genus *Rhaponticum*

The following are some species included in the genus *Rhaponticum*: *R. acaule* (L.) DC. , *Rhaponticum aulieatense* Iljin., *Rhaponticum australe* (Gaudich.) Soják., *Rhaponticum berardioides* (Batt.) Hidalgo., *Rhaponticum canariense* DC., *Rhaponticum centauroides* (L.) O.Bolòs., *Rhaponticum coniferum* (L.) Greuter., *Rhaponticum cossonianum* (Ball) Greuter., *Rhaponticum exaltatum* (Willk.) Greuter., *Rhaponticum heleniifolium Gren. & Godr., Rhaponticum insigne* (Boiss.) Wagenitz., *Rhaponticum integrifolium* C.Winkl., *Rhaponticum karatavicum* Regel & Schmalh., *Rhaponticum longifolium* (Hoffmanns. & Link) Dittrich, *Rhaponticum lyratum* C.Winkl. ex Iljin, *Rhaponticum namanganicum* ljin, *Rhaponticum nanum* Lipsky., *Rhaponticum nitidum* Fisch., *Rhaponticum orientale* (Serg.), *Rhponticum pulchrum* Fisch. & C.A.Mey., *Rhaponticum repens* (L.) Hidalgo., *Rhaponticum scariosum* Lam., *Rhaponticum serratuloides* (Georgi) Bobrov. https://compositae.org.

2.3.2. Traditional Uses of The *Rhaponticum* species

Literature reports suggest that *Rhaponticum* species have been used traditionally for the treatment of different ailments and disorders. The dried root of *Rhaponticum uniflorum* (L.) DC., called “Nuro” in Korea, is widespread throughout Asian countries. It has been used as herbal medicine to treat inflammatory diseases (Jeong et al., 2016). In China, the roots of *R. uniflorium* (Qizhou Loulu) are traditionally used for reducing fever, clearing heat and toxic materials, treatment of chronic gastritis, inflammation, alleviation of antioxidant, pain, anti-aging, and improvement of immunological functions (Yan et al., 2013).

Rhaponticum carthamoides, commonly known as Maral Root in Siberia and Mongolia, has been used for the treatment of overstrain and common weakness after illness (Petkov et al., 1984). Additionally, it has been used to improve mood and

concentration and as a tonic and anabolic, enhance physical and sexual (Skała et al., 2019; Winston & Maimes, 2007). Similarly, *Rhaponticum repens* is traditionally used for the treatment of stomach pain, fever, and dysentery (Khan et al., 2011).

2.3.3. Biological Properties of The *Rhaponticum* Species

Several studies have been reported different biological effects of the genus *Rhaponticum*. Preparations of *R. uniflorium* were proved to have biological properties, including antitumor, antioxidant, and anti-inflammatory activities (H. Chen et al., 2017). Moreover that, an alcoholic extract of *R. uniflorum* was reported to be affected on learning and memory of antisenescence and improving intelligence (XIAN et al., 2005). In addition, pharmacological and clinical investigations of *R. carthemoids* have a various effect on biochemical and physiological functions e.g., antioxidant, immunomodulatory activities, and adaptogenic properties as well as stimulate overall protein synthesis (Todorov et al., 2000). Furthermore, some other biological activities including anticancerogenic, antimicrobial, antiparasitic, and insect antifeedant effects have been reported for extracts of *R. carthamoide* (Le Bizec et al., 2002).

Moreover, some bioactive molecules were isolated from *Rhaponticum* species and tested for their biological potential. In general, the major constituents identified in these species are ecdysteroides that are responsible for most of their biological activities (Thiem et al., 2017). Ecdysteroides show a wide range of biological activities, especially cytotoxic and antitumor against cancer cells (Arakawa et al. 2013; Iranshahy et al. 2015). Additionally, several sesquiterpene lactones have also been demonstrated to possess pharmacological effects. such as antifeedant, anti-hyperlipidemic, anti-tumor action anti-inflammatory properties and anti-malarial (Elsebai et al., 2016).

2.3.4. Chemical Overview of The *Rhaponticum* Species

Phytochemical profiles of the *Rhaponticum* species have not been fully documented and the phytochemical information on the genus is still quite sparse. Predominantly*, Leuzea carthamoides*, *Rhaponticum uniflorium R. pulchrum and R. serratuloides* have been the most studied species. Literature reviews of the chemo

diversity of *Rhaponticum* species revealed the presence of more than one hundred compounds grouped into diterpenes, sesquiterpenes, triterpenes, sterols, thiophenes, phenolic acids and flavonoids. Most research has shown that genus *Rhaponticum* is very rich in terpenoids, essentially ecdysteroids (Kokoska. & Janovska, 2009b).

2.3.4.1. Ecdysteroids / Phytoecdysteroids

Recently, there has been a growing interest in ecdysteroids in biomedical research and pharmaceutical industry (Głazowska et al., 2018). Ecdysteroids are widespread constituents present in both the plant kingdom (phytoecdysteroids) and animals (zoo ecdysteroids), but are also found in fungi, and even in marine sponges. Ecdysteroids are hormones used by the crustacean and arthropod (insect) in the process of ecdysis (U. A. Baltaev, 2000). The theory that insect molting, and metamorphosis is managed by ecdysteroid hormones was confirmed by the isolation and structure elucidation of ecdysone as the first compound from silkworm pupae (Butenandt & Karlson, 1954). Afterward, 20-hydroxyecdysone was first isolated from crayfish, and this compound is now generally renowned as the main biologically active ecdysteroid in most invertebrate systems. In 1966, compounds structurally related to ecdysone (Ponasterone A, B, C, and D), were identified in leaves of *Podocarpus nakaii* Hay., (Nakanishi et al, 1966). That was the starting point for the term of phytoecdysteroids class (PEs) depending on the plant as an isolation source of steroidal analogous. Their roles in plants are still conjectural, so it is believed that they might provide protection against insect predators and soil nematodes (Speranza, 2010). From a pharmacological point of view, ecdysteroids with a natural composition are used for disorders of the central nervous, cardiovascular, reproductive systems and for weakening the functions of various organs (Sokolov, 2000). Furthermore, the best described property of almost every type of ecdysteroids is their capacity to act as adaptogens. Accumulating evidence indicates that oxygenated phytoecdysteroids could act as adaptogens (Bathori et al, 2008). A recent study reported that 20-hydroxyecdysone is a new non peptidic Mas receptor (Mas 1) activator which has significant anti-thrombotic, anti-inflammatory and antifibrotic activity in heart, kidney, and lung. Accordingly, (Dioh et al., 2021) proposed that the new Mas receptor activator BIO101 (a pharmaceutical formulation of 20E)

might be a new therapeutic option in COVID-19 patients with severe pneumonia and a high thrombotic risk.

Phytoecdysteroids (PEs) are widely distributed compounds and have been detected throughout the *Rhaponticum* genus and there are remarkable similarities in medicinal uses of most species (Table 2.1). Therefore, in that respect, PEs (in particular, 20-hydroxyecdysone) are considered a group of chemicals responsible for most of the biological properties (Kokoska & Janovska, 2009b)

From a chemical point of view, phytoecdysteroids are polar compounds with a polyhydroxylated cyclopentano[α]perhydro phenanthrene ring system. They are generally characterized by a basic skeleton containing 29 carbon atoms with a long sterol alkyl side chain on carbon-17 and the presence of a 7-en-6-one chromophore group in ring B (**Figure 2.1**). They contain hydroxy group on C-3 and the position 14 is generally hydroxylated (Chaubey, 2018).

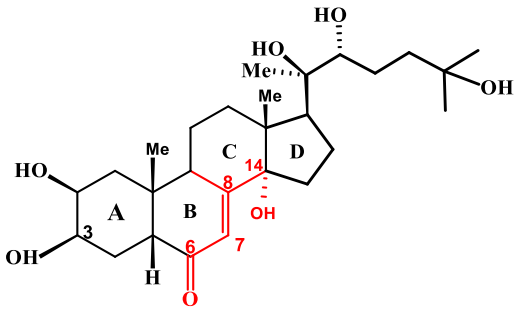

Figure 2. 1. Structure of the most common ecdysteroids, 20-Hydroxyecdyson.

In addition, phytoecdysteroids are classified as triterpenoids which are suitable to generate a very large number of derivatives. Their structural diversity results from variations in the number and/or the position of various substituents, mainly hydroxyl or keto groups) (Al Naggar et al, 2017). Over 400 different phytoecdysteroids have been described and this number is today still increasing (Das et al, 2020). It is believed that there are more than 1000 possible structures, which might exist in nature (Chaubey, 2018). Structures of some selected ecdysteroids previously isolated from the genus *Rhaponticum* are represented in **Table 2.1**.

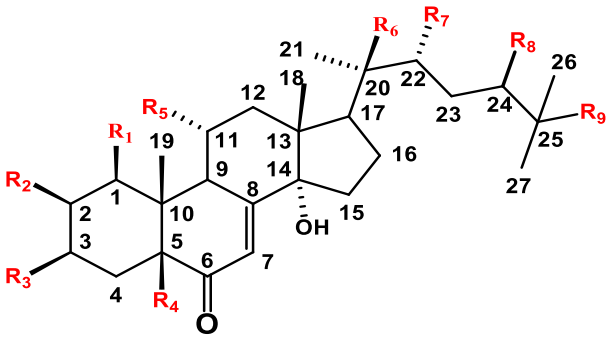

Table 2.1. Structures of some selected ecdysteroids previously isolated from the genus *Rhaponticum***.**

Ecdysteroid name	Plant	R_1	R_2	R_3	R_4	R_5	R_6	R_7	R_8	R_9	References
Integristerone A	*R. uniflorium*	OH	OH	OH	H	H	OH	OH	H	OH	(U. Baltaev., 1977)
24(28)- dehydromaki-sterone A		H	OH	OH	H	H	OH	OH	CH2=	OH	(U. Baltaev., 1978)
Rhapisterone C	*R. carthamoides*	H	OH	OH	H	H	OH	OH	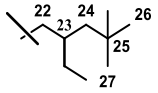		(U. A. Baltaev, 1992)
Carthamasterone A		H	OH	OH	OH	H	OH	OH	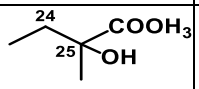		(Ramazanov et al., 1997)
Carthamasterone B		H	OH	OH	H	H	OH	OH	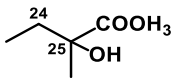		
Rhapisterone B		H	OH	OH	H	OH	OH	OH	OH(ξ)	H	(U. A. Baltaev, 1991)
Ajucasterone C 2, 3;20, 22 - Diacetonide		H	O--R		H	OH	O--R		H	H	(Y.-H. Zhang & Wang, 2001)
5-Deoxykalad esterone 20, 22-Acetonide		H	OH	OH	H	OH	O--R		H	H	
Turkesterone2-O-Cinnamate		H	O--R	OH	H	OH	OH	OH	H	OH	(Daniil N Olennikov et al., 2019)
Carthamasterone	*L. carthamoides*	H	OH	OH	H	H	OH	OH	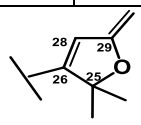		(J-P Girault et al., 1988)
Carthamoleusterone		H	OH	OH	H	OH	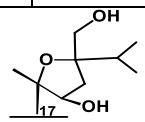				((Buděšínský et al., 2008)
Inokosterone20,22-Acetonide		H	OH	OH	H	OH	O--R		H	H	

2.3.4.1.1. NMR spectra of Steroids (Ecdysteroids)

The chemical nature of steroids (ecdysteroids) is diverse, the presence of angular methyl groups (at positions 18 and 19) is rather the norm than the exception. Ring A is often modified by an oxygen function at C3. Although, specific shift for the 7-en-6-one chromophore group of ring B in the downfield region and signals at 4 ppm indicates the presence of hydroxyl groups. However, Proton NMR spectra of ecdysteroids look very complicated. with often more than 30 protons found in that shift range, most of them appear in regions between 0.5 and 2.5 ppm which is often referred to as the steroid hump. Additionally, when the hydroxyl group acetylated, carbon atoms and protons close to these carbons undergo a characteristic shift. Since steroid spectra are often so crowded that the couplings cannot be simply extracted from the 1D proton NMR spectra. For that, in addition to (^{13}C and DEPT -135), two-dimension NMR is more valuable and gives good ways for assignment strategies (Schwalbe, 2014).

Other Metabolites

2.3.4.2. Diterpenes

There are very few reports on this class of secondary metabolites in the genus *Rhaponticum*. However, there has been a great interest due to the presence of diterpene lactone. Diosbulbin B (DIOB) was isolated for the first time from the aqueous extract of *Rhaponticum uniflorum* (**Figure 2.2**). DIOB has antitumor and anti-inflammatory properties, and it is also the main component leading to hepatotoxicity (Ji et al., 2020; X. Zhang et al., 2010).

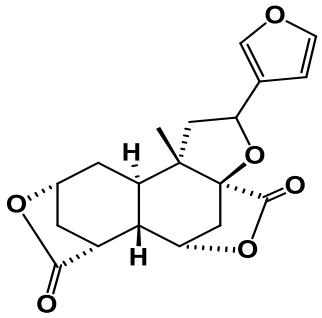

Figure 2. 2. Diosbulbin B (DIOB).

2.3.4.3. Sesquiterpenes

Sesquiterpenes are the most abundant of all terpenoids with approximately 5000 known compounds (Seigler, 2012). Sesquiterpenoids have been regarded as marker constituents of the family Asteraceae and the subtribe Centaureinae. Sesquiterpene lactones (SLs), a class of sesquiterpenoids, are one of the largest and the most important group of plant secondary metabolites. One plant species usually produces one type of sesquiterpene lactones, found mainly in flower and leaves in concentrations of 0.01% to 8% dry weight. In general, sesquiterpene lactones classified into the following groups (**Figure 2.3**), germacranolides (10-membered rings); eremophilanolides and udesmanolides (6/6-bicyclic compounds); hypocretenolides, pseudo guaianolides, and guaianolides (all 5/7-bicyclic compounds) (Chaturvedi, 2011).

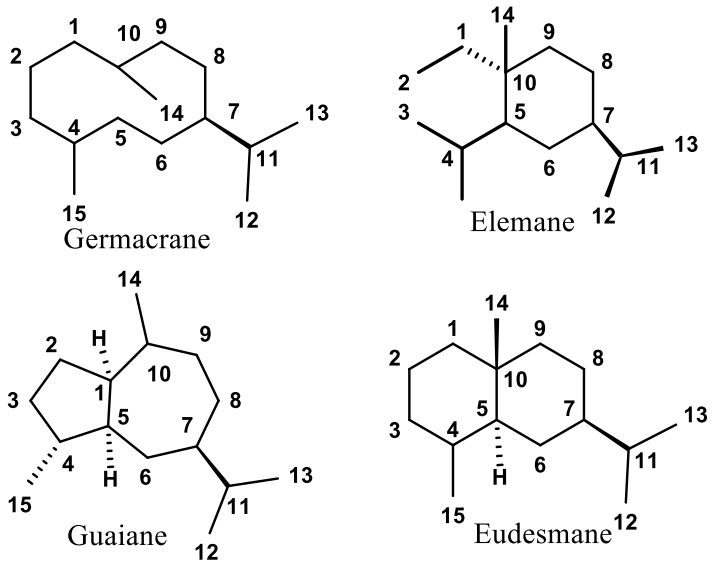

Figure 2. 3. General structures of sesquiterpene lactones.

In addition to germacrane, eudesmanes and guaianes are regarded as characteristic chemical markers for *Rhaponticum* genus (Olennikov, 2019), several studies have also shown the presence of numerous sesquiterpenes. The compounds rhaponticol, desacylnaropicrin, 8-desacylrepin, chlorohyssopifolin E, and repin were found in *R. uniflorium*, whereas *R. carthemoids* afforded repensolide, chlorojanerin, repdiolide, and janerin (Kokoska & Janovska 2009b; Olennikov, 2019) Other SLs including cebellin J, rhaserin, rhaposerin, rhaserolide, chlorohyssopifolin A, repdiolide, acroptilin, and series of chlorine-containing guaianolides were isolated from *R. serratuloides* (Berdin et al., 2001; Ifantis et al., 2013; X. Zhang et al., 2010). In addition, chlorojanerin, janerin, cebellin G, aguerin B, 19-deoxyjanerin, repdiolide and repensolide, 15-dechloro-15-hydroxychlorojanerin and cynaropicrin, were obtained from *R. pulchrum*. Some sesquiterpene lactones were identified from more than one species. For example, cynaropicrin as shown in **Figure 2.4** was isolated from the species of the genus *Rhaponticum*.

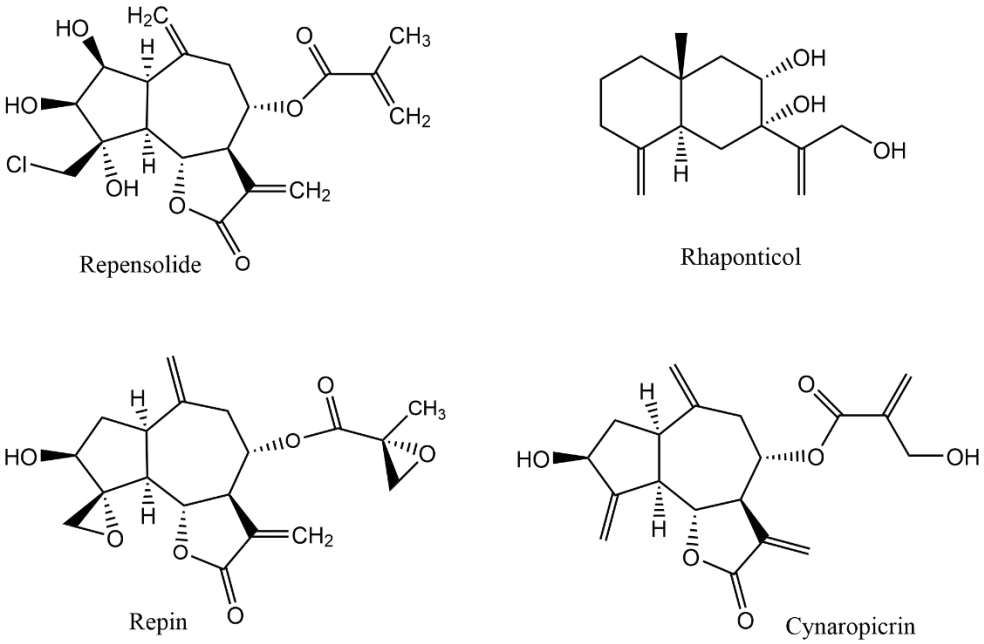

Figure 2.4. The chemical structures of sesquiterpenes detected from *Rhaponticum* species.

2.3.4.4. Triterpenes

Previous phytochemical investigations on *Rhaponticum* genus indicated the presence of different triterpene skeletons. The extract of the roots and aerial parts of *R. carthemoids* was reinvestigated by Vereskovskii et al. (1978) afforded triterpenoid glycosides including rhaponticosides A, B, C, D, E, F, G , and H., while carthamenol and carthamenyl acetate were isolated from underground parts (Kokoska & Janovska, 2009b). Besides, triterpenes have been detected in *R. unflorium*. (Y. Zhang et al, 2002) indicated the presence of 3-oxo-19α-hydroxyurs-12-en-28-oic acid, arjunic acid, pomolic acid, ursolic acid, and tormentic acid which were isolated for the first time from the roots part of *R.* uniflorium (**Figure 2.5**). Additionally, other compounds are present in *R. uniflorium* e.g., 3-O- -L-arabinopyranosyl-urs-12,18(19)-dien-28-oic acid -D-glucopyranosyl ester, 3 - hydroxyurs-12,18(19)-dien-28-oic acid -D-glucopyranosyl ester, 3 -hydroxyurs-12,19(29)-dien-28-oic acid -D-glucopyranosyl ester, 3-O- -L-arabinopyranosyl-urs-9(11),12-dien-28-oic acid -D-glucopyranosyl ester, 2 ,3 ,19 ,25-tetrahydroxyurs-12-en-23,28-dioic acid. (Zhang et al., 2009), were isolated two new triterpenoid saponins from the roots of *R. uniflorum* 3-O-[b-D-glucopyranosyl]-ilexolic

acid-28-O-[b-D-glucopyranosyl] ester and 3-O-[b-D-glucopyranosyl]-urs-12, 19 (29)-dien-oic acid-28-O-[b-D-glucopyranosyl] ester.

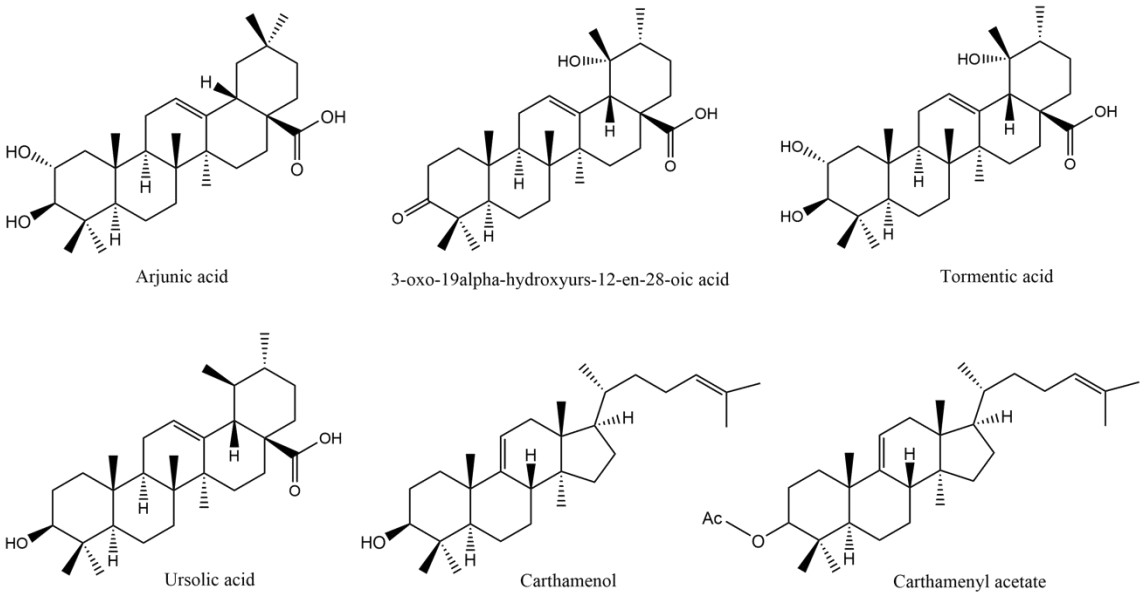

Figure 2.5. The chemical structures of triterpenes detected in *Rhaponticum* species.

2.3.4.5. Phytosterols

Phytosterols are a subgroup of steroids as an important class of bioorganic molecules. They are distributed in *Rhaponticum* species which serve as chemotaxonomic leads for this genus. Stigmasterol, β-sitosterol, and campesterol were detected in the roots of *R. uniflorium* (**Figure 2.6**), whereas these compounds were previously observed in the extract of *R. carthamoides* seeds (Biskup et al, 2009; X. Zhang et al., 2010). A comprehensive review of studies has found that some phytosterols display various biological activities, e.g., stigmasterol, used as a starting material in the production of synthetic progesterone and β-sitosterol, which was shown to act as an anti-inflammatory agent by inhibiting prostaglandin release in macrophages (Kaur et al., 2011).

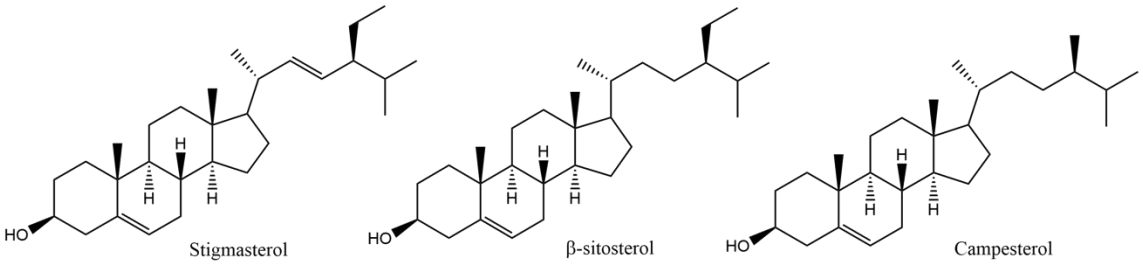

Figure 2.6. The chemical structures of phytosterols detected in *Rhaponticum* species.

2.3.4.6. Flavonoids

Flavonoids are based upon a fifteen-carbon skeleton consisting of two benzene rings linked via a heterocyclic pyrane ring (C) as shown in **Figure 2.7**. Most of the classification of flavonoids is depending on the level of substitution of the C ring, while individual compounds within a class differ in the substitution of the A and B rings. In this context, distribution of flavonoids in the genus *Rhaponticum* can be divided into several classes such as flavanones (e.g., hesperetin, and naringenin), flavones (e.g., flavone, apigenin, and luteolin), and flavonols (e.g., quercetin and kaempferol). (Kokoska & Janovska, 2009a; X. Zhang et al., 2010).

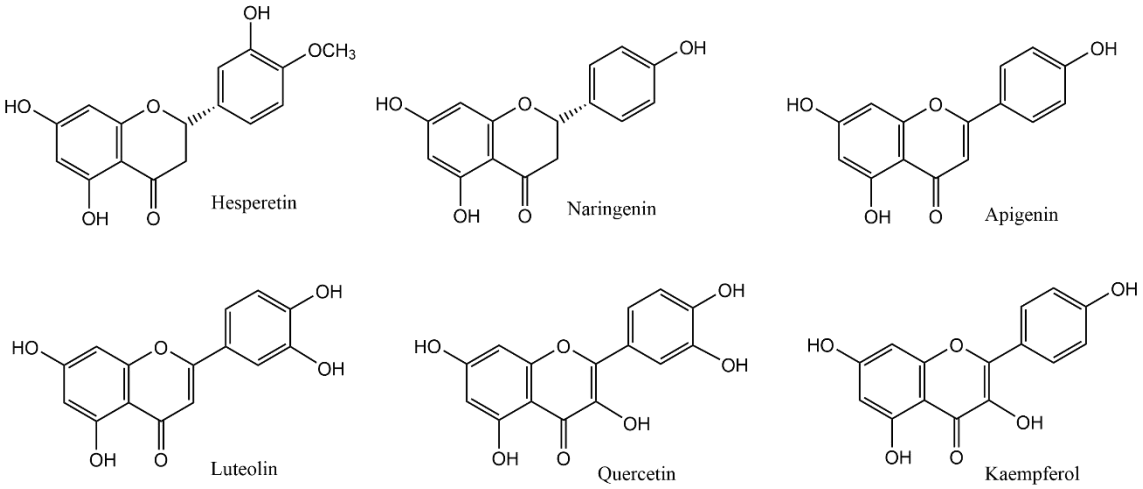

Figure 2.7. The chemical structures of flavonoids detected in *Rhaponticum* species.

2.3.4.7. Thiophens

In addition to the different classes of natural products mentioned above, other types of compounds were obtained from *Rhaponticum* genus. Thiophens (e.g., arctinal, arctinone-b, arctic acid, arctinol-b were isolated from *R. uniflorium* (Wei et al., 1997), while 2-(1,2-Dihydroxyethyl)-5-[(E)-heptene1,3-diyn-1-yl] 1-{5-[(E)-5,6-Dimethylhept-5-en-1,3-diynyl]- 2-thienyl}ethan-1,2-diol were reported from *R. carthemoids* (**Figure 2.8**).

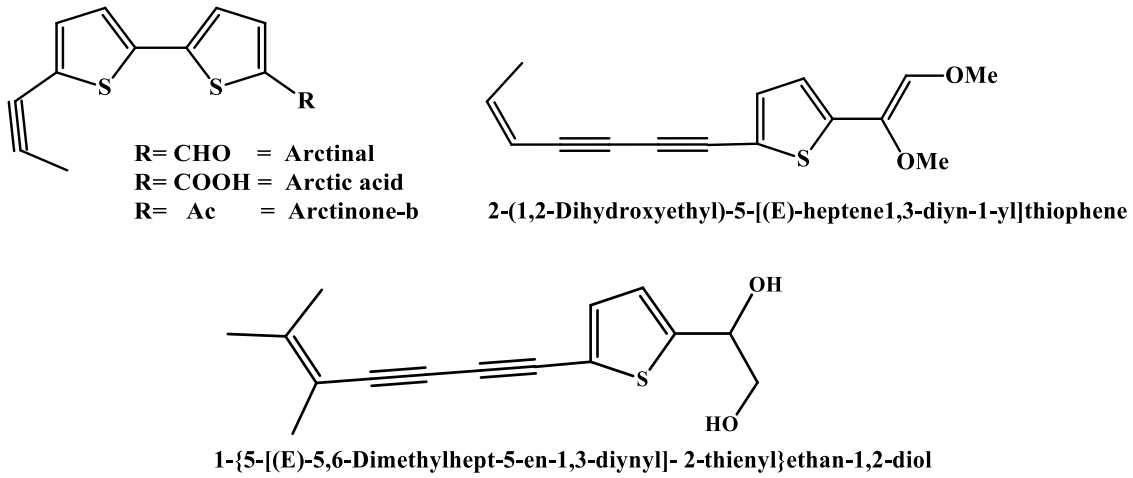

Figure 2. 8. The chemical structures of thiophens isolated from the genus *Rhaponticum*.

2.3.4.8. Volatile Constituents of The Genus *Rhaponticum*

Essential oils (Eos) are complex mixtures of volatile compounds produced by living organisms and can be obtained by different methods (physical means only), including low- or high-pressure distillation of different plant parts, or the use of liquid carbon dioxide or microwaves**.** The diverse applications of volatile oils account for the great interest in their study. In addition to fragrances, flavoring, and decorative cosmetics, they play an important role in the pharmaceutical industry due their biological properties (Baser & Buchbauer, 2009).

Chemically, essential oils are mixtures of hydrophobic aroma compounds, most of which are terpenoids. The constituents of essential oils are present as monoterpene and sesquiterpenoids including various cyclic and acyclic forms such as hydrocarbons, alcohols, aldehydes, ketones, esters, ether, peroxides, phenol epoxides (Bruno *et*

al.,2010). In the genus *Rhaponticum*, various investigations have been carried out to examine the chemical composition of essential oils of different species (**Figure 2.9**). (Lotocka& Geszprych., 2004) reported that the analysis of essential oils from rhizomes and roots, and basal and stem leaves of *R. carthamoides* plants cultivated in Polish climatic conditions was characterized by low content of essential oil (0.07% - 0.11% and - 0.08% - 0.09% in underground organs and leaves, respectively). The monoterpenes, especially geraniol (17.04–18.27%), were the most abundant in the essential oil from roots and rhizomes, whereas sesquiterpenes, represented by β-caryophyllene (24.65–32.30%), was identified as the most important compound in the leaves analyzed in their study. Similarly, essential oils obtained from *R. carthamoides* roots and rhizomes were analyzed by GC, GC– MS and GC–FTIR techniques. (Havlik et al., 2009). A total of 30 components were identified, accounting for 98.0% of total volatiles. A norsesquiterpene 13-norcypera-1(5),11(12)-diene (22.6%), followed by aplotaxene (21.2%) and cyperene (17.9%), were isolated and their structures were confirmed by 1D and 2D-NMR. Selinene type sesquiterpenes and aliphatic hydrocarbons were among minor constituents of the essential oil. In the same way, the components of the essential oil from *R. uniflorum* (L.) DC were analyzed by G/ MS, resulting in identification of 30 components, mainly terpenoids. (Zhu, Lu, & Chen, 1991).

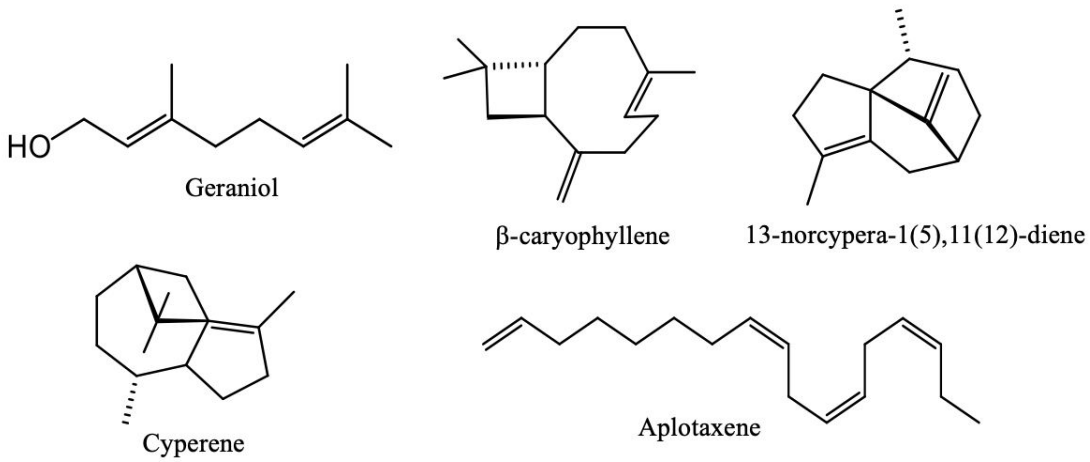

Figure 2.9. The chemical structures of the volatile compounds detected in *Rhaponticum* species.

2.4. Rhaponticum acaule (L.) DC.

Rhaponticum acaule (L.) DC. is an endemic species distributed in Tunisia, Algeria, Morocco (Greuter & von Raab-Straube, 2008) (**Figure 2.10**). In addition to growing in limited geographical areas in North Africa, it is also distributed in the Northwest area of Libya (S. M. Jafri & Elgadi, 1986).

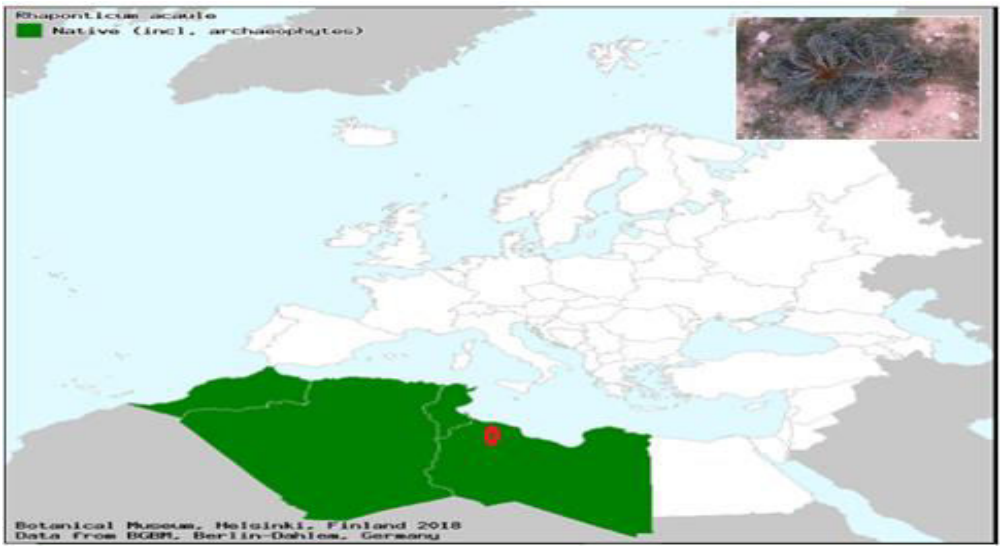

Figure 2. 10. Distribution map of *Rhaponticum acaule* (L.).

2.4.1. Botanical Description of the Plant

The epithet of the species name of *Rhaponticum acaule* is derived from the word acaulescent. *R. acaule* is characteristic as a monocephalic perennial herb, rosulate, leaves coriaceous, green hairy above and white arachnoid tomentose underneath; first few leaves sometimes entire, sinuate, rest bipinnatipartite, oblong-oblanceolate in outline, up to 25 cm long, long petiolate. Capitula up to 10 cm in diam., sessile in the middle of the tips; in fruiting purplish due to long exserted pappus setae. Involucral bracts 4(-5) rowed, coriaceous, linear-ovate, up to 40mm long (include. appendage), narrowly white, scarious margined, glabrous; appendages lanceolate, acute, with margins white, lacerated. Corolla deeply 5 lobed; lobes towards the apex inflated-lanceolate; anther lobes purplish; filaments hairy below the anther lobes. Cypsela 10X6mm, obpyramidal angular, ribbed, glabrous; pappus 25-30 long, deep brown to violaceous, setae barbellate, connate at the base (Jafri & El-Gadi, 1983) (**Figure 2.11**).

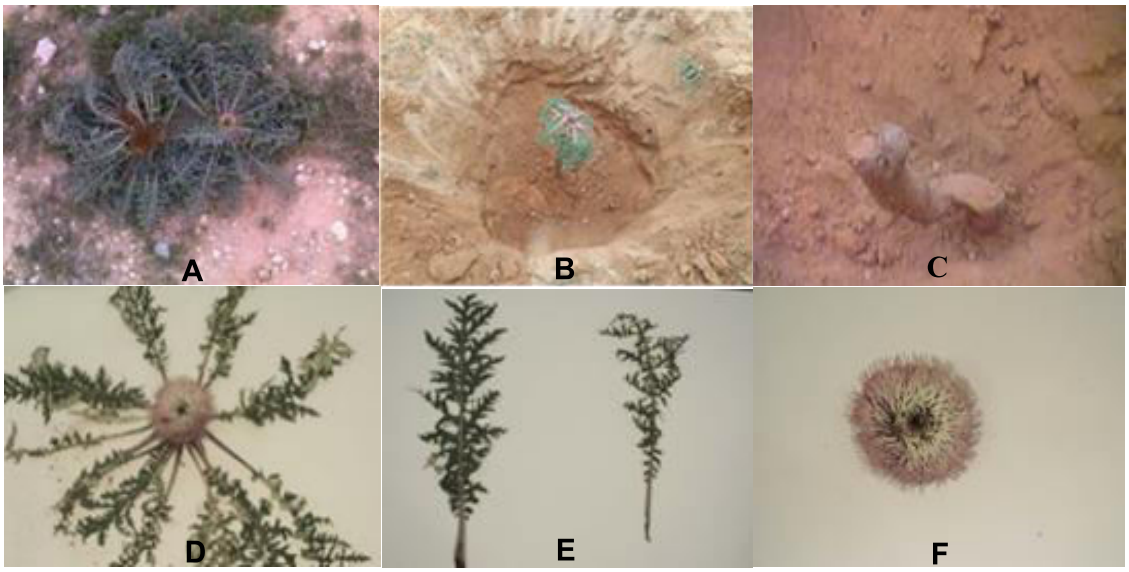

Figure 2. 11. A) Wild growth of *R. acaule* (L.), (B) Arial and ground parts of plant, (C) Rhizomes, (D) Leaves and capitulum, (Leaves-E, Capitulum-F).

2.4.2. Taxonomic classification

Domain	Eucaryota
Kingdom	Plantae
Subkingdom	Virideplantae
Division (phylum)	Tracheophyta
Subdivisions (Subphylum)	Euphyllophytina
Infra phylum	Radiatopses
Class	Magnoliopsida
Subclass	Asteridae
Order	Asterales
Suborder	Asterineae
Family	Asteraceae (compositae
Subfamily	Asteroideae (Tubuliflorae)
Trib	Cardueae (Cynareae)
Subtrib	Centaureinae
Genus	*Rhaponticum* L.
Species	*Acaule*.

Common local name in North Africa is Tafgha (التافغا).

Basionym

Cynara acaulis L. (1763)

Homotypic synonymes

Leuzea acaulis (L.) Holub (1973)

Stemmacantha acaulis (L.) Dittrich (1984)

Synonym(s) Heterotypic

Centaurea chamaerhaponticum Ball (1878), *Centaurea chamaerhaponticum* var. ochreuleuca Maire (1929), *Rhaponticum acaule* var. *ochroleucum* (Maire) Maire (1934), *Centaurea chamaerhaponticum* var. purpurea Emb. & Maire (1929), *Rhaponticum acaule* var. *purpureum* (Emb. & Maire) Maire (1934).

2.4.3. Traditional Use of *R. acaule*

Usually, the medicinal plants that are used are kept secret by the traditional practitioners. The use of ethnomedicinal information has led to the discovery of promising drug leads, which have significantly contributed to the pharmaceutical industry (Taylor et al., 2001). The information on traditional uses of *R. acaule* was collected through direct interviews with people living in villages in the northwest of Libya. The collected information included the local name, plant part used, human sicknesses treated, method of preparation, and how to be used. On the other hand, literature review indicates that *R. acaule* has been used traditionally to treat a disorder associated with inflammation (Rimbau et al., 1999), and the powdered roots have been used as an aperitif, depurative, digestive, stomachic and to treat gastrointestinal ailments, including ulcer (Bakhtaoui et al., 2014; Bendimerad-Mouttas et al., 2018). It is worth noting that the flower heads are eaten as artichokes (Ben Ismail, 2013).

2.4.4. Phytochemical and Biological Properties of *R. acaule*

Very few phytochemical and biological studies were conducted on *R. acaule*, however, the results of these studies confirm the ethnomedicinal uses of this plant. In one of the reports, aqueous, ethanol and chloroform extracts of underground part were administrated topically or intraperitoneal to investigate the anti-inflammatory activity in comparison with indomethacin (3mg/kg). The results showed that the ethanol and

chloroform extracts of *R. acaule* demonstrated promising activity on arachidonic acid induced edema (Rimbau et al., 1996). Boussaada et al., 2008., studied the essential oils from the capitula and the aerial parts of *R. acaule* obtained by steam distillation. The GC-MS analysis revealed the presence of 57 components, representing 95.5% and 96.3% of the two oils respectively and methyl eugenol, epi-13 manool, β-ionone, β-bisabolol, 1- octadecanol, phytol and farnesyl acetate were found to be the main components (**Figure 2.12**). Besides, the authors observed that the oils from both parts of the plant showed significant antibacterial activity against some species of bacteria.

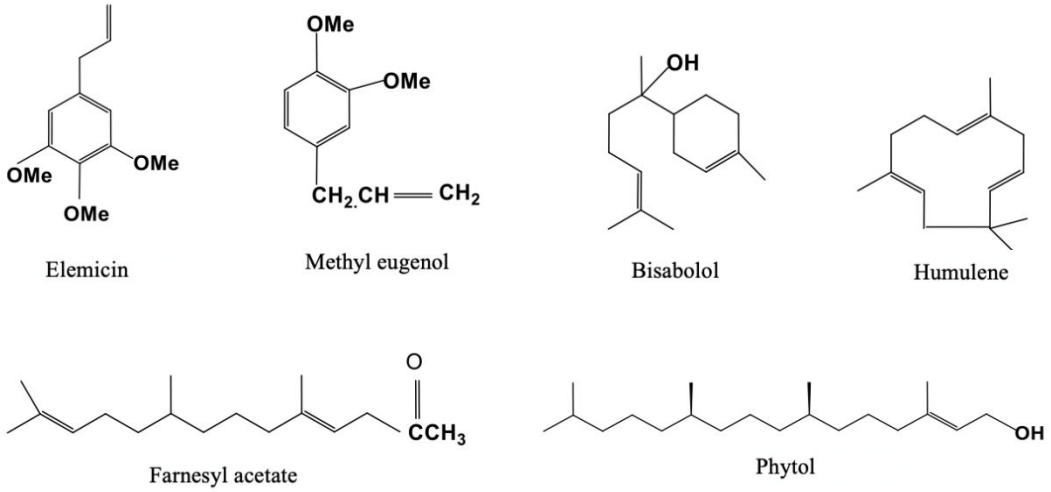

Figure 2. 12. Chemical structures of the main identified compounds from the oils of aerial parts of *R. acaule*.

Simultaneously, *R. acaule* exhibited growth inhibition and antifeedant activity against adults and larvae of confused flour beetle *Tribolium confusum*. The results of the study suggested that *R. acaule* may be used in grain storage against insects. In addition butanol and ethyl acetate extracts of *R. acaule* showed moderate antibacterial activity against tested bacterial strains and concurrently strong inhibition against the fungus *Trichophyton rubrum*. (Abdelkader et al, 2010).

Over and above that, studied the composition of essential oil from the roots of *R. acaule* growing wild in Algeria by hydrodistillation (HD) and by Head-Space Solid Phase Micro-Extraction (HS-SPME). observed that, Quantitative but not qualitative differences in the chemical composition of both samples depending on the extraction

method. Therefore, the authors proposed that HS-SPME extraction could be considered as an alternative technique for the isolation of volatiles from plants. (Benyelles et al., 2014).

In another study, antioxidant, antibacterial and anticoagulant activities of the methanolic extract of *R. acaule* fruit were evaluated (Benabdesselam et al, 2018). A study was carried out indicating that the main constituents in essential oils from the aerial part of *R. acaule* include germacrene D, methyl eugenol, (E)-β-ionone, β-caryophyllene, (E, E)-α-farnesene, bicyclogermacrene, and (Z)-α-bisabolene. This oil has free radical scavenging activities and demonstrated a strong α-glucosidase inhibition which plays a vital role in the treatments of diabetes mellitus (Mosbah et al., 2018). On the other hand, results evidenced that this oil exhibited an important xanthine oxidase inhibitory effect which is an important cause of treatment of gout diseases.

CHAPTER 3

3. MATERIAL AND METHODS

3.1 General

Classical column chromatography and a gradient Medium Pressure liquid Chromatography (Büchi MPLC equipped by Pump Modules C-601 & C-605 with a pump Controller C-610 and pump manager C-605) and a Büchi Fraction Collector C-615 were used for the isolation process. Melting points (mp) were measured using an Electrothermal IA9200 Digital 451 Programmable Melting Point Apparatus (Cole Parmer). Optical rotations were measured on a Schmidt + Haensch Polartronic MHZ-8 polarimeter. IR Spectra were measured on a PerkinElmer FT-IR spectrometer. NMR experiments in CD_3OD were performed on a Bruker DRX 500 spectrometers operating at 500 MHz for ^{1}H and 125 MHz for ^{13}C, respectively, using the XWIN NMR software package for the data acquisition and processing. Negative- and positive-mode HRMS were recorded on a Finnigan TSQ 7000 and HR-Mass Spectrometer and a UPLC-Quadrupole Orbitrap instrument. For lyophilization a CHRIST Alpha 1-4 LD Plus was used. X-ray diffraction measurements were made at 160 K on *Rigaku Oxford Diffraction SuperNova* and *Synergy* dual-source area-detector diffractometers. Büchi R-210 and Heidolph 4001 rotary evaporators were used.

3.2. Chemicals and Adsorbents

Acetone, ethyl acetate, toluene, *t*-butanol, methanol, dichloromethane, chloroform and pyridine (Merck, Fluka Analytical, Sigma-Aldrich) were the solvents throughout the studies. For thin-layer chromatography, silica gel 60 F_{254} (Merck) precoated plates were used. Silica gel 60 (0.063-0.200 mm, Merck), LiChroprep C-18 (0.063–200 mm, Merck) and Sephadex LH 20 were used for column chromatography. The TLC plates were sprayed with 1% vanillin in methanol and 5% H_2SO_4), followed by heating at 110 °C.

3.3. Plant Material

Rhaponticum acaule (whole plant) was collected from a specific region of the northwest Libya, Tarhunah city, during its flowering stage during March-April in 2016 [32º23’04.74” N, 13º27’21.20” E] and identified by Prof. Mohamed Abuhadra. Voucher

specimen number D6810764 has been deposited in the National Herbarium of the Faculty of Science, Botany Department, the University of Tripoli in Libya.

3.4.Chromatographic Methods

3.4.1. Thin Layer Chromatography

All fractions were subjected to TLC (NP, Kieselgel 60 F_{254} Aluminium 20×20 cm, Merck 5554). The mixtures of DCM-MeOH-H_2O (80:20:2, 70:30:3 or 61:32:7) was used as a solvent system for development. For the revelation, Plates were first examined under UV light using short (λ=254nm) and long (λ=366nm) wavelengths, and thereafter 1% Vanillin and 5% H_2SO_4 were used successively as a reagent. In most cases, plates heated at 110°C for a minute to allow the color to develop. So, after that, colorful spots at daylight and fluorescence at 366 nm can be detected.

3.4.2. Vacuum Liquid Chromatography (VLC)

Vacuum liquid chromatography is pretty simple and quick method which is capable to give good results in a short time period. It provides an ideal pretreatment of samples prior to further process of isolation. In this study, stepwise elution was performed to speed up the fractionation. Reversed-phase vacuum liquid chromatography (RP-VLC) was used as a nonpolar stationary phase packed with C-18 (25-40µm), and water-methanol mixtures was used as a polar mobile phase.

3.4.3. Column chromatography

Column chromatography was used for further purification of the fractions obtained via VLC using suitable stationary phase and mobile phase previously determined by TLC. The column was rinsed well with acetone and was completely dried before packing. A piece of glass wool was placed at the bottom of the column with the help of a glass rod. Silica slurry was prepared in the least polar system (wet method) and was poured from the top of the column approximately 2/3rd of the column with simultaneous draining of the solvent to aid proper packing of the column. Known amount of sample (mg or g) was mixed with minimum quantity of mobile phase and was poured down from the top of the column along the sides and was rinsed down with the

solvent. The lipophilic fractions (insoluble samples) were mixed separately with silica gel and mobile phase in an alternative way to get freely loose powders (dry method). The powder was applied on the surface of the adsorbent and elution was performed with a gradient system. Gradient elution method was followed to separate fractions from sample by using solvents from low polarity to high polarity in varying ratios. The flow rate was adjusted to ml/min and usually 10-15 ml of solvent was collected for each fraction. Fractions were analyzed by TLC and combined according to the band similarity and evaporated to dryness.

3.4.4. Size-Exclusion Chromatography (SEC)

This technique applied by using Sephadex LH-20 (a beaded, cross-linked dextran). Due to its dual character, LH-20 swell in water and a number of organic solvents. The swollen resin can be used for gel filtration separations of both hydrophilic and lipophilic compounds. In this study the Sephadex LH-20, was poured into the column after swelling in water for several hours, the sample was applied to the top as a concentrated solution in the same solvent. The column was eluted with the solvent system MeOH:H_2O (50:50) and the fractions were collected in small vials (about 5 ml per fraction).

3.4.5. GC/MS Analysis

The volatile oil was obtained from dried roots via steam distillation. In order to extract the oil, 180 g of the coarse powder was placed in a one-liter conical flask and linked to the Clevenger apparatus. 500 mL of distilled water was added to the flask and heated to the boiling point. The steam in combination with the oils had been distilled into a graduated cylinder for three hours after which separated from aqueous layer with the use of n-hexane as an auxiliary phase due to the slight quantity of the yield (A lower temperature was used because of intensive foaming). The oil composition was determined both by Gas Chromatography (GC) analysis which was carried out using an Agilent 7890B GC system. FID detector temperature was 300°C. To obtain the same elution order with GC-MS, simultaneous auto-injection was done on a triplicate of the same column applying the same operational conditions. Relative percentage amounts of

the separated compounds were calculated from FID chromatograms and Gas Chromatography-Mass Spectrometry (GC-MS) Analysis which was carried out with an Agilent 5977B GC-MSD system. Innowax FSC column (60 m x 0.25 mm, 0.25 μm film thickness) was used with helium as carrier gas (0.8 mL/min). GC oven temperature was kept at 60°C for 10 min and programmed to 220°C at a rate of 4°C/min and kept constant at 220°C for 10 min and then programmed to 240°C at a rate of 1°C/min. Split ratio was adjusted at 40:1. The injector temperature was set at 250°C. Mass spectra were recorded at 70 eV. Mass range was from *m/z* 35 to 450. The sample was dissolved in 10% n-hexane and 1μL was injected. Identification of the essential oil components was carried out by comparison of their relative retention times (t_R) with those of authentic samples or by comparison of their linear retention index (LRI) to series of *n*-alkanes. Computer matching against commercial (Wiley GC/MS Library, NIST Chemistry WebBook) [(McLafferty & Stauffer, 1989)]and in-house "Başer Library of Essential Oil Constituents" built up by genuine compounds and components of known oils, as well as MS literature data was used for the identification (B.A.C.I.S)., 1999; Joulain & König, 1998).

3.4.6. Extraction and Isolation of Ecdysteroids

The air-dried, ground, underground parts (roots and rhizomes, 600 g) of the plant were percolated with methanol (3 x 1.5 L) at room temperature. After filtration, the combined extract was evaporated on a rotary evaporator under reduced pressure at 40°C. The concentrated aqueous extract (150 g) was diluted with 200 mL of H_2O and partitioned successively using dichloromethane (200 mL x 3) and ethyl acetate (200 mL x 3) to give a dichloromethane (DCM, 2.8 g) and ethyl acetate extract (EtOAc, 4.81g). (**Figure 3.1**).

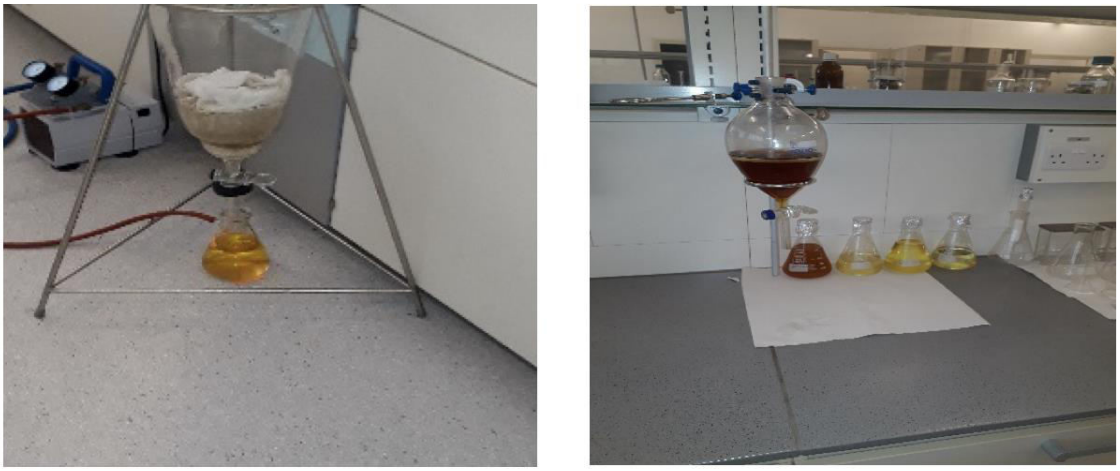

Figure 3. 1. Solid-liquid extraction (left) and liquid-liquid extraction (right).

The aqueous water phase (viscous brown syrup) was divided into two parts (40 ml and 30 ml) and after diluted with water, they were subjected separately to the vacuum liquid chromatography (VLC) using reversed-phase silica gel (LiChroprep C18, 100g) and employing H_2O and H_2O–MeOH mixtures with an increasing amount of MeOH (0→100% MeOH in H_2O). Elutes of 100 ml were collected each time. The similarity of fractions was examined by TLC plates, and according to the TLC profiles (qualitative matching of spots), these fractions were pooled into seven groups (A-G). Fraction A (426 mg), fraction B (802 mg), fraction C (313 mg), fraction D (850 mg), fraction E (4867 mg), fraction F (391 mg) and fraction G (178 mg). Fractions B, and E were dried and subjected to further column chromatography to isolate the compounds (RA-1, RA-2, RA-5, RA-6 and RA-8) (**Figure 3.2**).

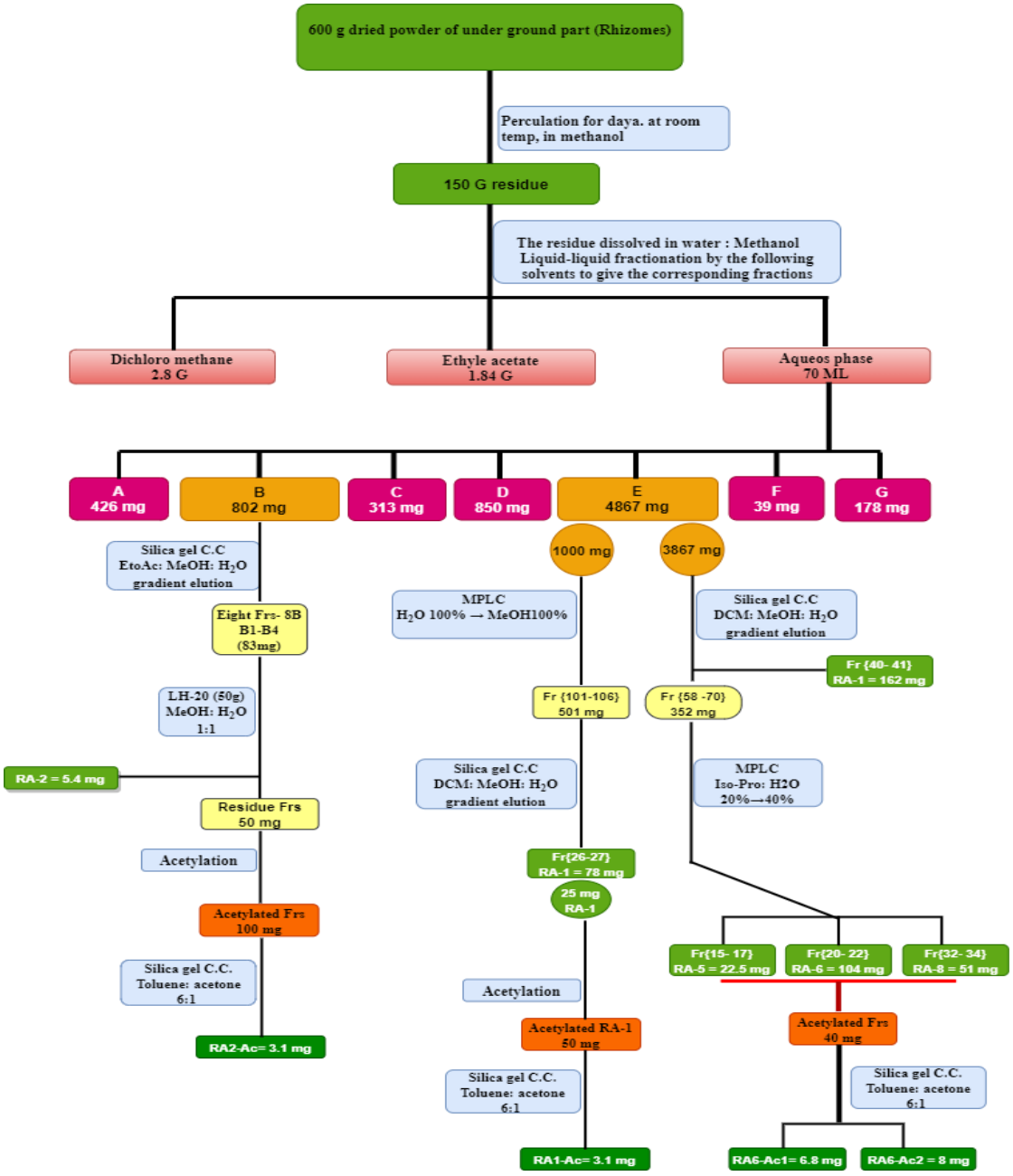

Figure 3.2. Isolation of compounds from the methanol extract of *R. acaule*.

3.4.6.1. Isolation of RA-2

A column of suitable size was chosen and packed with 80 g silica gel 70-230 mesh by adding a slurry of the adsorbent in solvent system EtOAc-MeOH-H_2O (100:10:4). Fraction B was dissolved in methanol and adsorbed on a small amount of silica gel 60 (5g) and fed to the column through a funnel as a dry sample (dry method). The mobile phase was added to the column and kept aside without disturbance for some

time for the settlement of the extract. The column was eluted with solvents in the order of increasing polarity (100:10:4 to 100:16.5:13.5). Fractions showing the similar appearance of R_f value and identification test, were pooled together and solvents evaporated to give 8 fractions which are coded as B8. Fractions [B1→B4, 83 mg] as crude of RA-2 (3), were applied to column chromatography (gel filtration) using Sephadex LH-20 (50 g) for the stationary phase and methanol-water (1:1) as the solvent system, which yielded pure 3 (5.4 mg). The remaining fractions rich in 3 (50 mg) were used for acetylation.

3.4.6.2. Isolation of RA-1

A part of fraction E (1000 mg) was submitted to MPLC using LiChroprep C18 as the stationary phase with a stepwise gradient of MeOH in H_2O (0-60% MeOH in H_2O). This yielded 150 fractions of 10 ml, which were combined and minimized into 22 fractions (Ea 1-22). The fraction Ea 8 was submitted to normal phase column chromatography and eluted with DCM-MeOH-H_2O (80:10:1 to 70:30:3) to give **RA-1** (78 mg). The remaining part of fraction E (3.867 g) was also subjected to a silica gel column (150 g) using DCM-MeOH-H_2O mixtures (80:10:1, 500 mL, 80:20:2, 500 mL, 75:25:2.5, 500 mL, 70:30:3500 mL) to give eleven subfractions (Eb1-11). Eb-6 contained pure **RA-1** (162 mg).

3.4.6.3. Isolation of RA-5, RA-6, and RA-8

The subfraction Eb9 (352 mg) was applied to RP-MPLC (Reverse phase medium pressure liquid chromatography) using H_2O (200 mL) and H_2O-*Iso*-PrOH mixtures with increasing amounts of *Iso*-PrOH in H_2O (20%- 40%; fraction volume 10 mL) to give **RA-5** (22.5 mg) and the mixture of **RA-6** & **RA-8** (180 mg).

3.5. Acetylation of Purified Compounds

In order to prove the proposed structures, the acetyl derivatives of the compounds were prepared. The compounds **RA-1** (78 mg), **RA-2** (50 mg) and the mixture of **RA-6** and **RA-8** (**4&5**, 91 mg) were treated separately with Ac2O (0.5 mL–1.0 mL) and pyridine (0.5 mL–1.0 mL) at room temperature overnight. The acetylation mixtures were poured into icy water and precipitates were washed with cold water. The

crude acetyl derivatives were purified by column chromatography over silica gel (25 g) using toluene-acetone (6:1) to give the acetylated derivatives, **RA-1ac** (**1a**, 34 mg), **RA-2Ac** (**3a,** 12 mg), **RA-6Ac1 (4a,** 20 mg) and **RA-6Ac2 (5a**, 33 mg).

CHAPTER 4

4. RESULTS AND DISCUSSION

Hydrodistillation of *R. acaule* roots provided a pale-yellow essential oil with a yield of 0.055% (v/w), on moisture-free basis. Analysis and identification by mass fragmentation and retention index revealed the presence of 14 compounds. The composition of the essential oil was given in **Table 4.1**. Three components that could not be identified by this method, while eleven components identified in the oil representing 73.1% of the total oil. The major compounds were determined as Aplotaxene (= 1, 8, 11, 14- heptadecatetraene) (34.6%) and carvacrol (11.1%), respectively (**Figure 4.1**). Besides that,a comparison of our study with the disseminated data concerning the essential oil of *R. acaule* and other species reported that 42 different volatile and semi-volatile compounds from roots of *R. acaule* growing in Algeria (Benyelles et al., 2014). The main groups of detected volatiles were aliphatic alcohols (69.2%), terpenes (5.5%), alkenes (5.2%), and alkynes (4.0%)., while 62 compounds were identified from essential oils of the hairy roots and roots of soil-grown plants of *R. carthamoides*. it is worth noting that the Aplotaxene is predominant component in *R. carthamoides* (Skała et al., 2016). Indeed, these differences could be elaborated by several factors such as weather conditions, soil, rainfall rate and harvested time (Barra, 2009).

Table 4.1. The essential oil composition of *Rhaponticum acaule* rhizomes.

LRI	**Compound Name**	**Relative Percentage Amounts (%) A**
1131	β-phellandrene	1.6
1146	1-butanol	2.0
1176	α- phellandrene	1.0
1211	Limonene	4.5
1243	Amyl furan (=2-pentyl furan)	6.0
1287	*p*-cymene	2.0
1362	Undecanal	2.6
1363	Unidentifed	7.8
1597	4-methylguaiacol	5.2
1822	1,8,11-heptadecatriene	2.6
1884	Aplotaxene (=1,8,11,14-heptadecatetraene)	34.6

2109	Unidentifed	8.0
2201	Unidentifed	11.3
2238	Carvacrol	11.1
Total		73.1

A: Essential oil of *Rhaponticum acaule* rhizomes, LRI: Linear retention indices calculated against *n*-alkanes, %: calculated from FID data, tr: Trace (<0.1%).

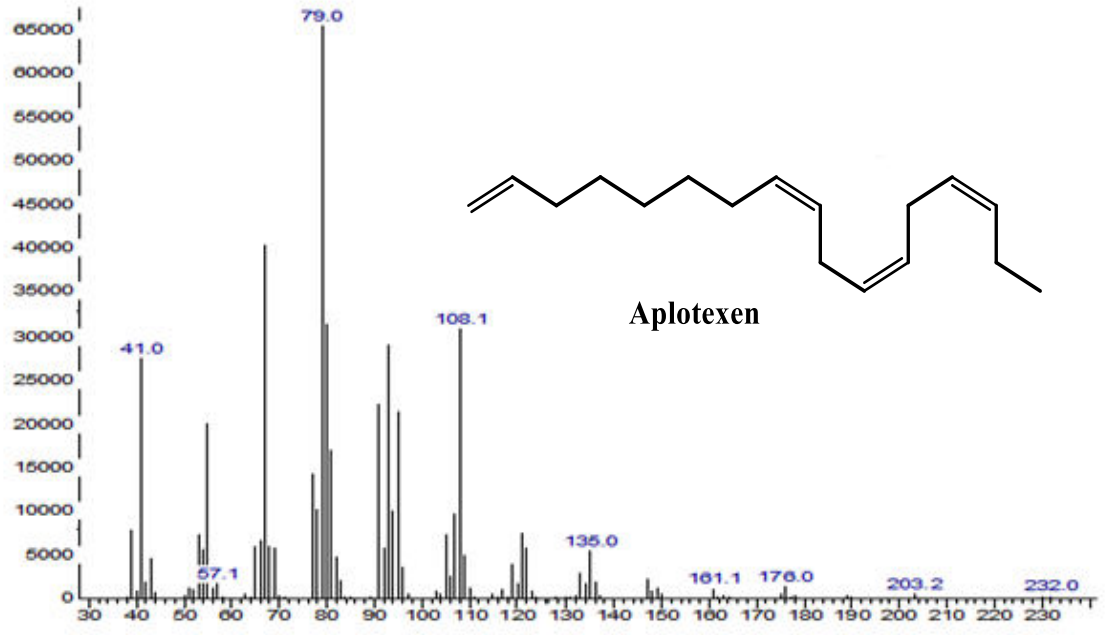

Figure 4.1. 70 eV mass spectrum of Aplotaxene (=1,8,11,14-heptadecatetraene).

On other hand, air-dried and powdered plant material of *R.acaule* (roots and rhizomes, 600 g) was percolated by methanol (3 x 1.5 L) at room temperature for 3 days. After filtration, the solvent was removed under reduced pressure at 40 to afforded 150g of crude extract (extract % Yield= 23%). The concentrated crude extract was dissolved in water (200 mL) and portioned successively using dichloromethane (200 mL x 3) and ethyl acetate (200 mL x 3) to give a dichloromethane extract (DCM 2.8g) and an ethyl acetate extract (EtOAc 1.84g), respectively. The remaining water phase was evaporated down to a volume of 70 mL under vacuum at 40 C° yielding a brown syrup. Following

the chromatographic methods described in the section 3.4.6, five ecdysteroides were isolated and coded as RA-1, RA-2, RA-5, and RA-6&8.

The structures of the isolated compounds were established by chemical (acetylation) and spectroscopic methods including UV, IR,HRMS, 1DNMR: 1HNMR, 13CNMR,DEPT-135.,and 2DNMR: COSY, NOESYHSQC, HMBC.

4.1. RA-1 (20-hydroxyecdysone)

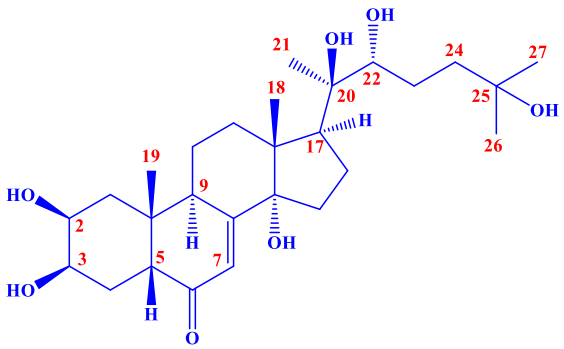

Chemical Formula: $C_{27}H_{44}O_7$
Exact Mass: 480,31
Molecular Weight: 480,64

20-Hydroxyecdysone (RA-1): $[\alpha]_D^{20}$ +29.3° (c 0.15, MeOH).

RA-1 was obtained as a white amorphous compound. The negative ion HR-MS of RA-1 (**Spectrum 4.1.1**) gave a quasimolecular ion $[M-H]^-$ peak at m/z 479.3037, which corresponds with the molecular formula $C_{27}H_{43}O_7$ with a Mr of 480.31 (calc. 479.30) and six degrees of unsaturation. The positive ion HR-MS spectrum (**Spectrum 4.1.2**) exhibited pseudo-molecular ion peaks $[M+H]^+$ at m/z 481.3157 and $[M+Na]^+$ at m/z 503.2975 (calcd for $C_{27}H_{44}O_7Na$). These results indicate the molecular weight of **RA-1** to be 480.3087 ($C_{27}H_{44}O_7$). The IR spectrum of **RA-1** (**Spectrum 4.1.3**) exhibited absorption bands for hydroxy and α,β-unsaturated ketone functionalities at 3379 cm^{-1} and 1648 cm^{-1}, respectively. In the UV spectrum, the maximum absorption at 230 nm was indicative of the presence of an α,β-unsaturated carbonyl system.

The spectra of ^{13}C-NMR and DEPT-135 of **RA-1** (Spectrum 4.1.5) indicated the presence of five methyl, eight methylene, seven methine (three oxygenated and one olefinic), and seven quaternary (three oxygenated, one olefinic, and one carbonyl)

carbon atoms (**Table 4.2**). The ^{1}H-NMR spectrum of **RA-1** (**Spectrum 4.1.4**) showed the presence of five tertiary methyl resonances at δ 0.89, 0.96, 1.19, 1.20 and 1.21 ppm (all singlets). Additional prominent signals were one olefinic proton at δ 5.81 (d, *J* = 2.2 Hz, H-7), and three oxymethine resonances at δ 3,95 (br d, *J* = 2.7 Hz, H-3), 3.84 (ddd, *J* = 11.6, 4.4 and 2.7 Hz, H-2) and 3.32 (br d, *J* = 11.3 Hz, H-22). Signals at higher field than those of all methylene protons were observed at δ 2.38 (dd, *J* = 12.6 and 4.1 Hz, H-5) and 2.40 (dd"t", *J* = 4.5 Hz, H-17). The proton signal at δ 3.16 (dd, J = 10.0, 7.3 and 2.2 Hz) was assigned as H-9 based on the ^{1}H-^{1}H correlations with the olefinic proton (H-7) and methylene protons (H_2-11) in a COSY experiment (Spectrum 4.1.6). The full assignment of the ^{1}H and ^{13}C-NMR resonances (**Table 4.2**) revealed the presence of an ecdysteroid skeleton with a double bond between C-7 and C-8, and a ketone functionality at C-6. With the help of ^{1}H, ^{13}C-NMR and DEPT-135 and 2D-NMR (COSY and HSQC, **Spectrum 4.1.6-4.1.8**) experiments it was possible to deduce four main fragments (A–D, **Figure 4.2**). In addition to five methyl resonances, intramolecular connectivities were established with the help of a HMBC experiment (**Spectrum 4.1.9**). The building of the skeleton was mainly based on the ^{13}C, ^{1}H-long range correlations between the carbon atoms of the fragments A–D and the methyl signals (Zerbe and Jurt, 2013). The relative configuration of the molecule was established by the coupling constants from NOESY and ROESY experiments. The small coupling constants between the H-2 and H-3 protons indicated that both hydroxy groups at C-2 and C-3 are on the same side of the molecule (**Spectrum 4.1.10**). ROESY correlations between H-2, H-3 and H-9 confirmed these assumptions.

Table 4.2. The ^{1}H and ^{13}C-NMR Data for RA-1 (20-hydroxyecdysone).

C/H	DEPT	δ_C, ppm	δ_H ppm, *J* (Hz)	HMBC (from C to H)
1	CH_2	37.33	1.79 dd (13.0/11.6) 1.43 dd (13.0/4.4)	Me-19
2	CH	68.66	3.84 ddd (11.6/4.4/2.7)	H-3
3	CH	68.47	3.95 br d (2.1)	
4	CH_2	32.81	1.75† 1.71†	
5	CH	51.74	2.38 dd (12.6/4.1)	H-7, Me-19
6	C	206.46	-	
7	CH	122.12	5.81 d (2.2)	H-9

8	C	167.98	-	
9	CH	35.04	3.16 ddd (10.0/7.3/2.2)	
10	C	39.25	-	
11	CH_2	21.47	1.80† 1.71†	H-9, H-7
12	CH_2	32.47	2.14 ddd "dt" (12.8/12.8/5.0) 1.88 br dd (12.8/3.0)	Me-18
13	C	48.60	-	Me-18
14	C	85.21	-	H-7, Me-18
15	CH_2	31.76	1.98 m 1.60 m	
16	CH_2	21.47	1.95† 1.70†	
17	CH	50.49	2.40 dd "t" (4.5)	Me-18, Me-21
18	CH_3	18.05	0.89 s	
19	CH_3	24.41	0.96 s	
20	C	77.90	-	Me-21
21	CH_3	21.04	1.20 s	H-22
22	CH	78.37	3.32 br d (11.3)	Me-21,
23	CH_2	27.29	1.63 ddd (12.1/13.0/3.3) 1.26 ddd (12.1/13.0/4.3)	H-22
24	CH_2	42.35	1.79 dd (13.0/4.3) 1.43 dd "t" (13.0/13.0)	H-22
25	C	71.29	-	Me-26, Me-27
26	CH_3	28.96	1.19 s	Me-27
27	CH_3	29.70	1.21 s	Me-26

†) *J* values are not clear due to overlapping.

With all of this, our results come in line with the results of other studies, and comparison of the NMR data of **RA-1** with those of known compounds revealed that this compound is 20-hydroxyecdysone (J. P. Girault & Lafont, 1988; Kubo, Matsumoto, & Hanke, 1985). 20-Hydroxyecdysone has been reported from the invertebrates and in plants (Horn & Bergamasco, 1985). Some of the plants rich in 20-hydroxyecdysone are *Aerva* (Saleem et al., 2013) , *Ajuga* (Calcagno *et al*., 1996; T. Chen *et al*., 2018; Coll *et al*., 2007; Sena Filho et al. 2008), *Leuzea* (syn. *Rhaponticum*) (Vokáč *et al*., 2002), *Silene*, (Girault et al., 1990), and *Vitex* (Suksamrarn et al., 2002) species.

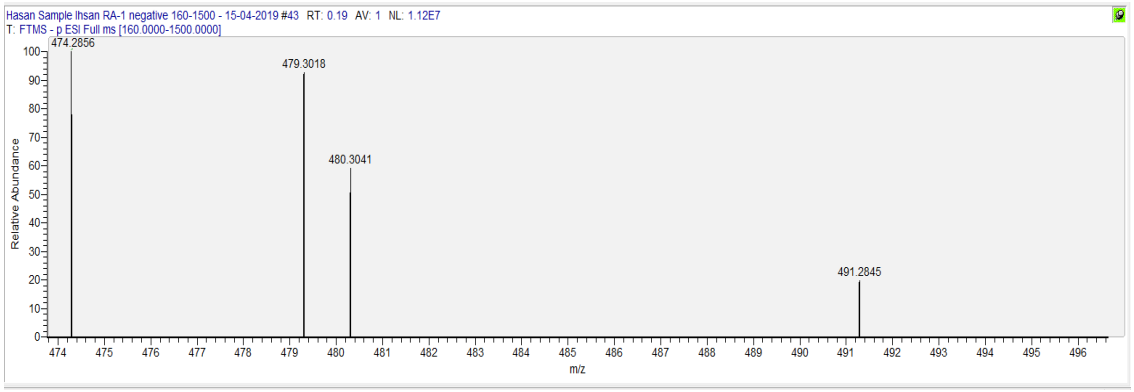

Spectrum 4.1.1. (-)-HRMS of 20-hydroxyecdysone (RA-1) $[M-H]^-$ m/z 479.3018.

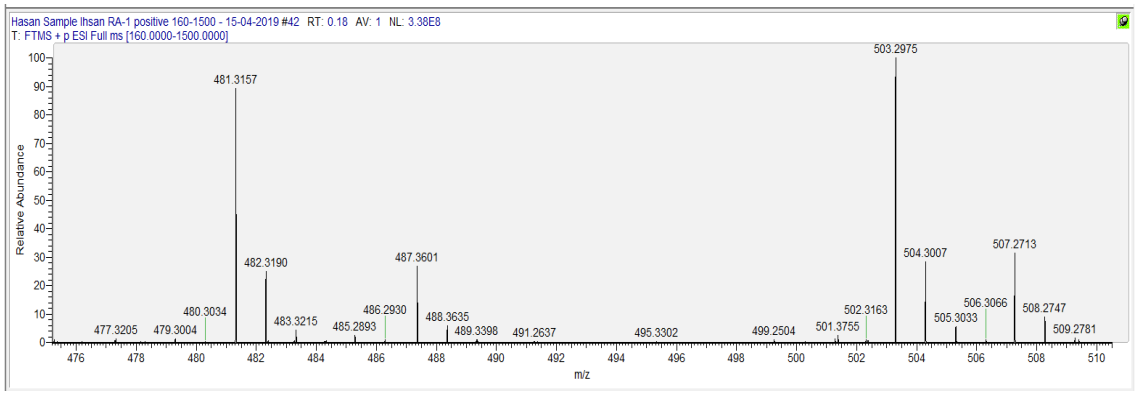

Spectrum 4.1.2. (+) HRMS of 20-hydroxyecdysone (RA-1) $[M]^+$ m/z 481.3157; $[M+Na]^+$ m/z 503.2975.

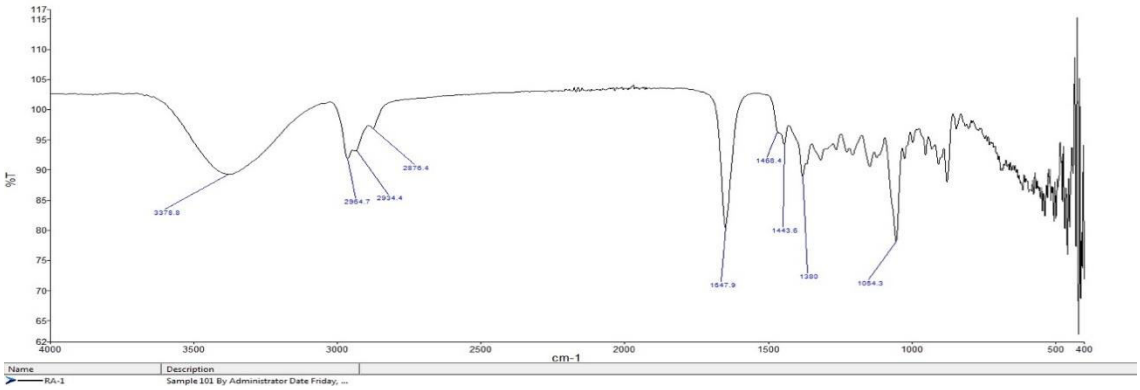

Spectrum 4.1.3. FT-IR of 20-hydroxyecdysone (RA-1).

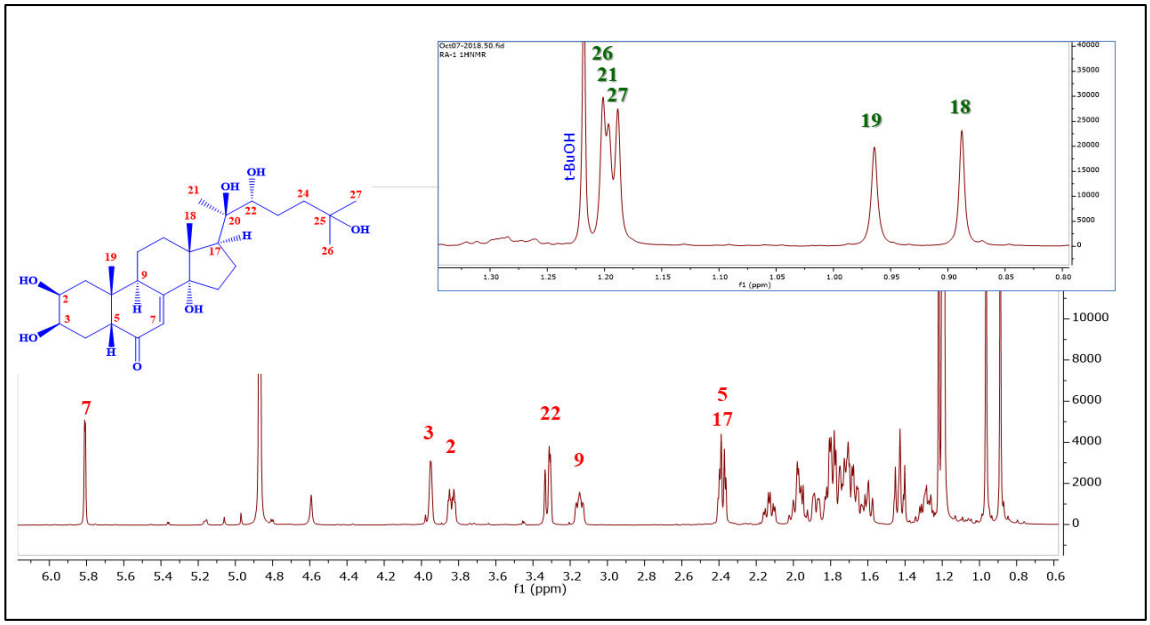

Spectrum 4.1.4. ^{1}H-NMR Spectrum of RA-1 (20-hydroxyecdysone) (500 MHz, MeOD).

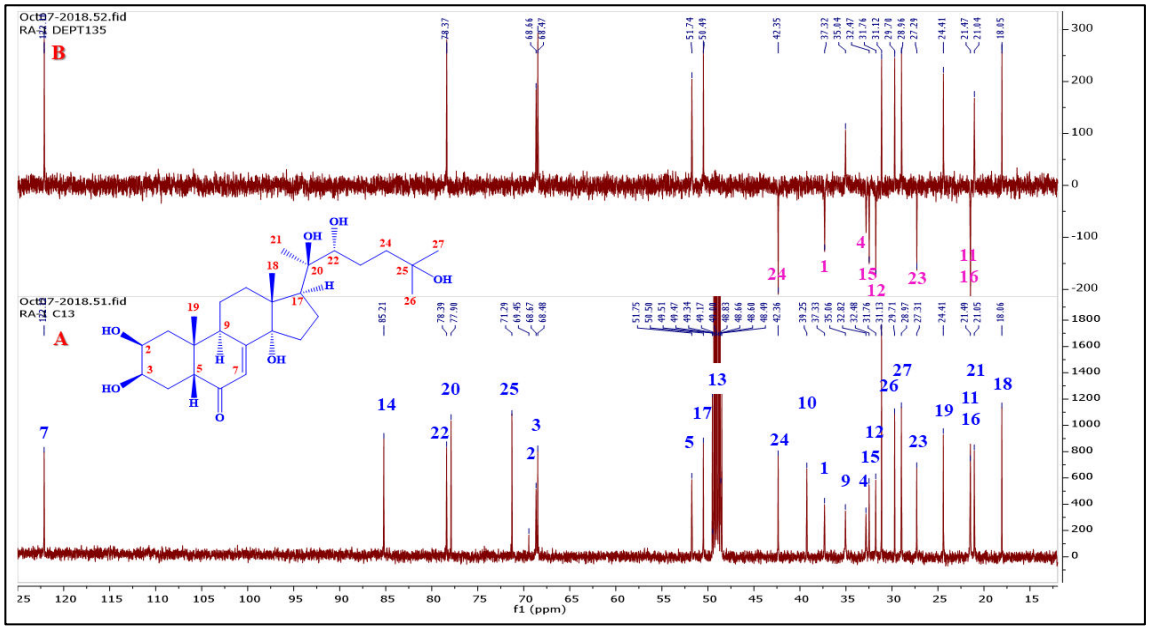

Spectrum 4.1.5. ^{13}C-NMR (A) (125 MHz, MeOD) and DEPT-135 (B) Spectra of RA-1 (20-hydroxyecdysone).

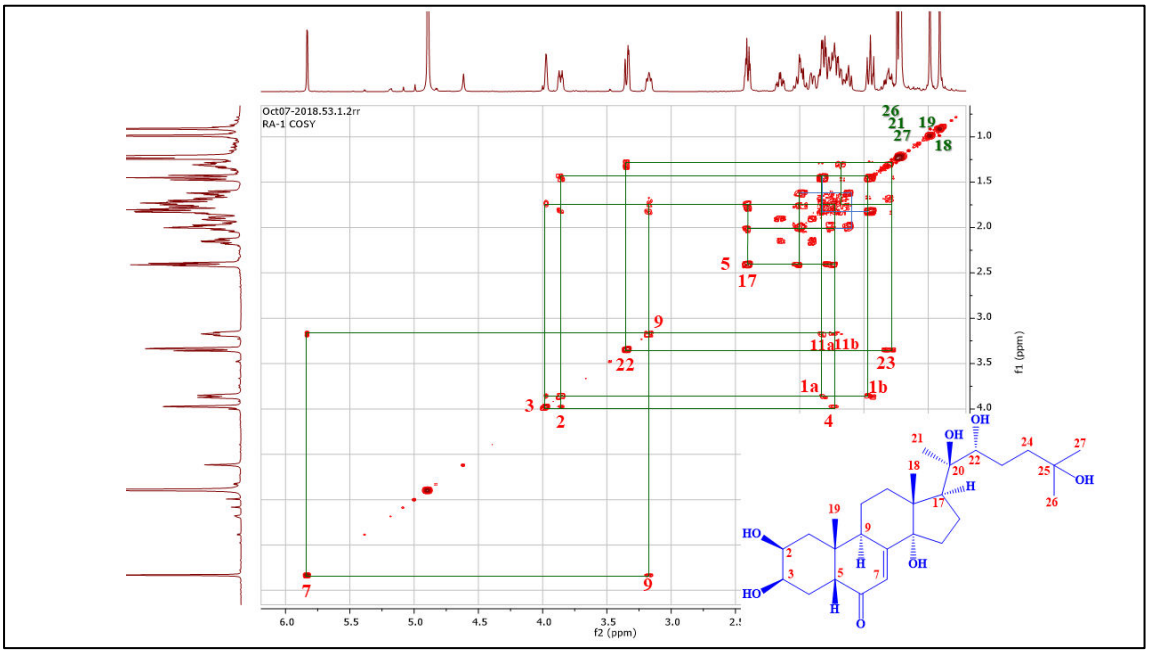

Spectrum 4.1.6. COSY of RA-1(20-hydroxyecdysone).

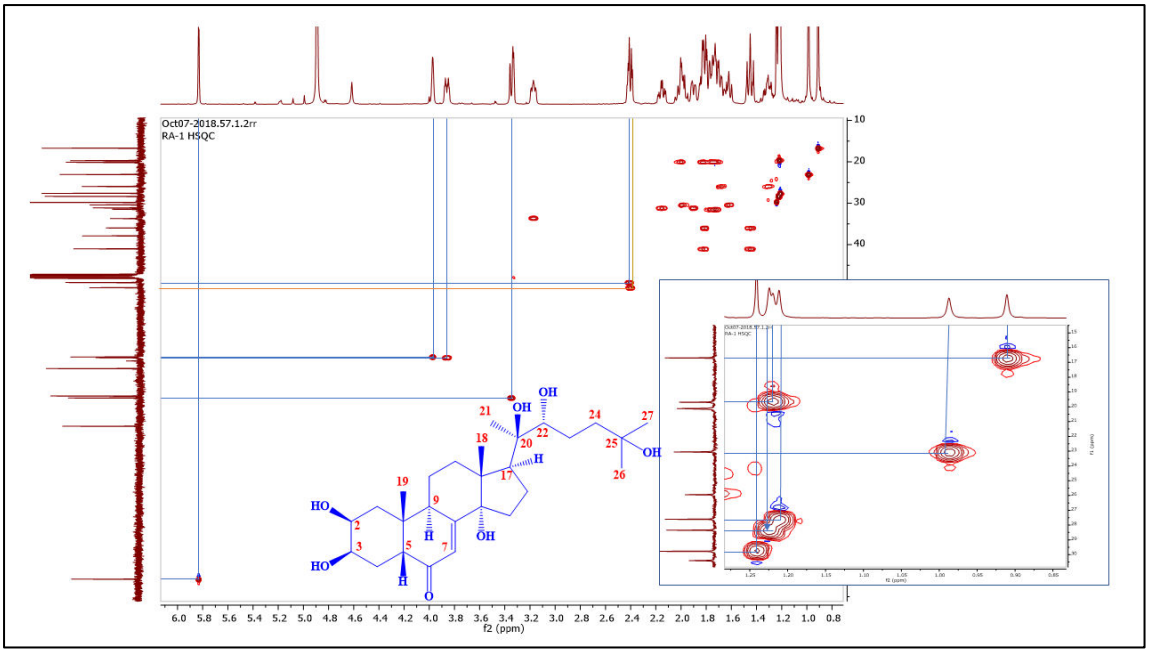

Spectrum 4.1.7. HSQC of RA-1 (20-hyroxyecdysone).

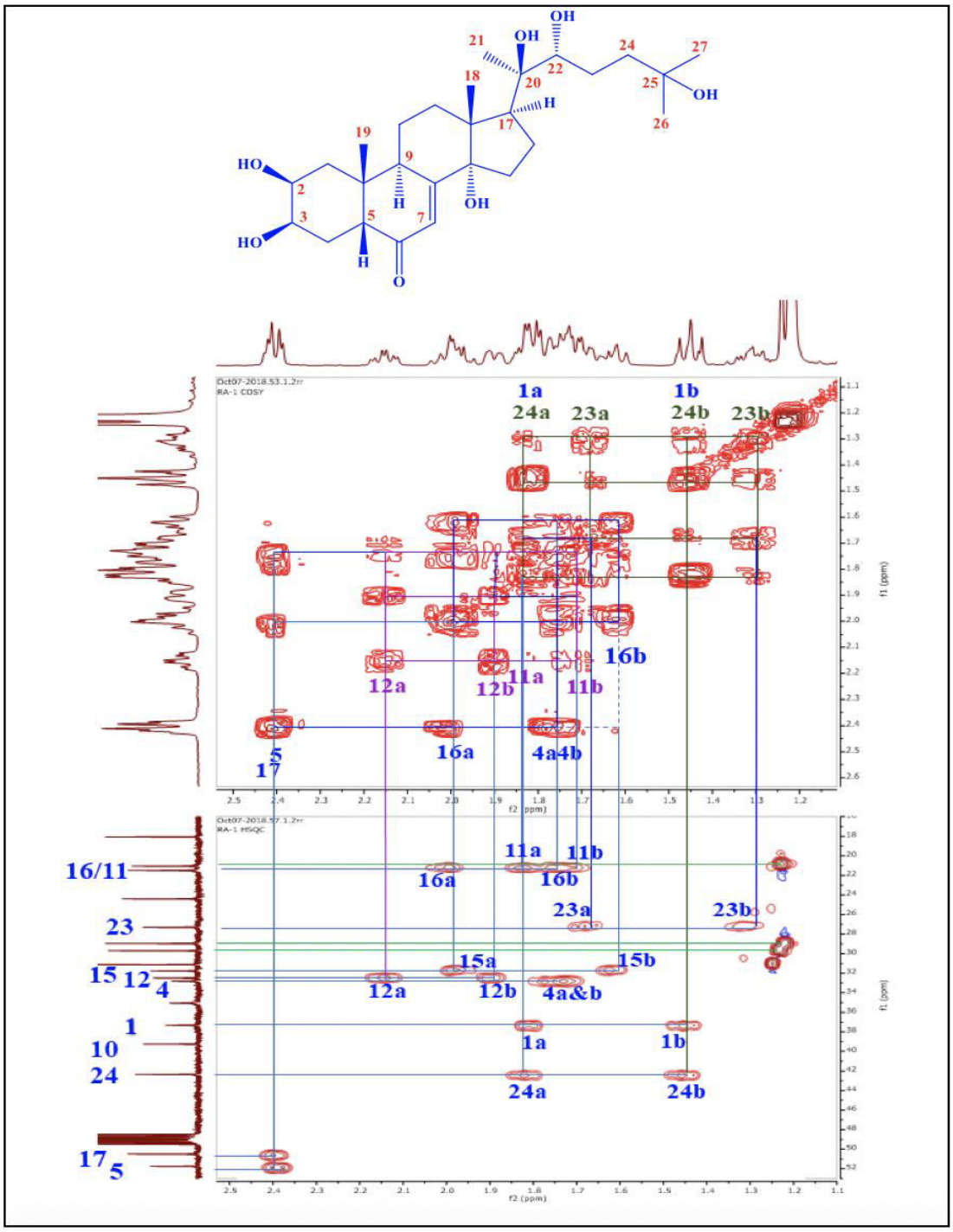

Spectrum 4.1.8. COSY and HSQC Spectra of RA-1 (20-hydroxyecdysone) (^{1}H: 1.1 – 2.5 ppm; ^{13}C: 16 – 54 ppm).

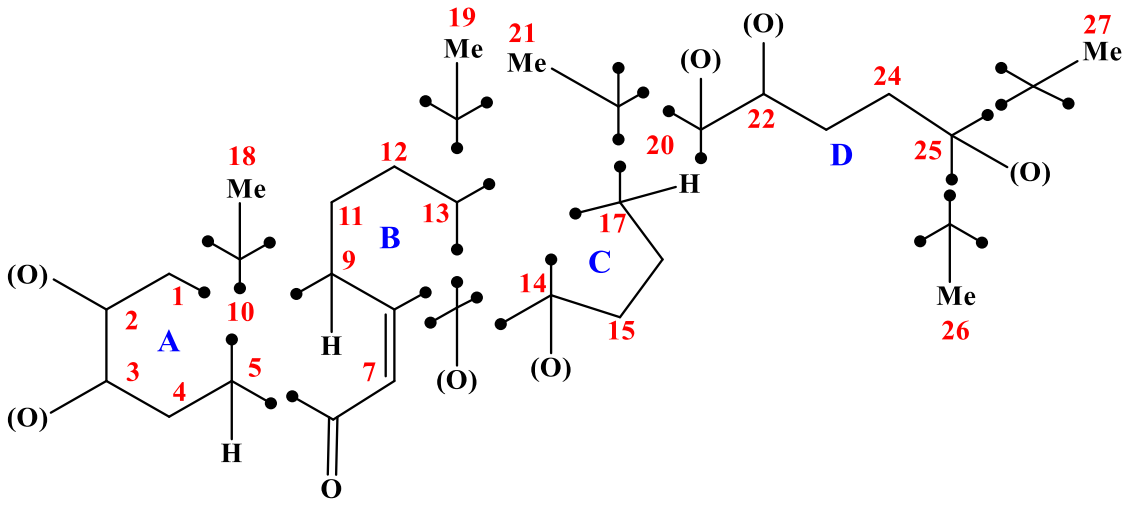

Figure 4.2. Molecular Fragments of RA-1 (20-hydroxyecdysone).

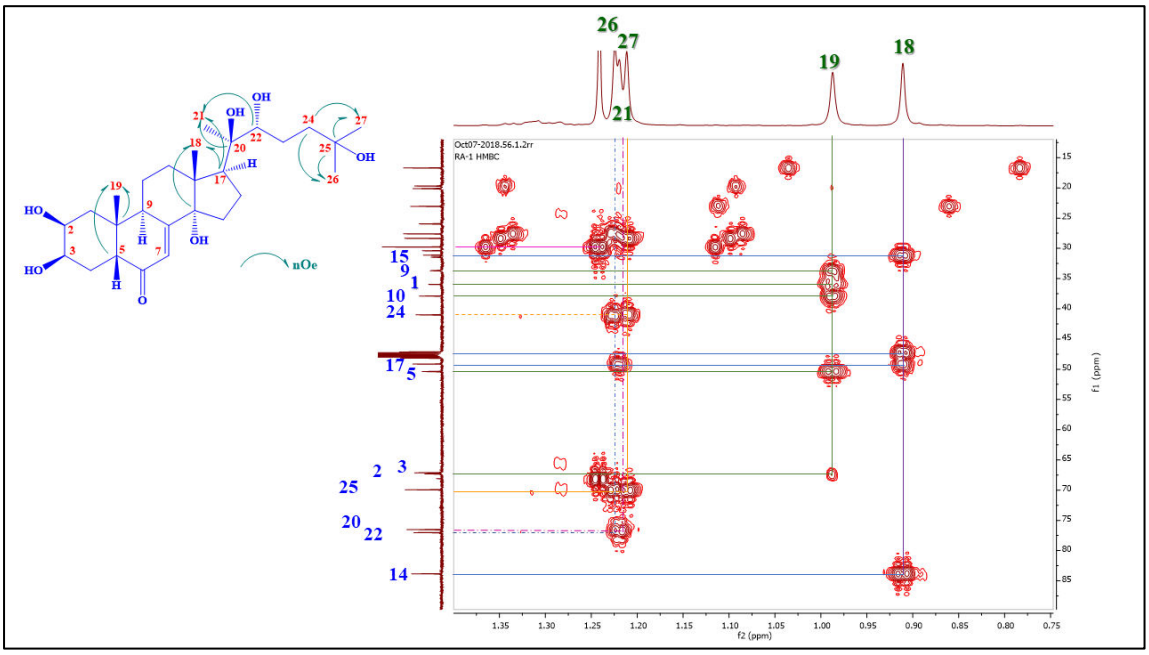

Spectrum 4.1.9. HMBC of RA-1 (20-hydroxyecdysone).

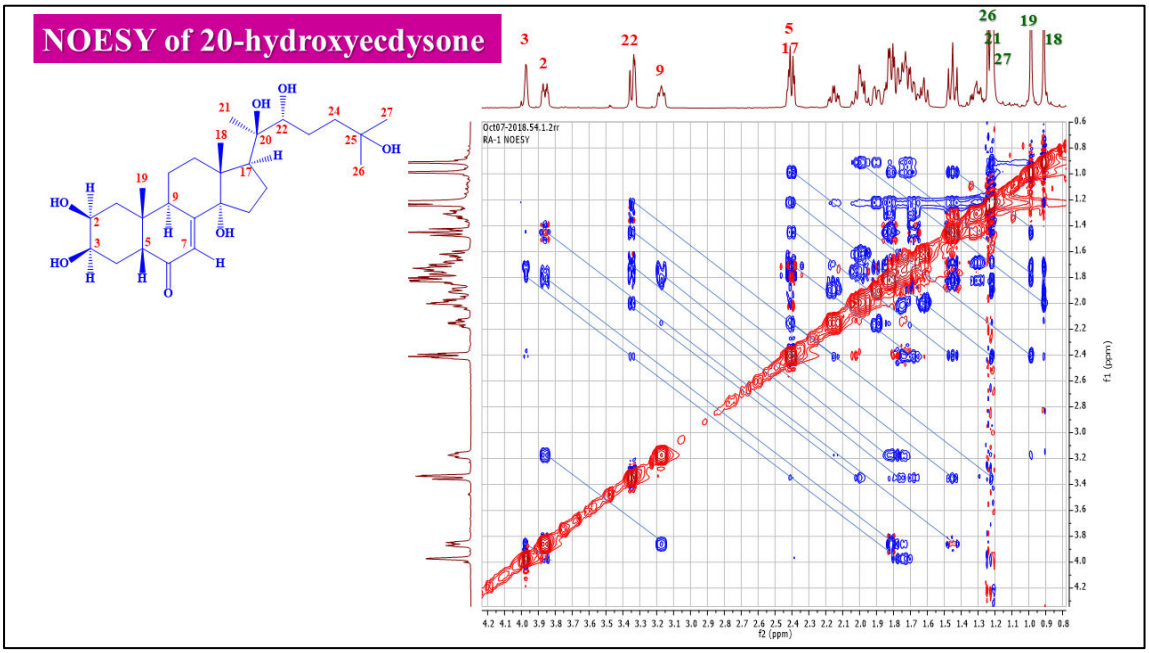

Spectrum 4.1.10. NOESY of RA-1 (20-hydroxyecdysone).

4.1.1. RA-1Ac = RA-21Ac (2,3,22-triacetyl-20-hydroxyecdysone)

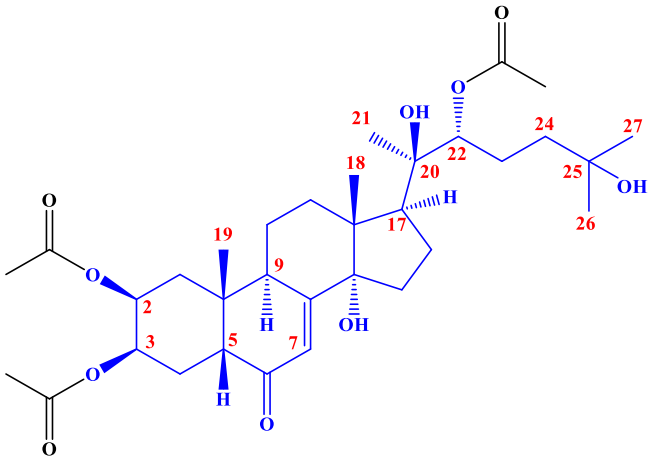

Chemical Formula: $C_{33}H_{50}O_{10}$
Exact Mass: 606,34
Molecular Weight: 606,75

RA-1Ac (2,3,22-triacetyl-20-hydroxyecdysone): $[\alpha]_D^{20}$ +48.9° (c 0.17, MeOH).

In order to prove the absolute stereochemistry of **RA-1**, the acetyl derivative was prepared. Mild acetylation of **RA-1** with Ac_2O in pyridine yielded a triacetyl-derivative,

2,3,22-triacetoxy-20-hydroxyecdysone (**RA-Ac1**). The IR spectrum of **RA-Ac1** (**Spectrum 4.1.2.1**) exhibited absorption bands for hydroxy and ester carbonyl and α,β-unsaturated ketone groups at 3442 cm^{-1}, 1722 cm^{-1} and 1656 cm^{-1}, respectively. The negative ion HR-MS of **RA-Ac1** gave a quasimolecular ion $[M-H]^-$ peak at m/z 605.3344 (**Spectrum 4.1.2.2**), The positive ion HR-mass spectrum exhibited pseudo-molecular ion peaks $[M+H]^+$ at m/z 607.3457 (**Spectrum 4.1.2.3**) and $[M+Na]^+$ at m/z 629.3285 (Spectrum 4.1.2.4). These results are in accordance with the calculated molecular weight of **RA-Ac1**, 606.3404 ($C_{33}H_{50}O_{10}$). The ^{1}H-NMR spectrum of **RA-Ac1** (**Spectrum 4.1.2.5**) exhibited three acetoxy methyl resonances at δ_H 2.12 s, 1.99 s and 2.01 s ppm. The downfield shifts of more than approximately 1.0 ppm for the geminal protons of the secondary hydroxy groups located at C-2, C-3 and C-22 showed the sites of acetylation (δ 5.06, H-2; 5.35, H-3 and 4.85, H-22). All protons and carbon atoms of **RA-Ac1** were assigned clearly (**Table 4.3**) with the help of 1D (^{1}H, ^{13}C-NMR and DEPT-135) (**Spectrum 4.1.2.6**) and 2D-NMR (COSY, HSQC, HMBC, NOESY and ROSY) (**Spectrum 4.1.2.7- 4.1.2.11**).

Table 4.3. The ^{1}H and ^{13}C-NMR Data for RA-1Ac (2, 3, 22-triacetyl-20-hydroxyecdysone).

C/H	DEPT	δ_C, ppm	δ_H ppm, *J* (Hz)	HMBC (from C to H)
1	CH_2	33.99	1.89† 1.54†	Me-19
2	CH	68.64	5.06 ddd (12.2/2.8/2.8)	H-3
3	CH	67.06	5.35 br s	
4	CH_2	29.18	1.82† 1.75†	
5	CH	50.94	2.38†	H-7, Me-19
6	C	202.2	-	
7	CH	121.57	5.81 br s	H-9
8	C	164.69	-	
9	CH	33.58	3.13 dd"t" (8.0)	
10	C	38.35	-	Me-19
11	CH_2	20.39	1.80† 1.65†	H-9, H-7

12	CH_2	31.07	2.15† 1.85†	Me-18
13	C	47.50	-	Me-18
14	C	84.43	-	H-7, Me-18
15	CH_2	31.46	2.03† 1.61†	
16	CH_2	20.47	1.86†	H-17
17	CH	49.52	2.38†	Me-18, Me-21
18	CH_3	17.45	0.85 s	H-17
19	CH_3	23.82	1.03 s	
20	C	77.02	-	H-22, Me-21
21	CH_3	21.19	1.27 s	H-22
22	CH	79.78	4.85 br d (9.6)	Me-21
23	CH_2	24.73	1.75† 1.50†	
24	CH_2	40.26	1.49† 1.40†	Me-26, Me-27
25	C	70.61	-	Me-26, Me-27
26	CH_3	28.56#	1.20 s	Me-27
27	CH_3	30.25#	1.23 s	Me-26

Additional acetoxy signals (***C***OCH_3): δ 175.57, 170.35 and 170.31; (CO***C*****H_3**): δ_C 21.14, 21.14, and 21.08; δ_H 2.12 s, 2.12 s, 1.99 s and 2.01 s.

†) *J* values are not clear due to overlapping. #) Interchangeable.

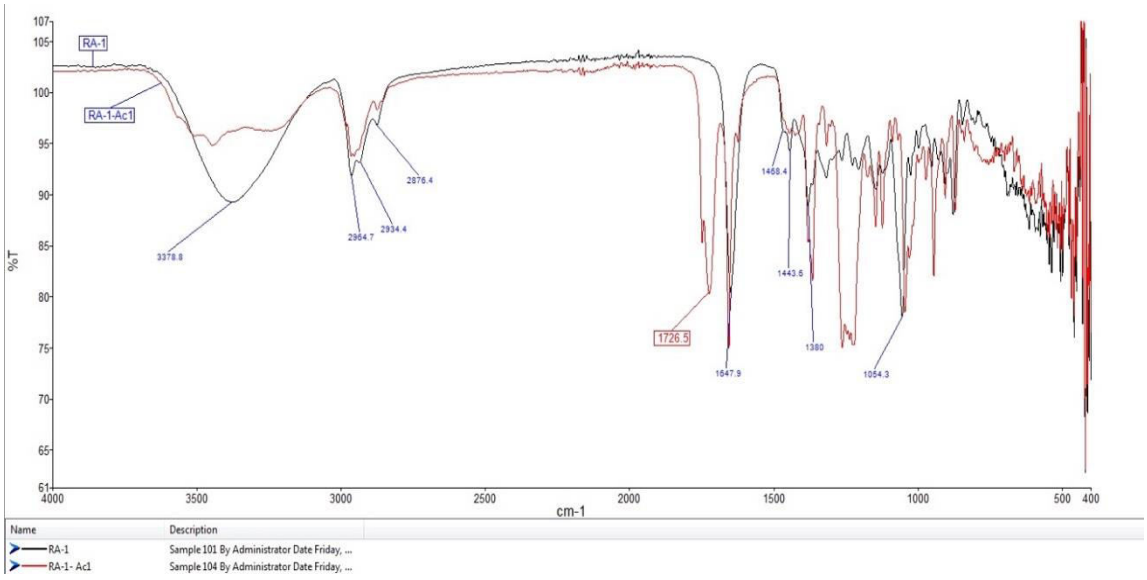

Spectrum 4.1.1.1. FT-IR of 2,3,22-triacetyl-20-hydroxyecdysone (RA-1Ac).

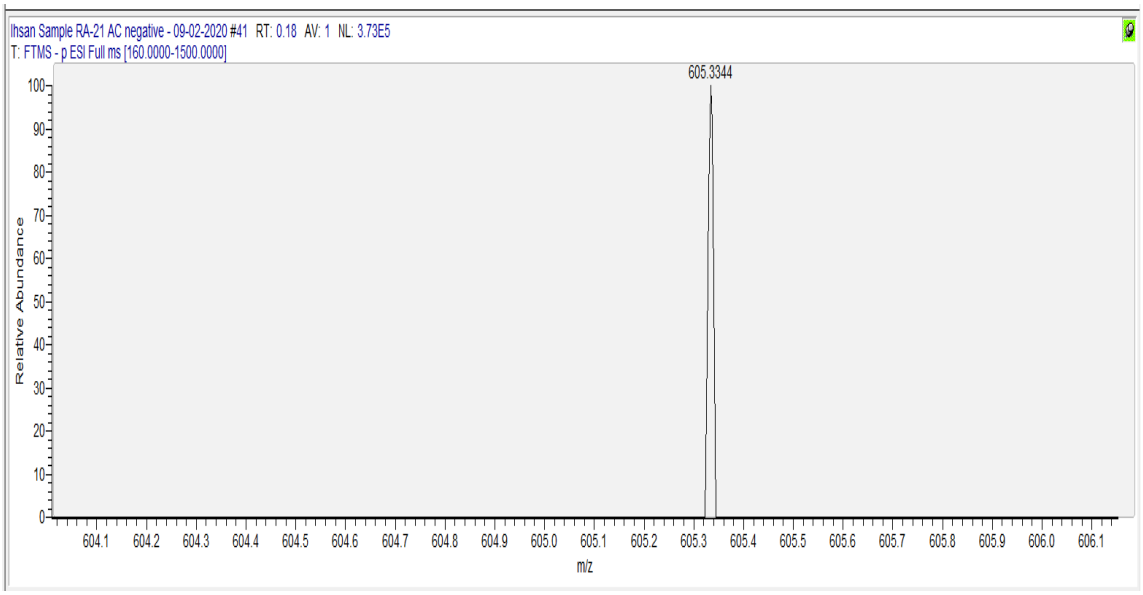

Spectrum 4.1.1.2. (-)-HRMS of 2,3,22-triacetyl-20-hydroxyecdysone (RA-1Ac) [M-H]- m/z 605.3344.

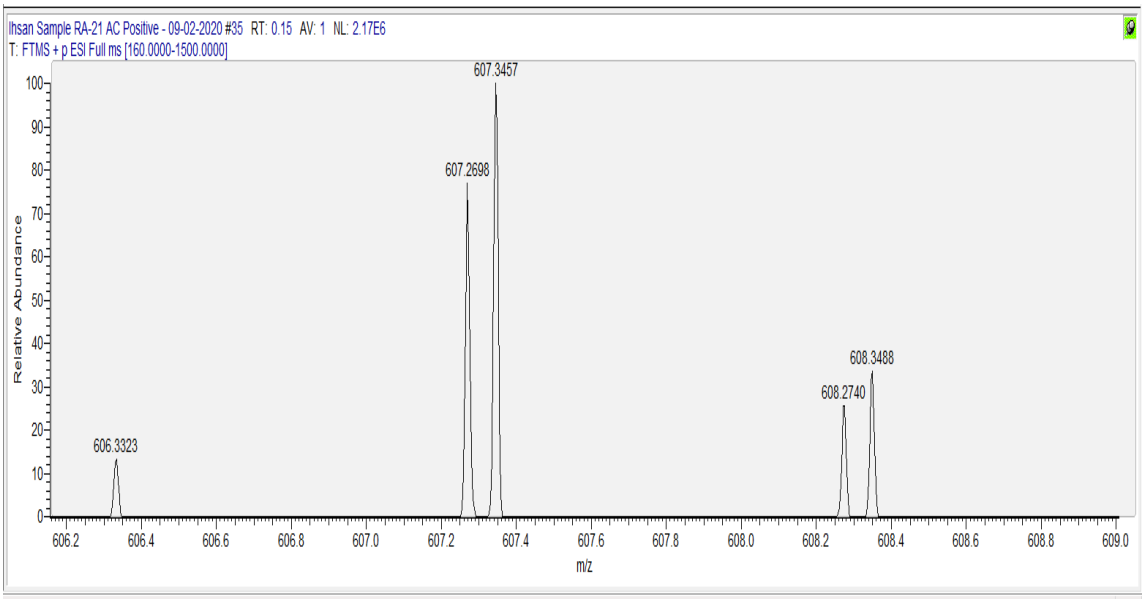

Spectrum 4.1.1.3. (+)-HRMS of 2,3,22-triacetyl-20-hydroxyecdysone (RA-1Ac)[M]+ m/z607.3457.

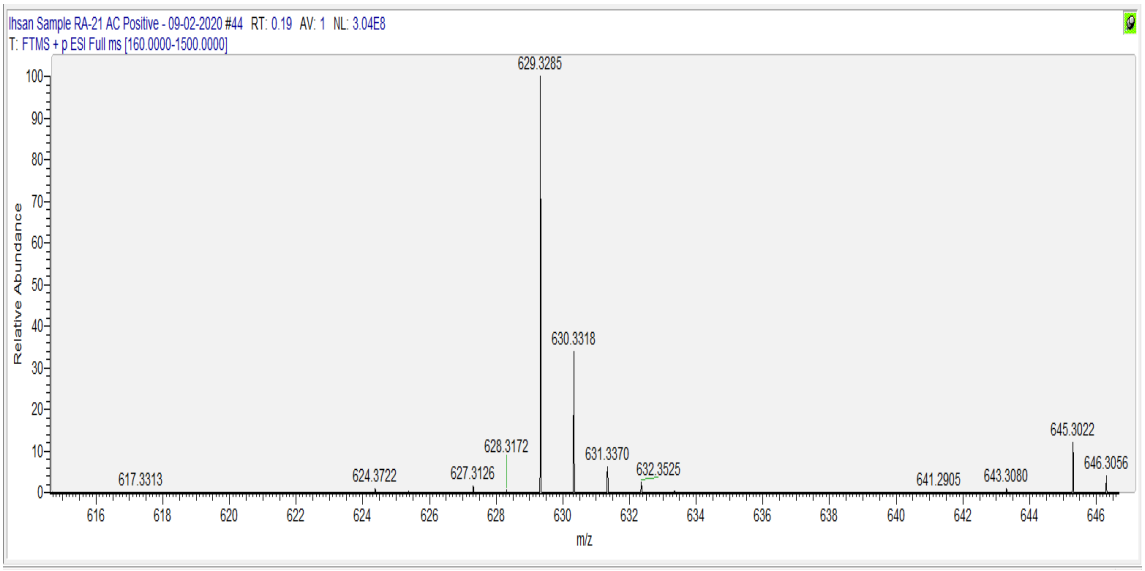

Spectrum 4.1.1.4. (+)-HRMS of 2,3,22-triacetyl-20-hydroxyecdysone (RA-1Ac) [M+Na]+ m/z 629.3285.

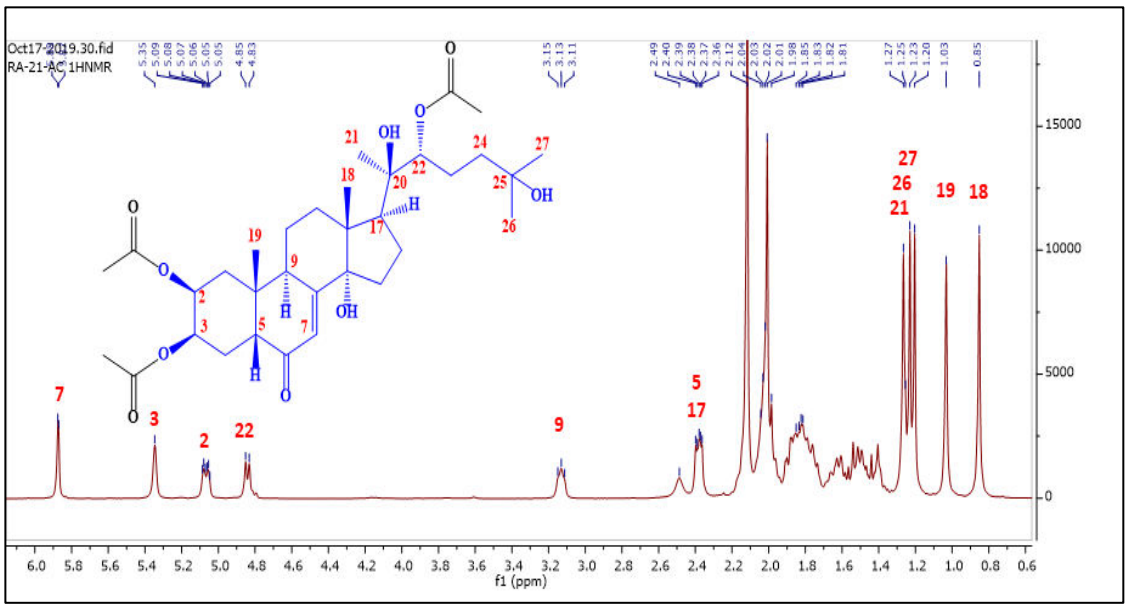

Spectrum 4.1.1.5. ^{1}H-NMR Spectrum of 2,3,22-triacetyl-20-hydroxyecdysone (RA-1Ac) (500 MHz, MeOD).

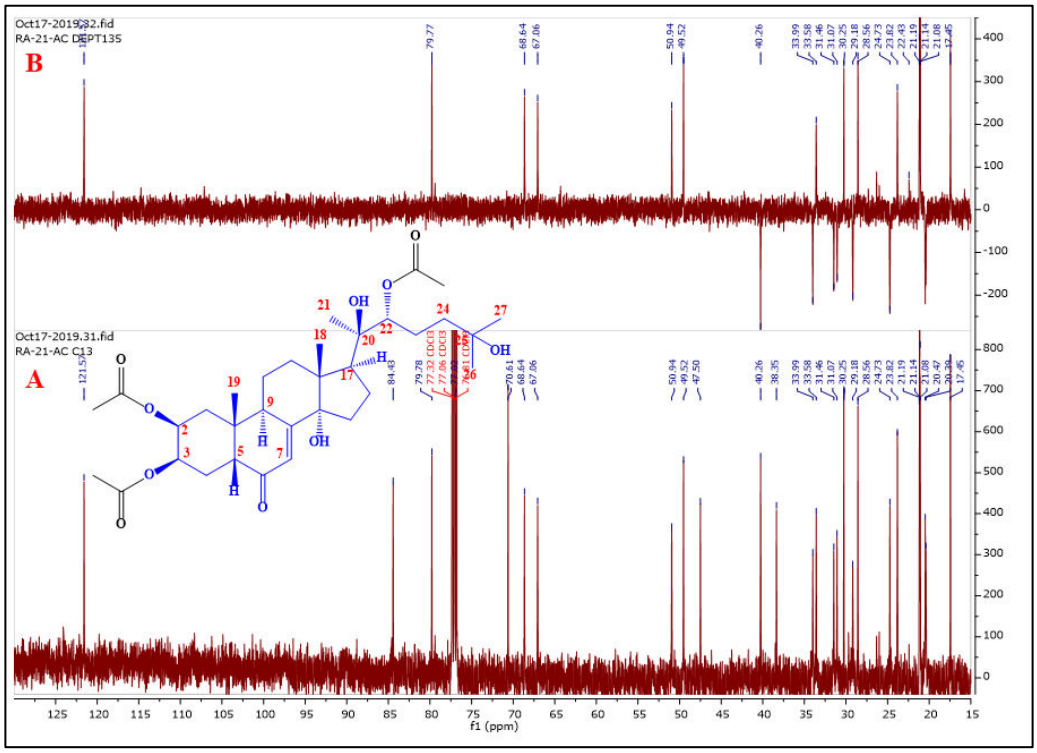

Spectrum 4.1.1.6. ^{13}C-NMR (A) (125 MHz, MeOD) and DEPT-135 (B) Spectra of 2,3,22-triacetyl-20-hydroxyecdysone (RA-1Ac).

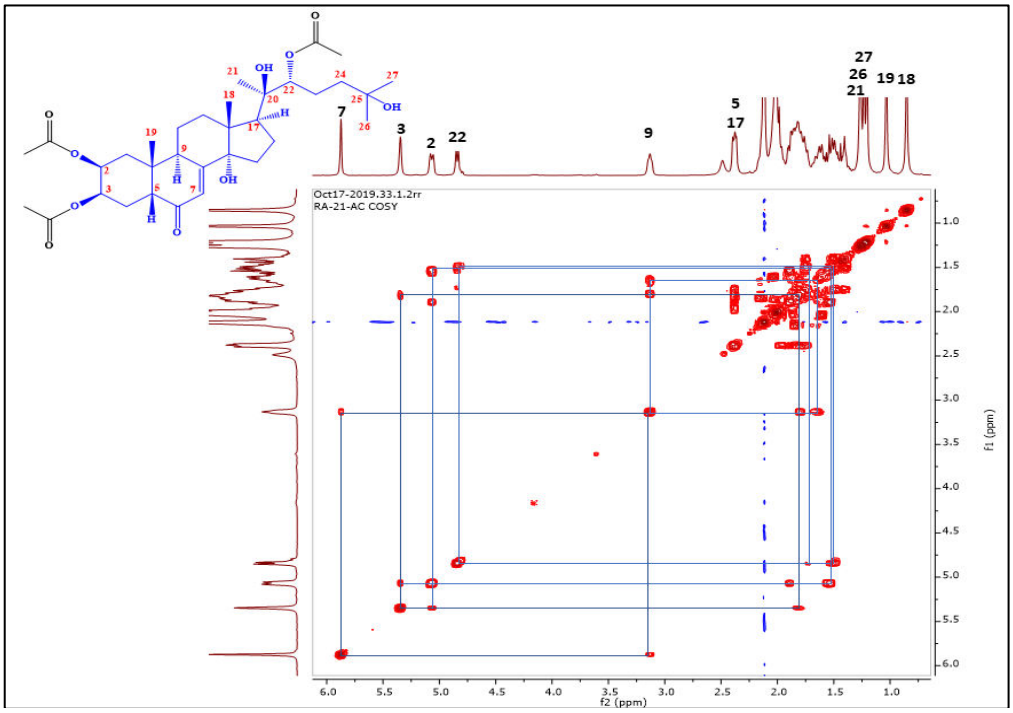

Spectrum 4.1.1.7. COSY of 2,3,22-triacetyl-20-hydroxyecdysone (RA-1Ac).

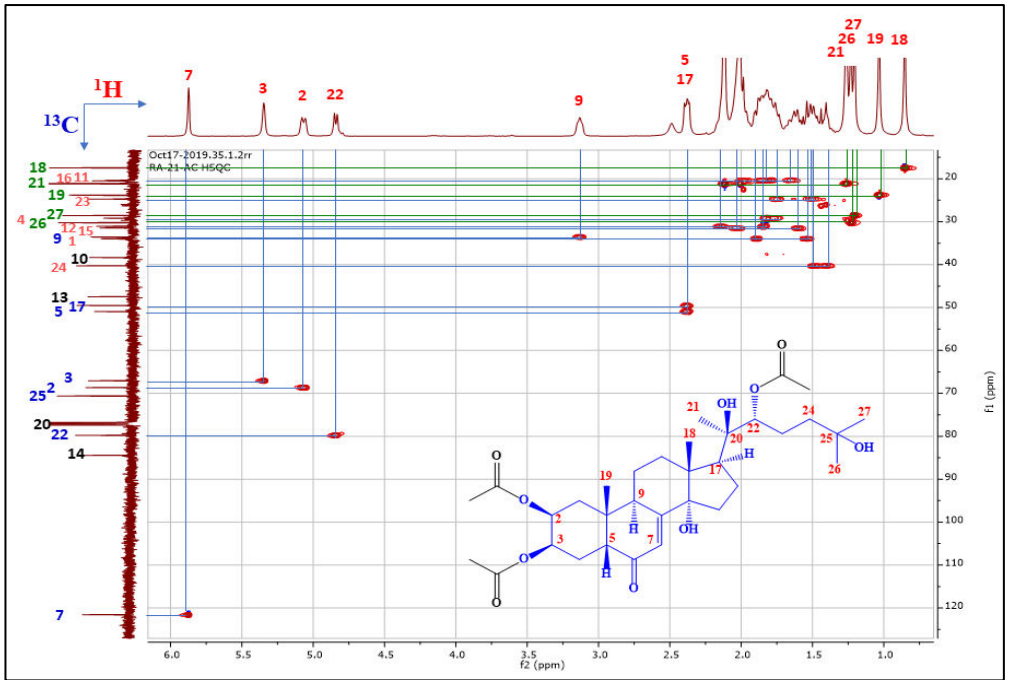

Spectrum 4.1.1.8.1. HSQC of 2,3,22-triacetyl-20-hydroxyecdysone (RA-1Ac) (^{1}H: 0.5 – 6.5 ppm; ^{13}C: 10 – 130 ppm).

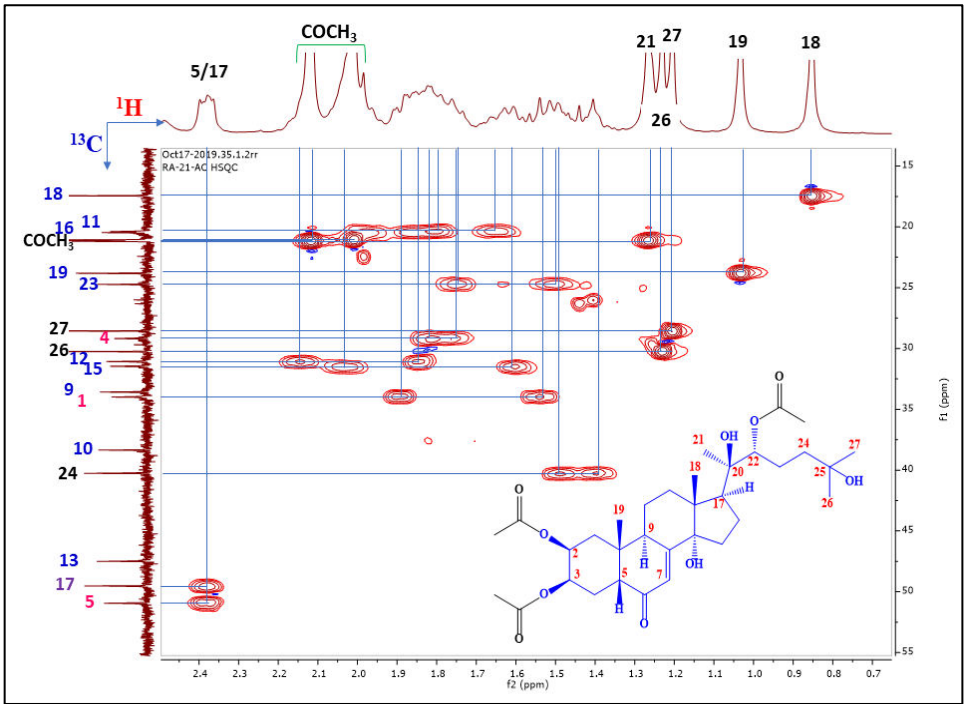

Spectrum 4.1.1.8.2. HSQC of 2,3,22-triacetyl-20-hydroxyecdysone (RA-1Ac) (^{1}H: 2.5 is – 0.7 ppm; ^{13}C: 15 – 55 ppm).

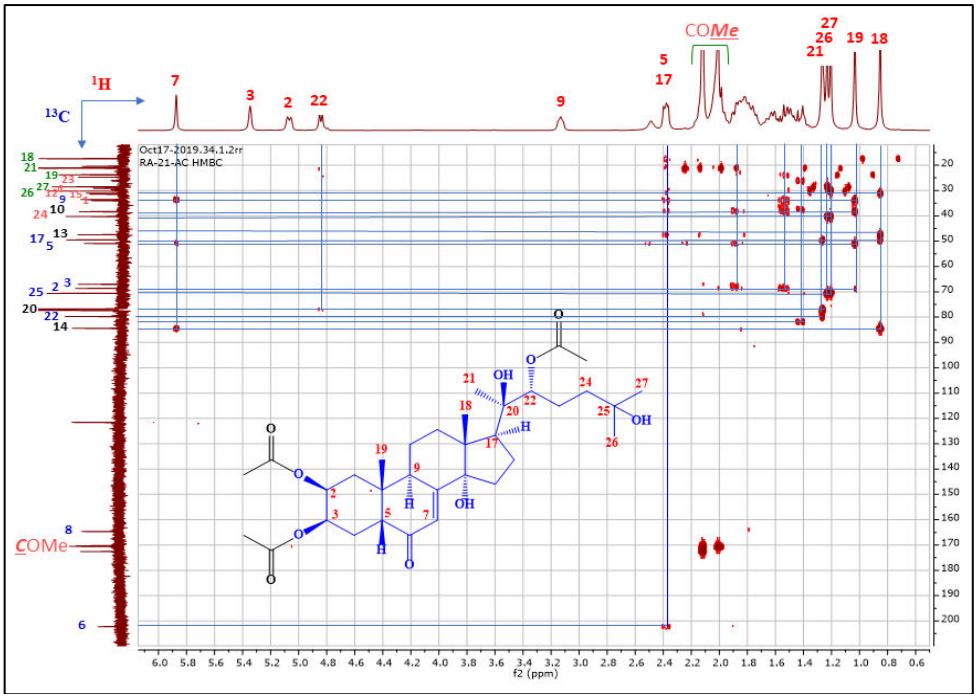

Spectrum 4.1.1.9.1. HMBC of 2,3,22-triacetyl-20-hydroxyecdysone (RA-1Ac) (^{1}H: 6.2 – 0.5 ppm; ^{13}C: 10 – 210 ppm).

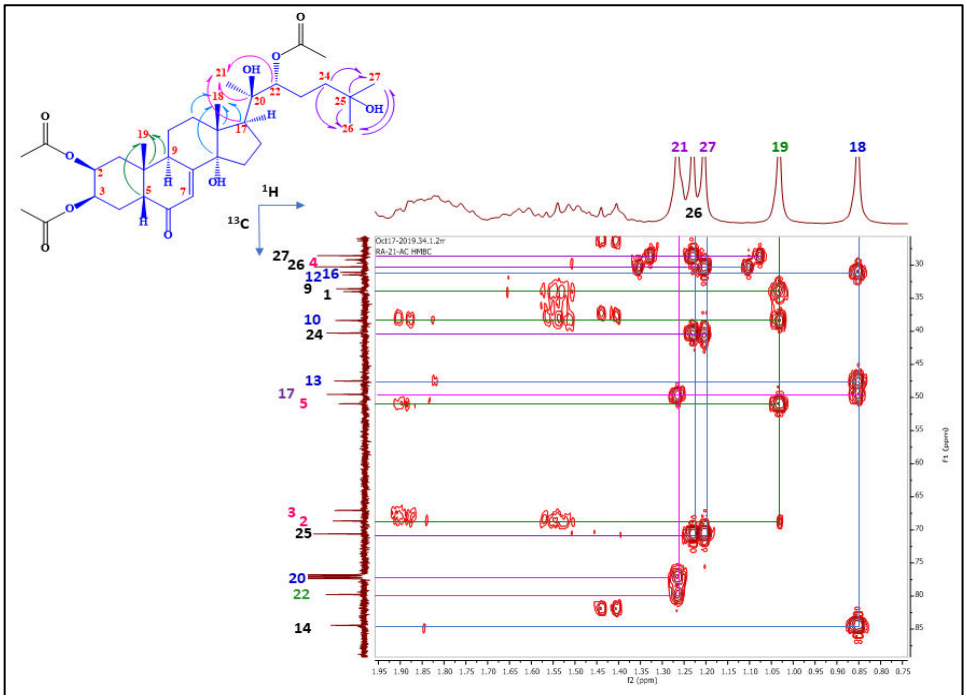

Spectrum 4.1.1.9.2. HMBC of 2,3,22-triacetyl-20-hydroxyecdysone (RA-1Ac) (^{1}H: 2.0 – 0.7 ppm; ^{13}C: 20 – 90 ppm).

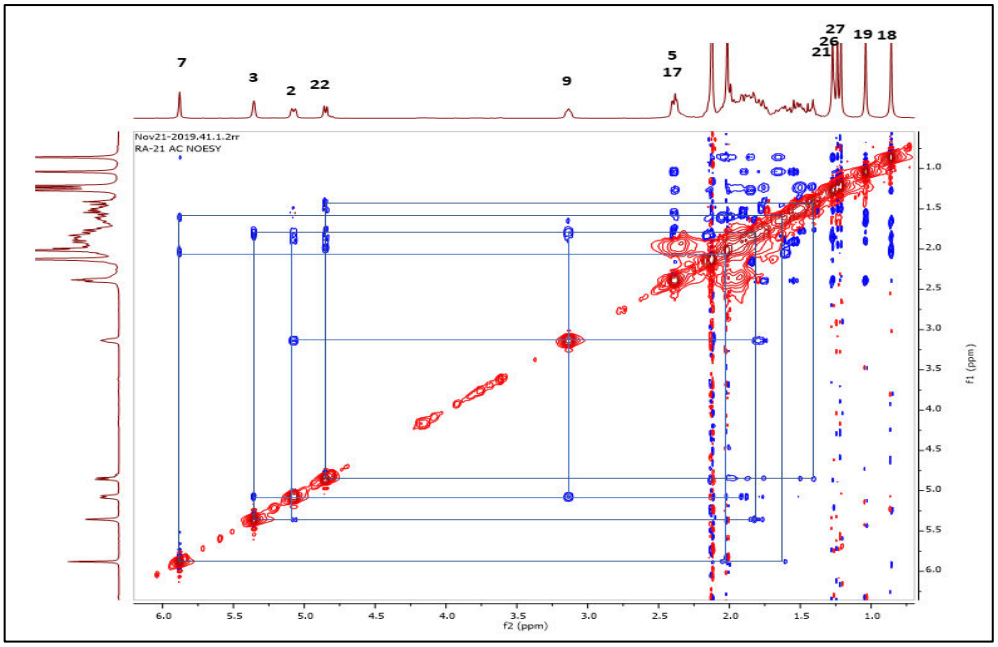

Spectrum 4.1.1. 10. NOESY of 2,3,22-triacetyl-20-hydroxyecdysone (RA-1Ac).

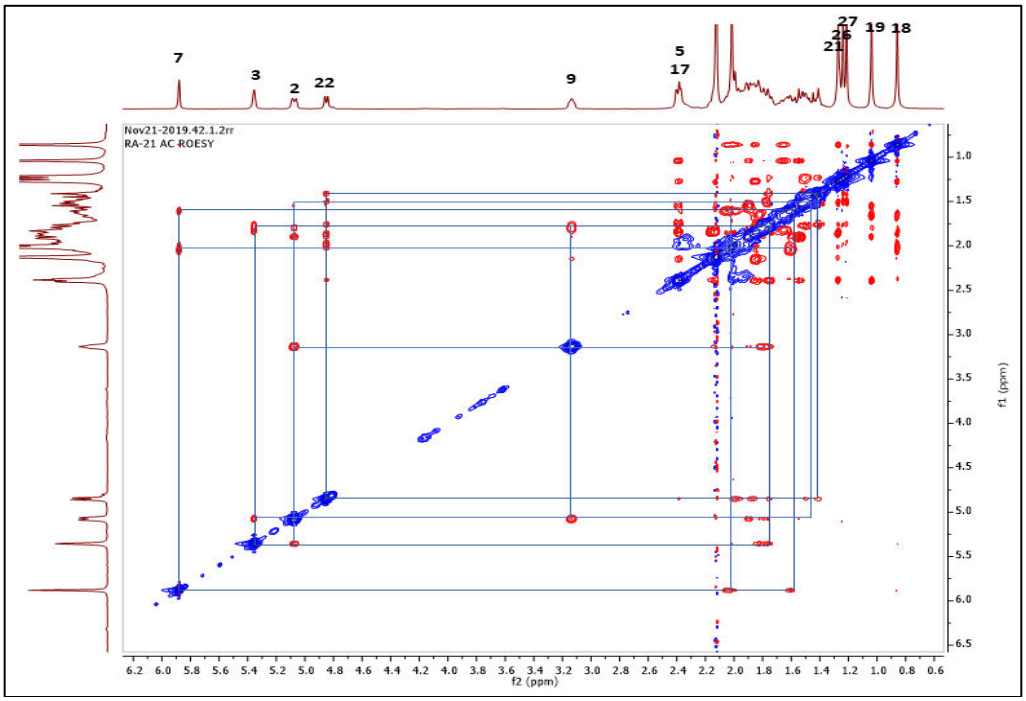

Spectrum 4.1.1.11.1. ROESY of 2,3,22-triacetyl-20-hydroxyecdysone (RA-1Ac).

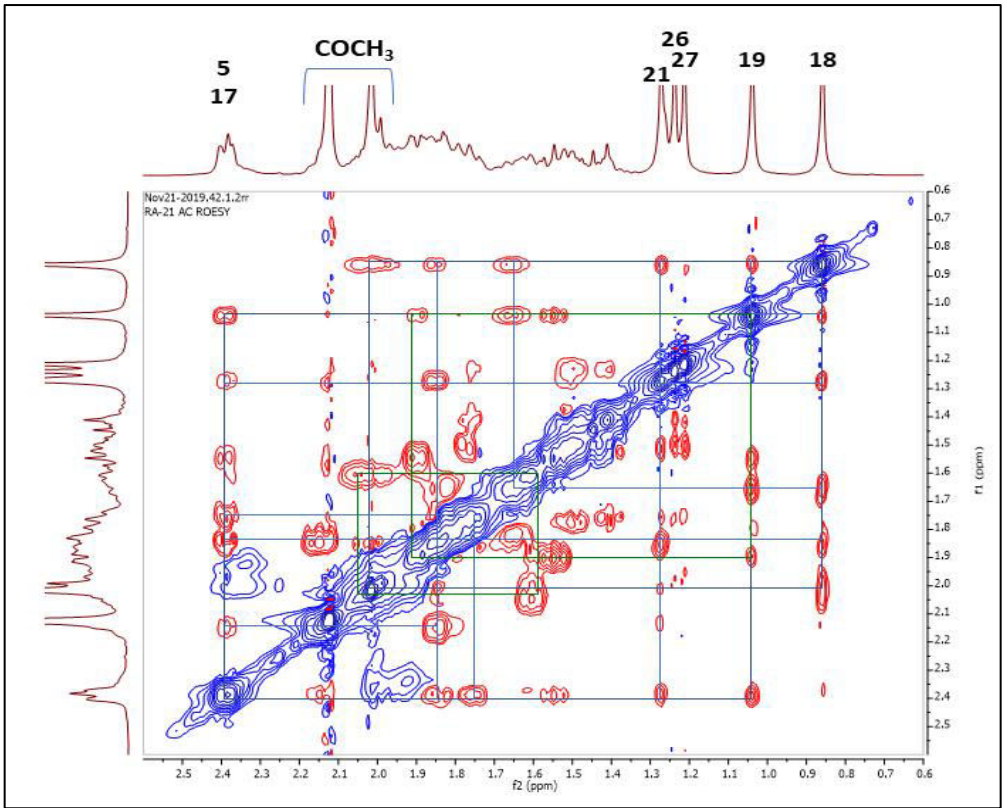

Spectrum 4.1.1.11. 2. ROESY of 2,3,22-triacetyl-20-hydroxyecdysone (RA-1Ac) (3.0 – 2.5 ppm).

In the molecular structure of **RA-1Ac**, cyclohexane ring A has a chair conformation with the acetyl substituents at C-2 and C-3 in *cis*-disposed equatorial and axial positions, respectively. The ring junction with ring B is *cis* with the methyl substituent in an axial position. Ring B has a distorted half-chair conformation. The cyclohexane ring C also has a chair conformation with the methyl and hydroxy substituents in axial positions and the ring junction with ring D is *cis*. Ring D has a distorted half-chair conformation twisted on the C-13–C-14 bond, but slightly distorted towards an envelope conformation. The methyl and hydroxy substituents are in *trans*-disposed axial positions; the side-chain substituent is in an equatorial position. Overall, the rings B, C and D form an approximately planar central section of the molecule, with the alkyl sidechain and ring A and its acetyl substituents pendant at each end to one side of this plane.

The structure and absolute configuration of **RA-1Ac** was finally confirmed by an X-ray crystal-structure determination (**Figure 4.3**). Compound **RA-1Ac** was crystalized from MeOH to give colourless needle-shaped crystals of **RA-1Ac**·2.5H_2O. The asymmetric unit contains one molecule of the steroid and two and a half molecules of water, with the latter water molecule situated close to a two-fold axis, so it is necessarily disordered about that axis with site occupation of 0.5. The acetyl group at C-2 is disordered unequally over two conformations. Refinement of the absolute structure parameter (Parsons et al., 2013) yielded a value of 0.07(6), which confidently confirms that the refined model represents the true enantiomorph with the 2*S*,3*R*,5*R*,9*R*,10*R*,13*R*,14*S*,17*S*,20*R*,22*R*-configuration.

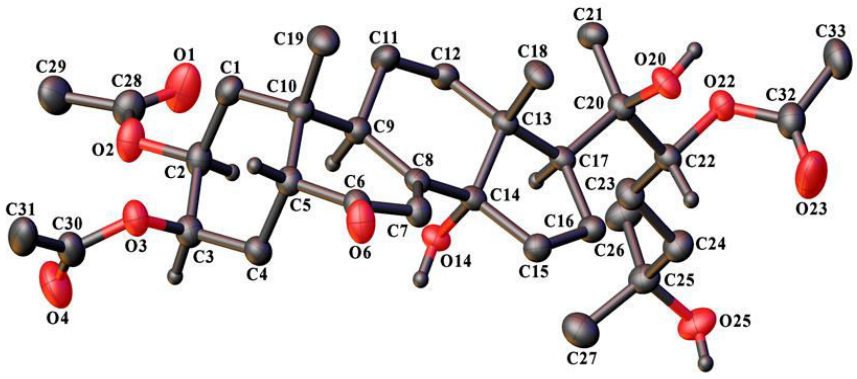

Figure 4.3. Displacement ellipsoid plot of the molecular structure of RA-1Ac (50% probability ellipsoids; only the major disorder conformation of the acetyl substituent at C-2 is shown).

Intermolecular O–H···O hydrogen bonds link the steroid and water molecules into a three-dimensional supramolecular framework (**Figure 4.4**). The hydroxy substituent at C-20 interacts with the keto O-atom in a neighbouring steroid molecule. This interaction links the steroid molecules into extended chains which run parallel to the [0 1 0] direction and have a graph set motif (Bernstein, Davis, Shimoni, & Chang, 1995) of C (10). The other hydroxy groups interact with the O-atoms of water molecules. The two full-occupancy water molecules each accept one hydrogen bond from a steroid molecule and donate two hydrogen bonds to two different steroid molecules. The half-occupancy water molecule, O-8, only donates a single hydrogen

bond to a steroid molecule. It does not interact with its counterpart across the two-fold axis because the sites are too close to one another to be occupied simultaneously. These findings are in accordance with those of 20-hydroxyecdysone (Fábián *et al*., 2002; Rele *et al*., 2003).

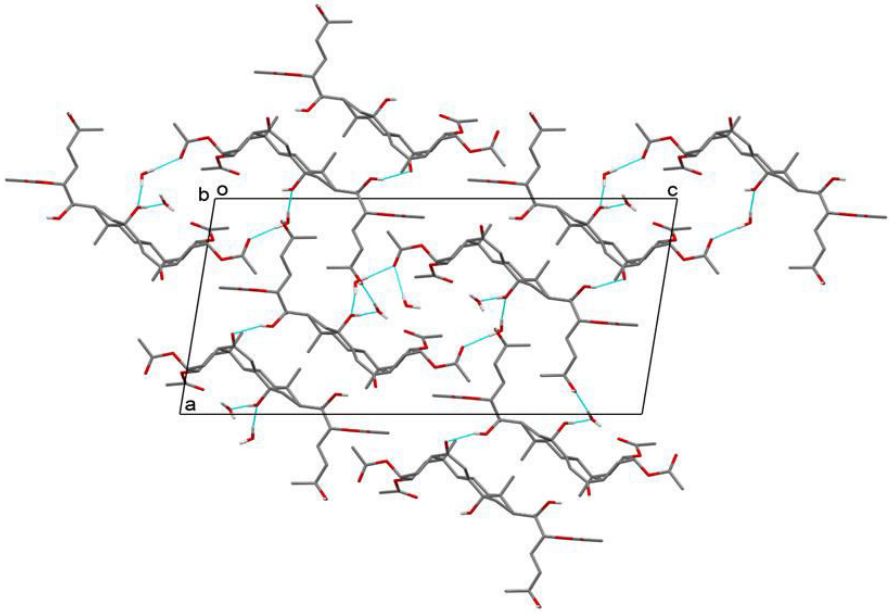

Figure 4.4. The packing of RA-1Ac·2.5H_2O viewed down the *b*-axis and showing the hydrogen-bonding network (uninvolved H-atoms have been omitted for clarity).

4.2. RA-5 (11α,20-dihydroxyecdysone)

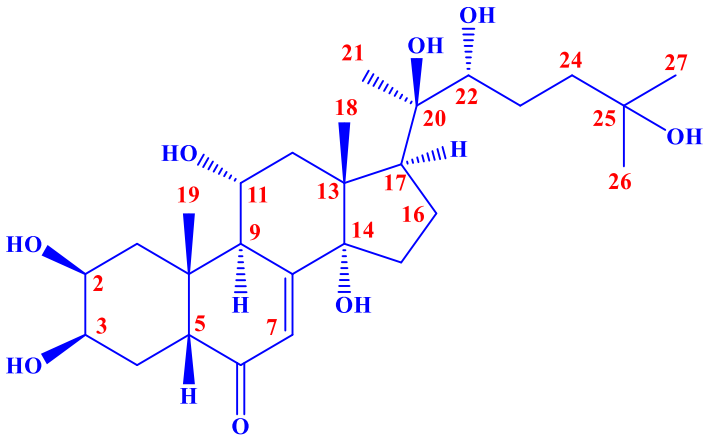

Chemical Formula: $C_{27}H_{44}O_8$
Exact Mass: 496,30
Molecular Weight: 496,64

RA-5 (Turkesterone): $[\alpha]_D^{20}$ +18.7° (c 0.107, MeOH).

RA-5 was obtained as an amorphous compound and its molecular formula was deduced as $C_{27}H_{44}O_8$ by a positive ion HRMS peak (**Spectrum 4.2.1**) at m/z 519.2926 $[M+Na]^+$ and as well as a negative ion HRMS peak (**Spectrum 4.2.2**) at m/z 495.2956 $[M-H]^-$. The difference in molecular weight between the compounds **RA-1** and **RA-5** is 16 Daltons, which indicated the presence of an additional oxygen atom in **RA-5**. The IR spectrum of **RA-5** (**Spectrum 4.2.3**) exhibited absorption bands at 3368 cm^{-1} and 1653 cm^{-1} for hydroxy and α,β-unsaturated ketone functional groups, respectively. The UV spectrum showed an absorption maximum at 230 nm, which indicated the presence of a α,β-unsaturated carbonyl system, as found for **RA-1**.

The ^{13}C-NMR and DEPT-135 of **RA-5** (**Spectrum 4.2.6**) indicated the presence of five methyl, seven methylene, eight methine (four oxygenated and one olefinic), and seven quaternary (three oxygenated, one olefinic, and one carbonyl) carbon atoms. The ^{1}H-NMR of **RA-5** (Spectrum 4.2.4; Table 4.4) displayed five tertiary methyl groups at δ 0.87 (Me-18), 1.06 (Me-19), 1.19 (Me-26), 1.21 (Me-27) and 1.22 ppm (Me-21) and an olefinic proton at δ 5.81 (d, J = 2.2 Hz), which showed allylic COSY correlation with a methine proton at δ 3.16 (dd, J = 9.0 and 2.5 Hz) and was assigned as H-9. This proton

(H-9) was in the same spin system as an oxymethine at δ 4.11 (ddd, J = 12.0, 9.0 and 6.6 Hz, H-11) and methylene protons at δ 2.22 (dd "t", J =12.0 Hz, H-12_{eq}) and 2.17 (dd, J = 12.0 and 6.6, H-12_{ax}) (Spectrum 4.2.7). This is the major difference between the spectra of compounds **RA-1** and **RA-5**, and the most noticeable change of the spectrum of **RA-5** is the shift in the H-11 signal from (δ 1.8, 1.65) to (δ 4.11), where the latter consists of an additional hydroxy functionality at C-11 of the molecular fragment C of **RA-1**. The chemical shifts were assigned unambiguously from the HSQC and HMBC. NOESY correlations in **RA-5** between H-11 and Me-18 (δ 0.87) and Me-19 (δ 1.06) revealed the equatorial position of the hydroxy functionality at C-11. The absence of NOESY correlations between H-9 and H-11 confirmed that these protons are on the opposite sides of the molecule (Spectrum 4.2.10 and 4.2.11). These observations indicated that the structure of **RA-5** is turkesteronen, which has been reported as being in several *Ajuga*(Guibout, Mamadalieva, Balducci, Girault, & Lafont, 2015; Sena Filho et al., 2008; Usmanov, Gorovits, & Abubakirov, 1973, 1975), *Rhaponticum* (syn. *Leuzea* spec.) (Buděšínský et al, 2008) *Silene* (Mamadalieva *et al*., 2002), and *Vitex* (Sena Filho et al., 2008; Suksamrarn et al., 2002) species. It has also been found in the mushroom *Tapinella panuoides* (Vokáč *et al*.,1998). The synthesis and biological activities of turkesterone 11α-acyl derivatives have been reported by (Dinan *et al*., 2003).

Table 4.4. The ^{1}H and ^{13}C-NMR Data for RA-5 (11α,20-dihydroxyecdysone).

C/H	DEPT	δ_C, ppm	δ_H ppm, *J* (Hz)	HMBC (from C to H)
1	CH_2	39.0	2.58 dd (12.7/5.0) H-1eq 1.38 dd (12.7/12.7) H-1ax	Me-19
2	CH	68.9	4.02 ddd (12.0/7.0/3.4)	H-3
3	CH	68.5	3.96 br s	H-5
4	CH_2	33.2	1.78† 1.70†	H-5
5	CH	52.7	2.34 dd (13.2/2.9)	H-7, Me-19
6	C	206.5	-	H-1eq, H-5
7	CH	122.7	5.81 d (2.2)	H-5, H-9
8	C	165.7	-	H-9

9	CH	42.9	3.16 dd (9.0/2.5)	H-5, H-7, Me-19
10	C	39.9	-	H-5, H-9, Me-19
11	CH	69.5	4.11 ddd (15.8/10.2/6.6)	H-9, H-7, Me-18
12	CH_2	43.7	2.22dd “t” (12.0/12.0) 2.17 dd (12.0, 6.3)	Me-19
13	C	48.5	-	Me-18
14	C	84.8	-	H-7, H_2-12, Me-18
15	CH_2	31.8	1.97 m 1.60 m	H-17
16	CH_2	21.5	1.99† 1.75†	
17	CH	50.3	2.43 dd “t” (8.3)	Me-18, Me-21
18	CH_3	18.9	0.87 s	H_2-12
19	CH_3	24.6	1.06 s	H-5, H-9
20	C	77.8	-	Me-21, H-22
21	CH_3	21.0	1.22 s	H-22
22	CH	78.4	3.33 br d (10.5)	Me-21,
23	CH_2	27.3	1.67 m 1.30 m	
24	CH_2	42.3	1.81 m 1.44 m	H-22, Me-26, Me-27
25	C	71.3	-	Me-26, Me-27
26	CH_3	29.0	1.19 s	Me-27
27	CH_3	29.7	1.21 s	Me-26

†) *J* values are not clear due to overlapping.

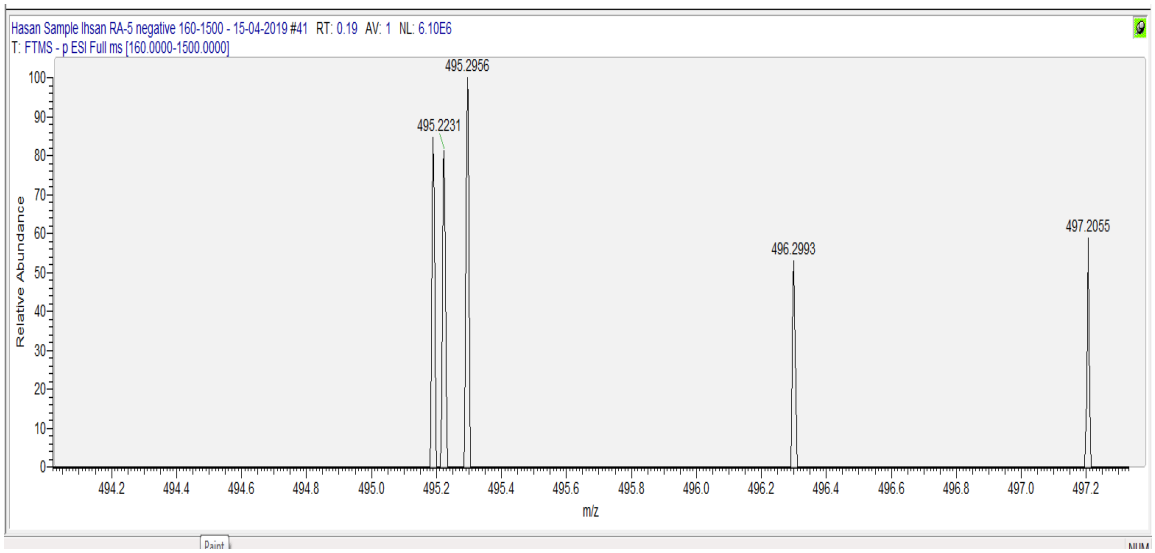

Spectrum 4.2.1. (+)-HRMS of Turkesterone (RA-5) [M]+ m/z 497.3104; [M+Na]+ m/z 519.2926.

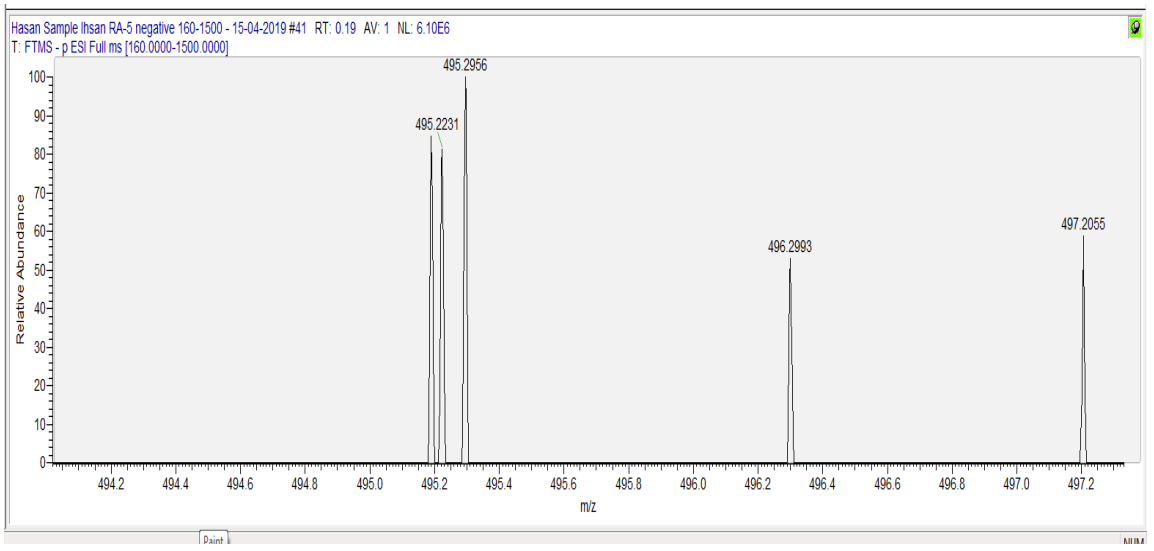

Spectrum 4.2.2. (-)-HRMS of Turkesterone (RA-5) [M-H]- m/z 495.2956.

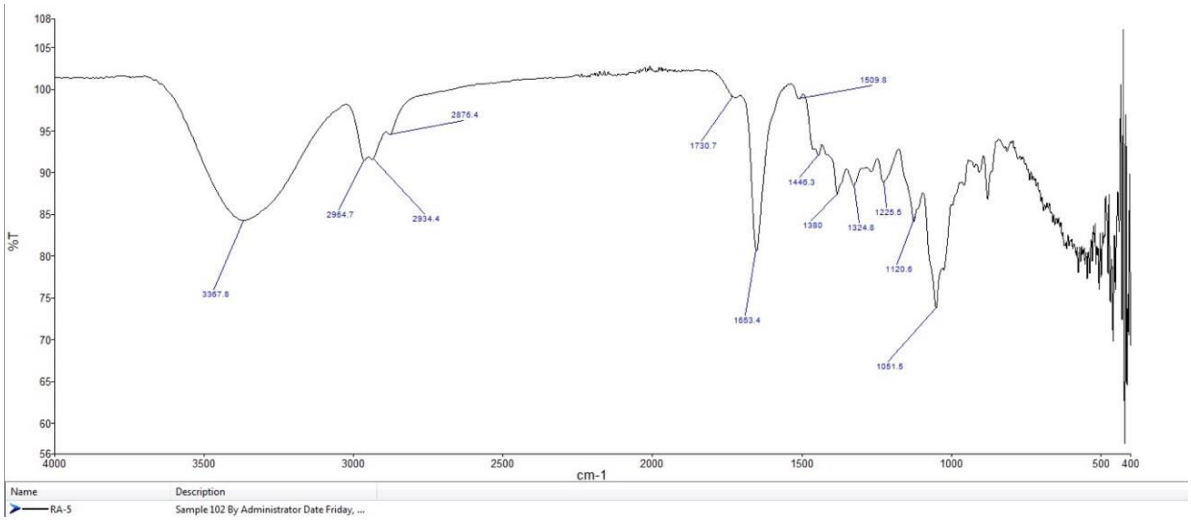

Spectrum 4.2.3. FT-IR of Turkesterone (RA-5).

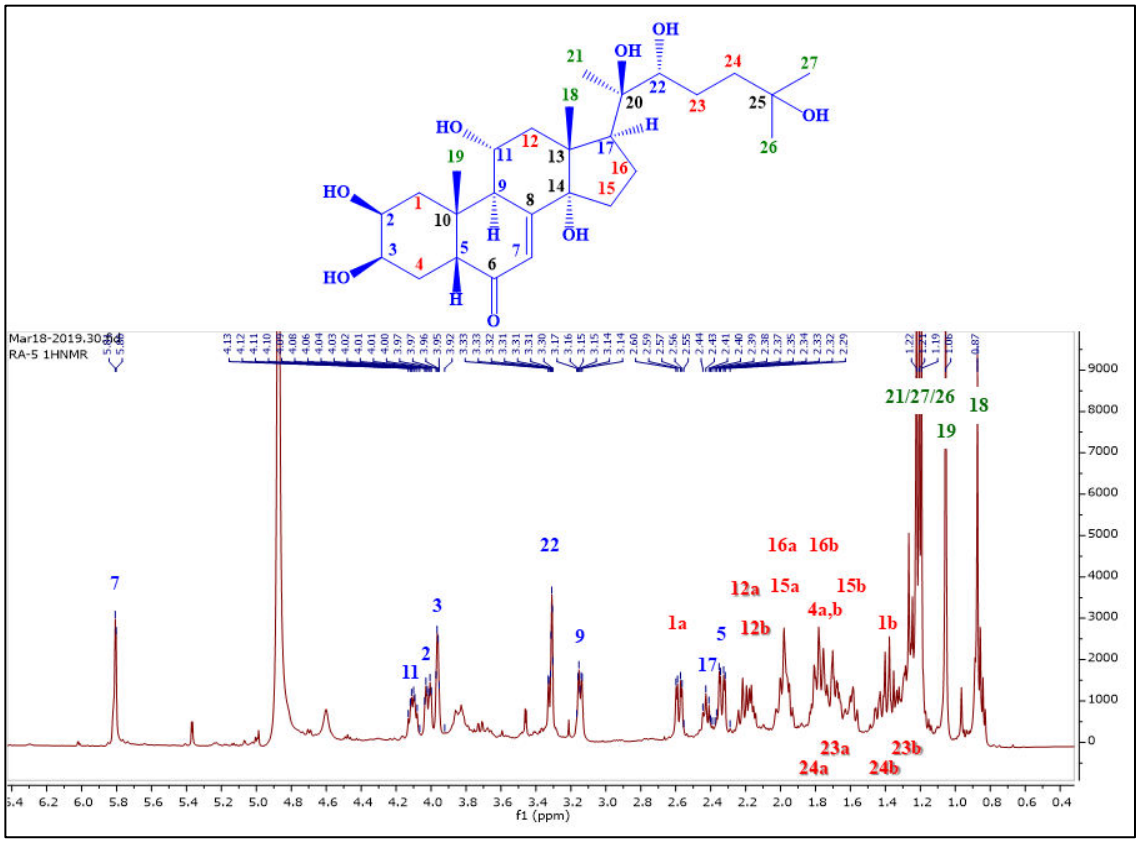

Spectrum 4.2.4. ^{1}H-NMR of RA-5 (Turkesterone) (500 MHz, MeOD).

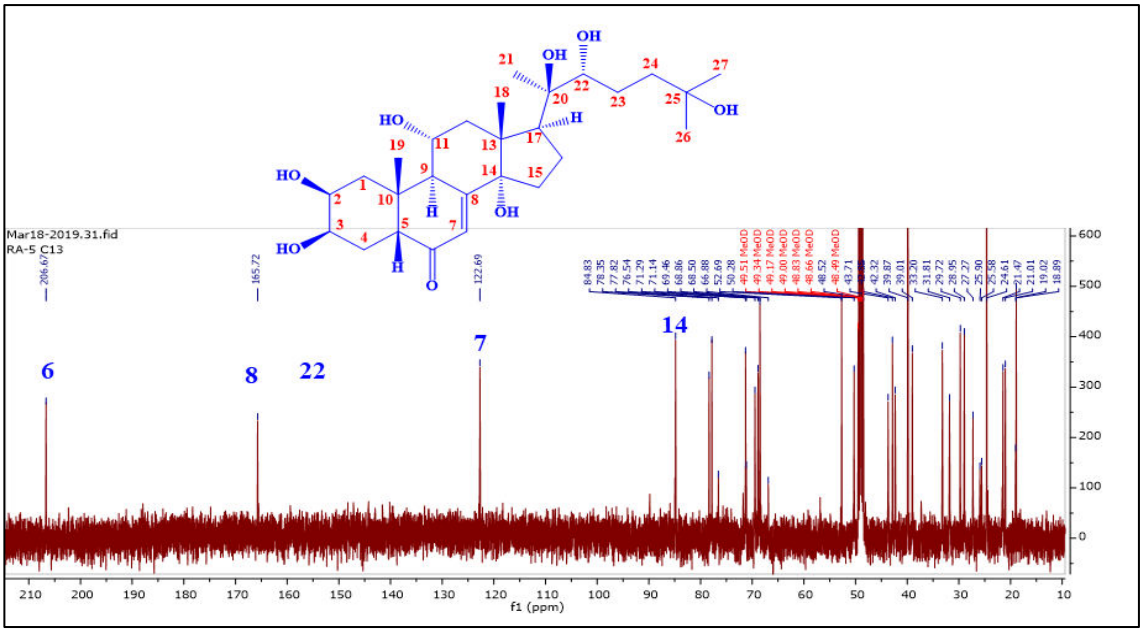

Spectrum 4.2.5. ^{13}C-NMR of RA-5 (Turkesterone) (125 MHz, MeOD).

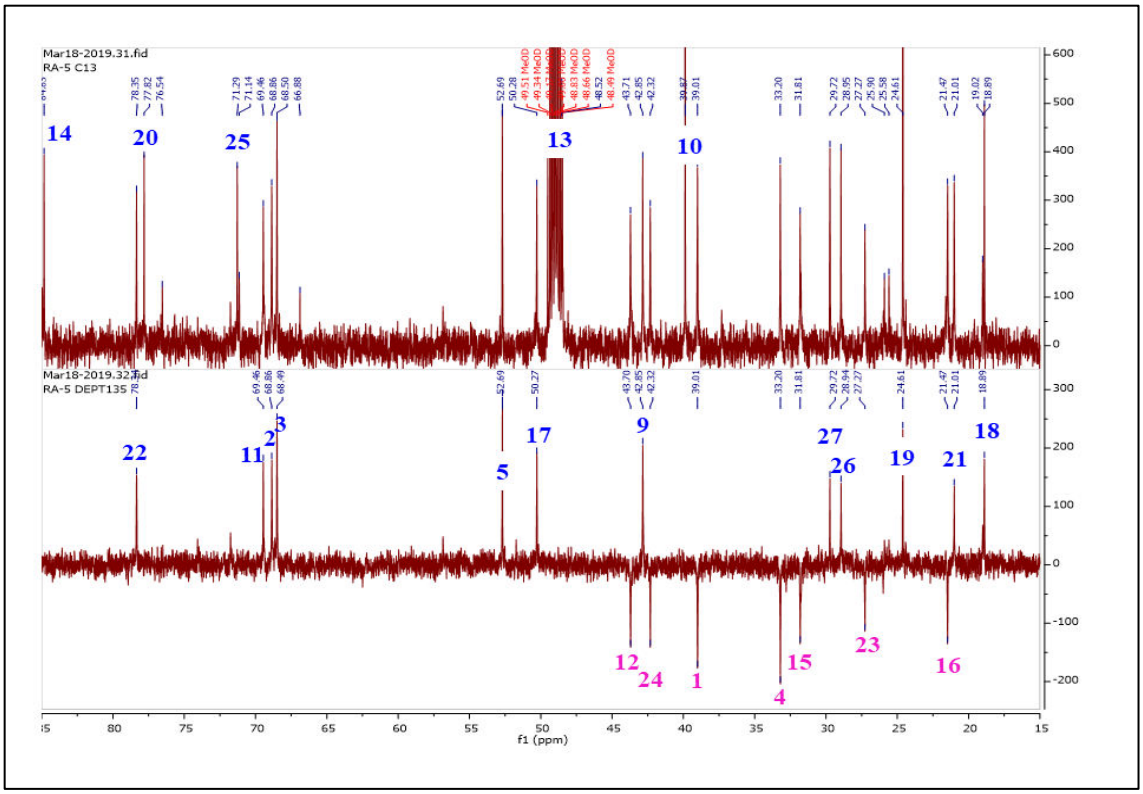

Spectrum 4.2.6. ^{13}C-NMR and DEPT-135 of RA-5 (Turkesterone) (125 MHz, MeOD)

.

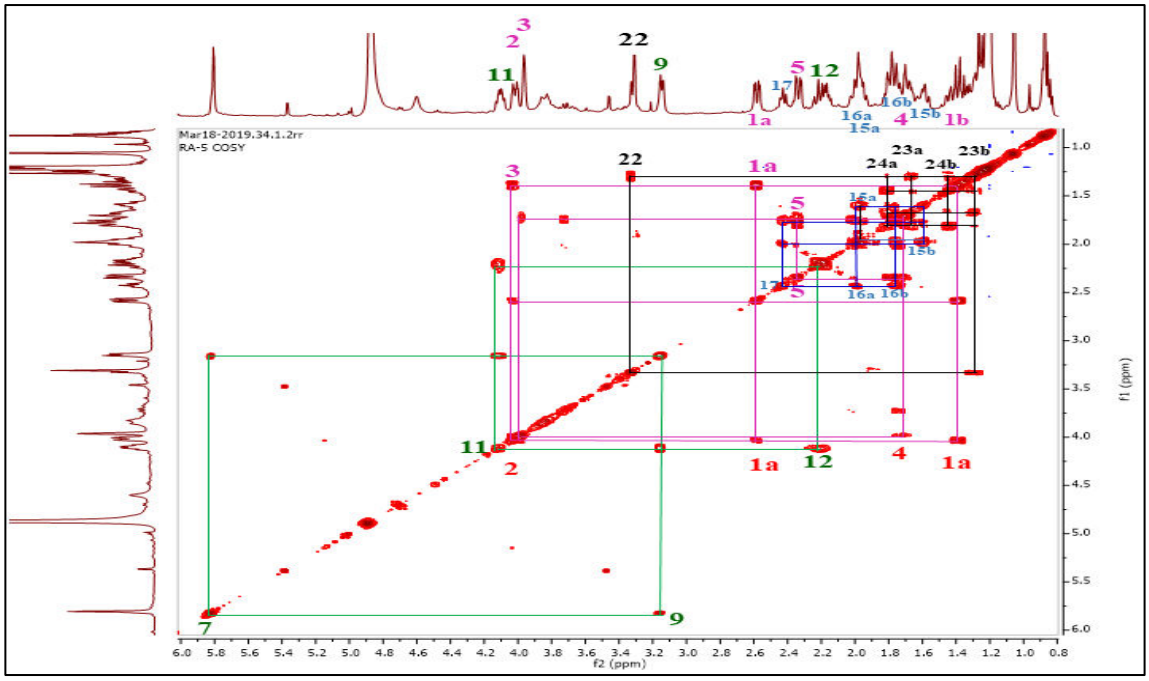

Spectrum 4.2.7. ^{1}H,^{1}H-Homonuclear Correlated Spectrum (COSY) of RA-5 (Turkesterone).

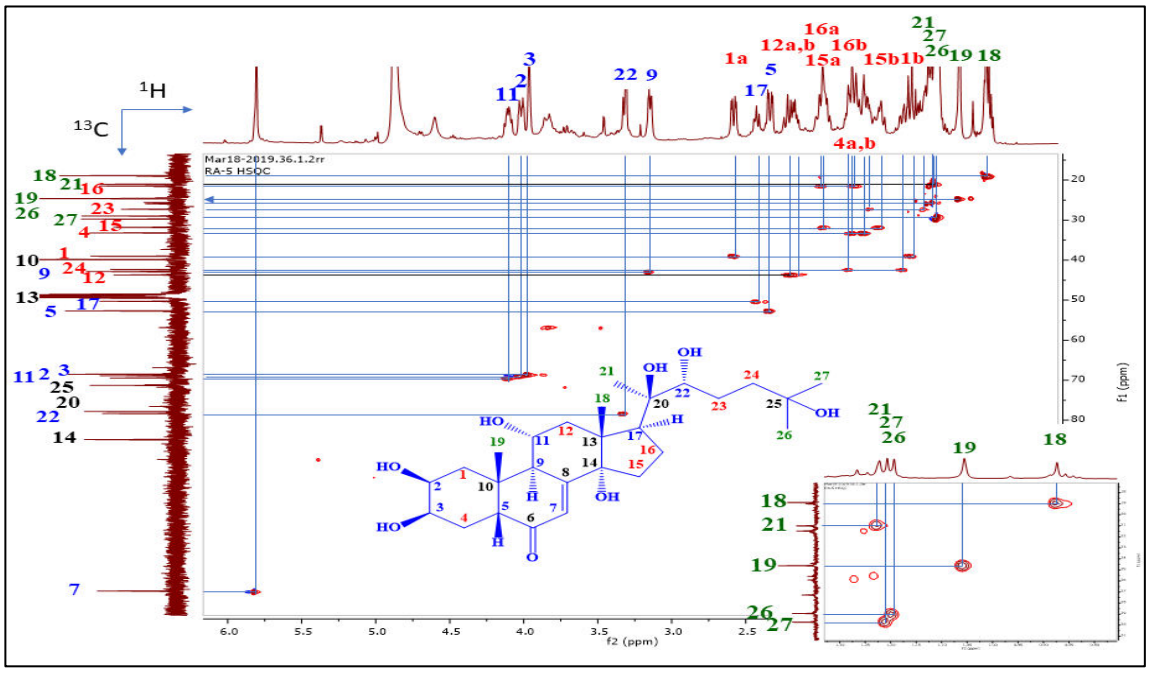

Spectrum 4.2.8. ^{1}H,^{13}C-Heteronuclear Correlated (HSQC) of RA-5 (Turkesterone) (1H: 6.2 – 0.5 ppm; ^{13}C: 10 – 130 ppm).

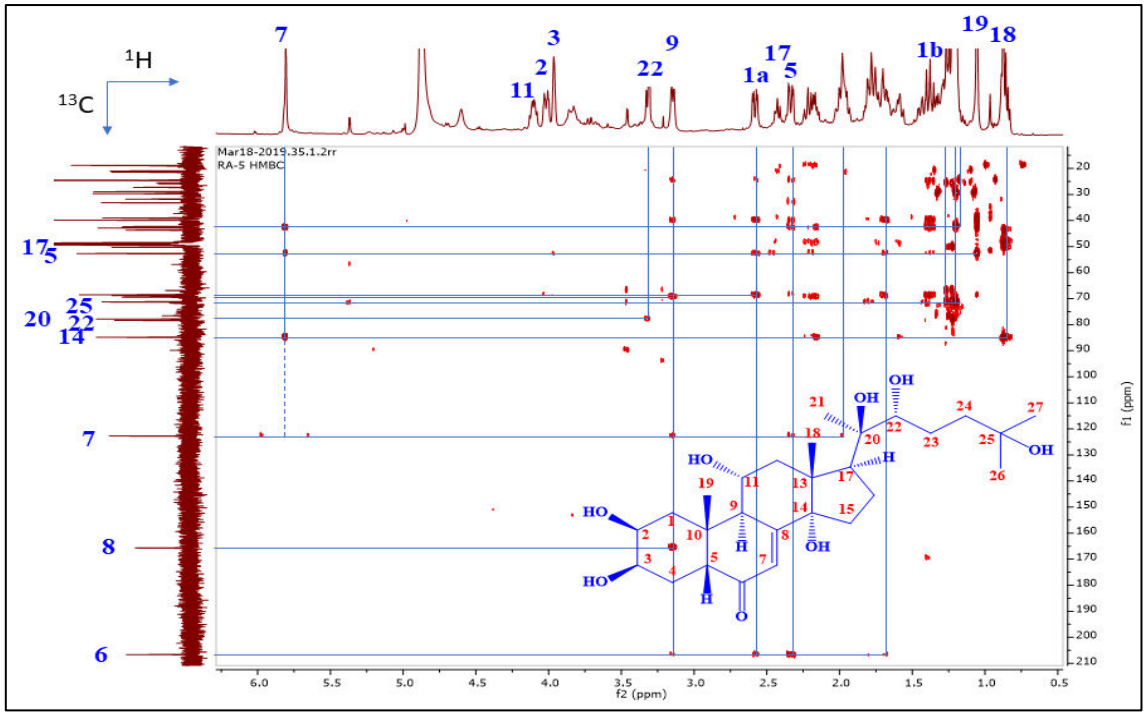

Spectrum 4.2.9. 1. HMBC (^{1}H,^{13}C-Heteronuclear Long-Range Correlated Spectrum) of RA-5 (Turkesterone) (^{1}H: 6.2 – 0.5 ppm; ^{13}C: 10 – 210 ppm).

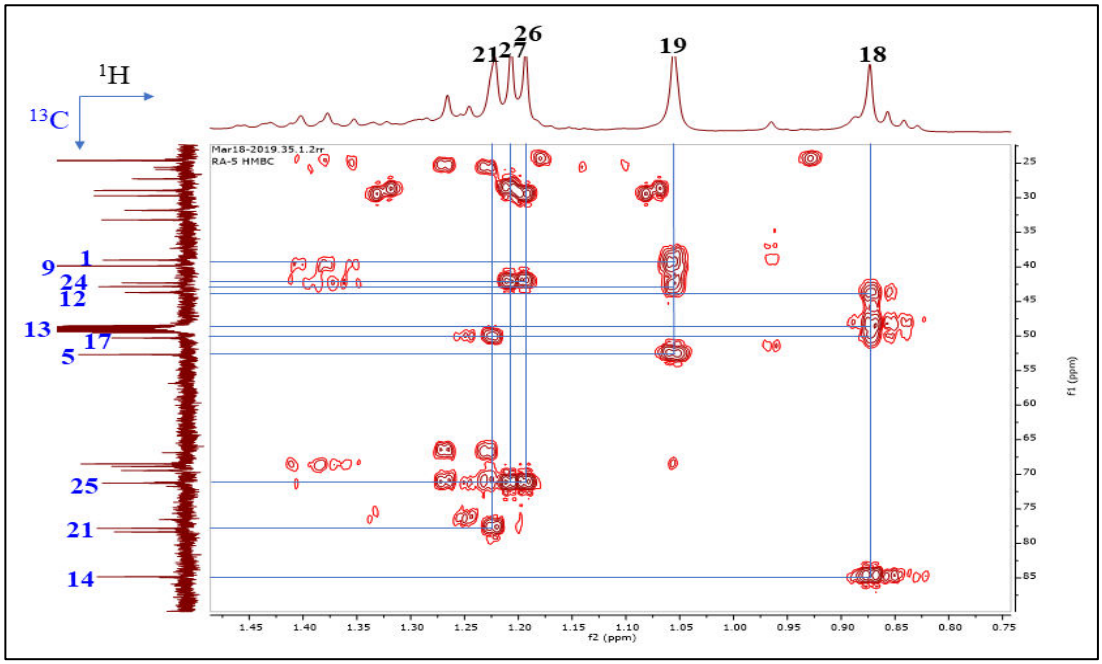

Spectrum 4.2.9.2. HMBC (^{1}H,^{13}C-Heteronuclear Long-Range Correlated of 2 (RA-5: Turkesterone) (^{1}H: 1.50 – 0.75 ppm; ^{13}C: 20 – 90 ppm).

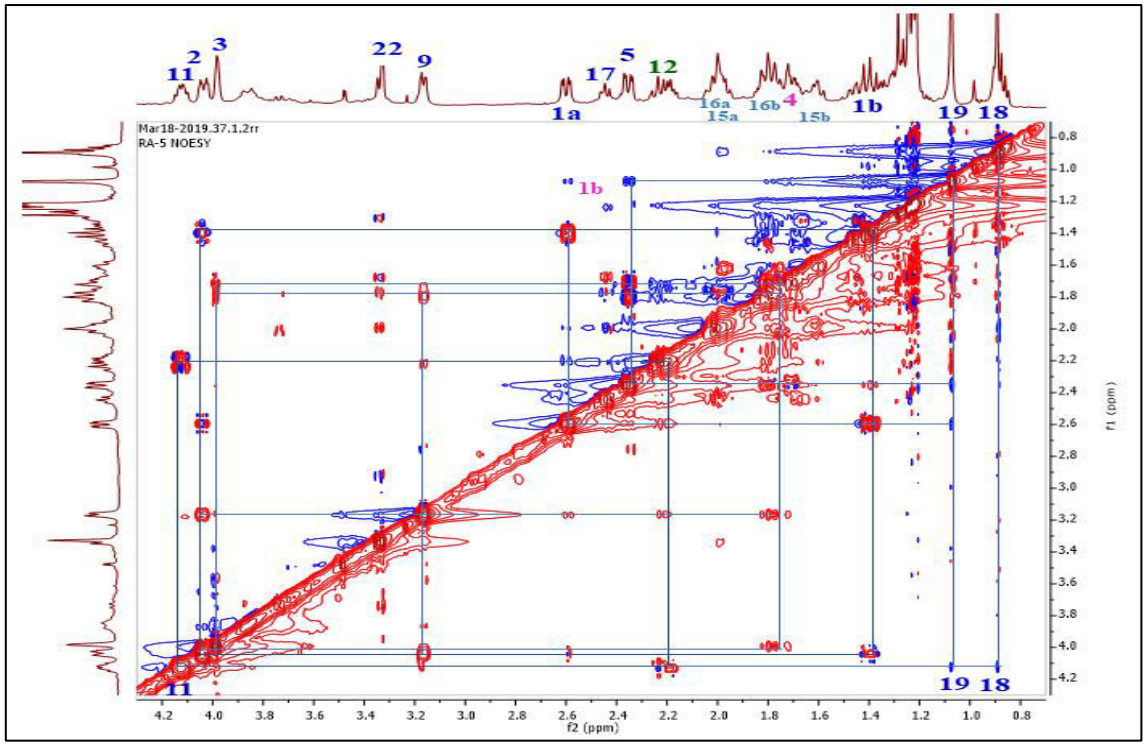

Spectrum 4.2.10. NOESY of RA-5 (Turkesterone).

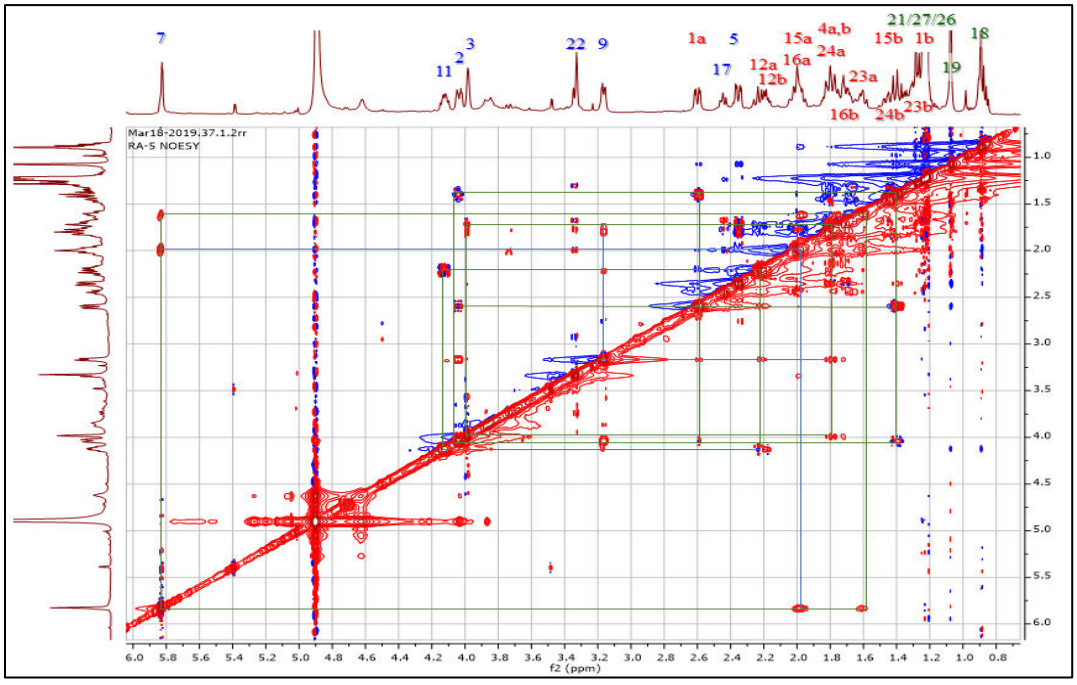

Spectrum 4.2.11. ROESY of RA-5 (Turkesterone).

4.3.1 RA-2 (Acaulesterone)

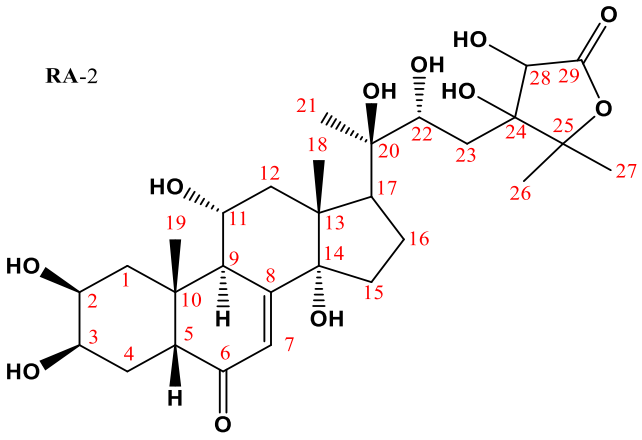

Chemical Formula: $C_{29}H_{44}O_{11}$
Exact Mass: 568,29
Molecular Weight: 568,66

Unsaturation Degree: {[(29x2)+2] – 44/2 = 8}. UD = [(2C)+2] – H/2 = 8.

RA-2 (Acaulesterone): $[\alpha]_D^{20}$ +35.0° (c 0.08, MeOH).

RA-2Ac =2,3,11,22,28-pentaacetyl-acaulesterone (3a): $[\alpha]_D^{20}$ +35.9° (c 0.117, MeOH).

RA-2 was obtained as a white amorphous solid. The positive ion HRMS and negative ion HRMS gave $[M-H]^-$ and $[M+H]^+$ at m/z 569.2950 and 567.2810, respectively (Spectrum 4.3.1 and 4.3.2), which corresponds with the molecular formula $C_{29}H_{44}O_{11}$ (calc. Mol. Wt. 568.2884) with eight degrees of unsaturation {[(29x2)+2] – 44/2 = 8}. UD = [(2C)+2] – H/2 = 8. The IR spectrum of **RA-2** (Spectrum 4.3.3) exhibited absorption bands at 3326, 1736, 1656 cm^{-1} and 1021 cm^{-1}, which were assigned to hydroxy, lactone carbonyl, α,β-unsaturated ketone and ether functionalities, respectively. The ^{1}H-NMR spectrum of compound **RA-2** (**Spectrum 4.3.4**) exhibited five tertiary methyl resonances at δ 0.89, 1.06, 1.27, 1.41 and 1.46 ppm (all s, Me-18, Me-19, Me-21, Me-26, and Me-27) (Table 4.5). The ^{13}C-NMR and DEPT-135 of **RA-2** (**Spectrum 4.3.5**) showed resonances for 29 carbon atoms, which were attributed to the presence of five methyl, six methylene, nine methine (five oxygenated and one olefinic), and nine quaternary (four oxygenated, one olefinic, and two carbonyl) carbon atoms. The ^{1}H-NMR spectrum of **RA-2** strongly supported a similar steroid skeleton to that of

RA-5 with the same substitution patterns; one olefinic proton at δ 5.82 (d, *J* = 2.4 Hz, H-7) and five oxymethine resonances at δ 4.56 (s, H-28), 4.12 (ddd, *J* = 12.0, 8.9, 6.3 Hz, H-11), 4.01 (ddd, *J* = 11.7, 7.2 and 2.8 Hz, H-2), 3.98 (ddd "brd", *J* = 2.7 Hz, H-3) and 3.29 (br d, *J* = 11.1 Hz, H-22). Proton H-9 was observed at δ 3.16 (dd, J = 8.9 and 2.6 Hz). A COSY experiment clearly indicated that H-9 was in the same spin system as the olefinic proton (H-7), oxymethine at δ 4.12 (H-11) and methylene protons at δ 2.21 and 2.17 (H-12a and H-12b), similar to the observations made for **RA-5** (**Spectrum 4.3.6.1 and 4.3.6.2**). The remaining ten carbon resonances and the corresponding proton resonances were consistent with the presence of three methyl, one methylene, two methine (both oxygenated), and four quaternary (three oxygenated, one carbonyl) carbon atoms. Two additional carbon resonances indicated that the substituents at C-24, assigned as C-28 and C-29, were the most significant differences between the side chain of **RA-1** and **RA-5** (**Spectra 4.3.7.1 and 4.3.7.2**). With the help of 2D experiments (COSY, HSQC and HMBC), the assignment of the proton and carbon resonances of the tetracyclic steroid nucleus and the side chain was established clearly. In the COSY experiment, one oxygenated methine (δ 3.29, br d, *J* = 11.1 Hz, H-22) and two methylene resonances (δ 1.89 and 1.71; H-23a and H-23b, resp.) were observed as an ABX system (**Spectrum 4.3.6.1**). One of the four quaternary carbon resonances at δ 77.6 showed long range correlation with the methyl signal at δ 1.27 (Me-21); it was attributed to C-20. Two quaternary carbon resonances at δ 89.3 and 80.0 showed long-range correlations with the other methyl resonances at δ 1.41 and 1.46, which were assigned as Me-26 and Me-27. Therefore, the two oxygenated quaternary carbon resonances were assigned as C-24 and C-25, respectively. HMBC (Spectrum 4.3.8.1 and 4.3.8.2) showed long-range correlation between the carbonyl signal at δ 176.9 and a single with one proton intensity at δ 4.56, which were assigned as C-29 and H-28, respectively. Additionally, the methylene carbon resonance of the ABX system at δ 35.2 (C-23) also showed long-range correlation with the proton resonance at δ 4.56 (H-28). These findings supported the presence of a five-membered lactone ring at the side chain (**Figure 4.5**). NOESY and ROESY (**Spectrum 4.3.9, 4.3.10.1 and 4.3.10.2**) experiments showed the expected correlations for a tetracyclic steroid nucleus and confirmed the

same substitutions that were observed for compound **RA-5**. Moreover, ROESY correlations were observed between one of the methyl groups (Me-26) located at C-25 and the methine and the methylene protons of C-28 and C-23, respectively.

Table 4.5. The ^{1}H and ^{13}C-NMR Data for RA-2 (Acaulesterone) (1H: 500 MHz; 13C: 125 MHz; CD_3OD).

C/H	DEPT	δ_C, ppm	δ_H ppm, *J* (Hz)	HMBC (from C to H)
1	CH_2	39.0	2.58 dd (12.8/4.3) 1.38 dd "t" (12.8)	
2	CH	68.9	4.01 ddd (11.7/7.2/2.8)	
3	CH	68.5	3.98 ddd "brd" (2.7)	H_2-4
4	CH_2	33.2	1.79 brd 1.70 †	
5	CH	52.7	2.36 dd (13.0/3.6)	Me-19, H-7
6	C	206.7	-	
7	CH	122.9	5.82 d (2.4)	
8	C	165.4	-	
9	CH	42.9	3.16 dd (8.9/2.6)	
10	C	39.9	-	Me-19
11	CH	69.4	4.12 ddd (12.0/8.9/6.3)	
12	CH_2	43.6	2.21dd "t" (12.0/12.0) 2.17 dd (12.0, 6.3)	
13	C	48.5	-	Me-18
14	C	85.0	-	H-7, Me-18
15	CH_2	21.5	2.01† 1.82†	
16	CH_2	31.9	2.01m 1.62 m	
17	CH	50.2	2.35 dd "t" (8.3)	Me-21
18	CH_3	18.8	0.89 s	
19	CH_3	24.6	1.06 s	
20	C	77.6	-	Me-21
21	CH_3	20.8	1.27 s	
22	CH	73.4	3.80 br d (11.1)	Me-21
23	CH_2	35.2	1.89 ddd "brd" (15.9) 1.71†	H-28
24	C	89.3	-	Me-26, Me-27
25	C	80.0	-	Me-26, Me-27
26	CH_3	24.7	1.41# s	Me-27
27	CH_3	22.3	1.46#s	Me-26
28	CH	74.4	4.56 s	
29	C	176.9	-	

†) *J* values are not clear due to overlapping; #) Interchangeable.

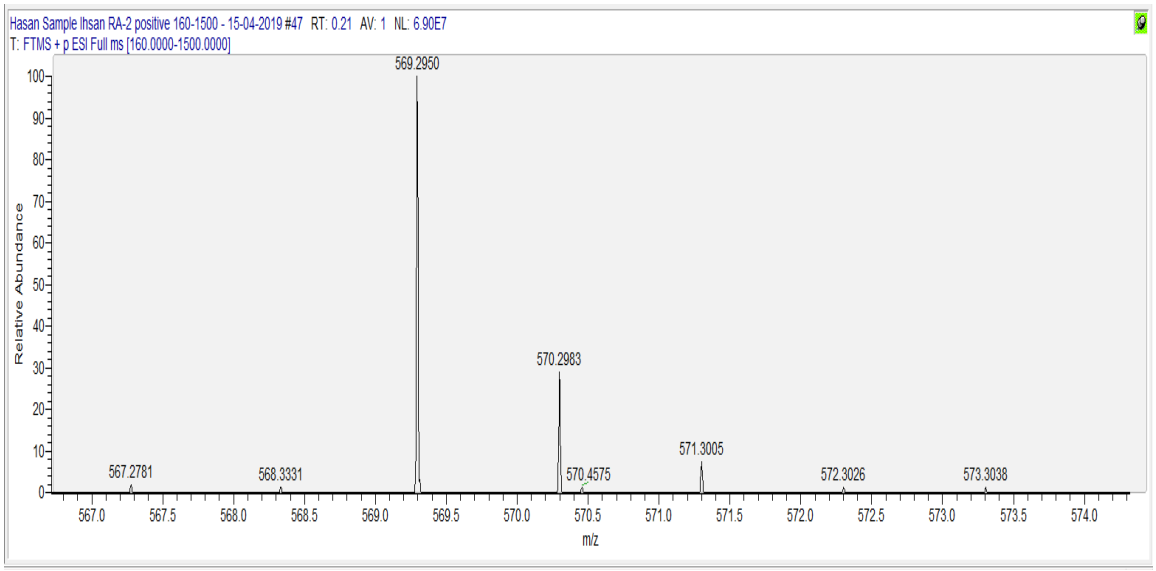

Spectrum 4.3.1. Positive ions HRMS of RA-2 (Acaulesterone) [M]+ m/z 569.2950.

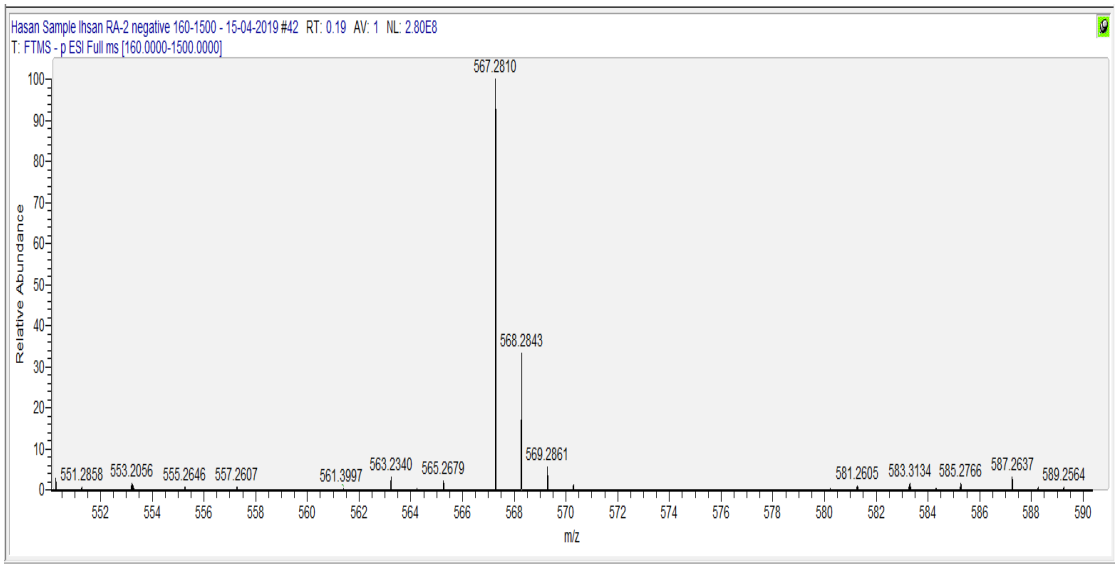

Spectrum 4.3.2. Negative ions HRMS of RA-2 (Acaulesterone) [M-H]- m/z 567.2810.

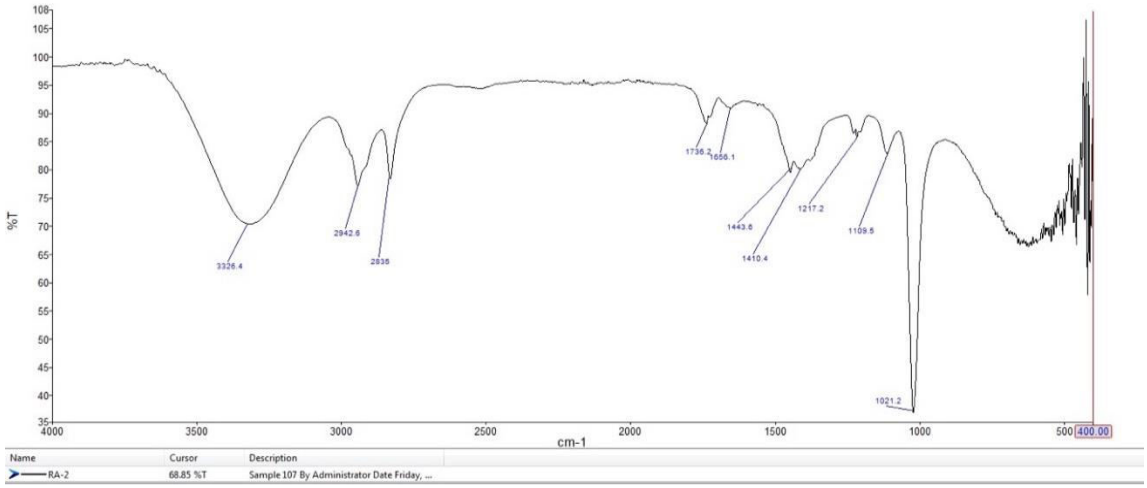

Spectrum 4.3.3. FT-IR of RA-2(Acaulesterone).

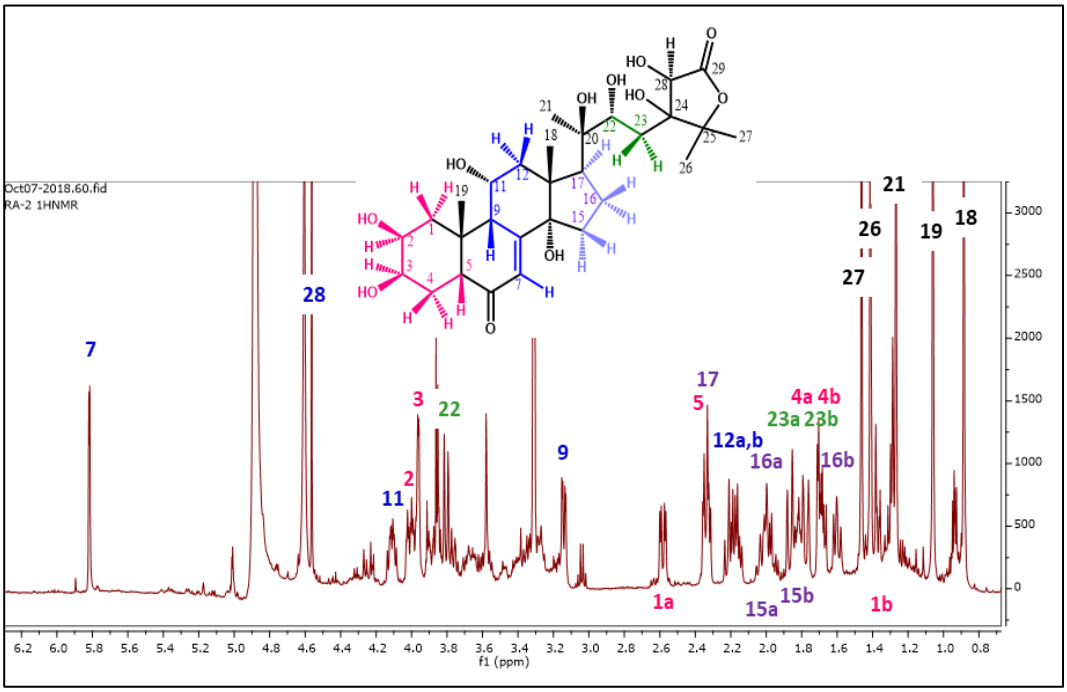

Spectrum 4.3.4. ^{1}H-NMR Spectrum of compound RA-2 (Acaulesterone) (500 MHz, MeOD).

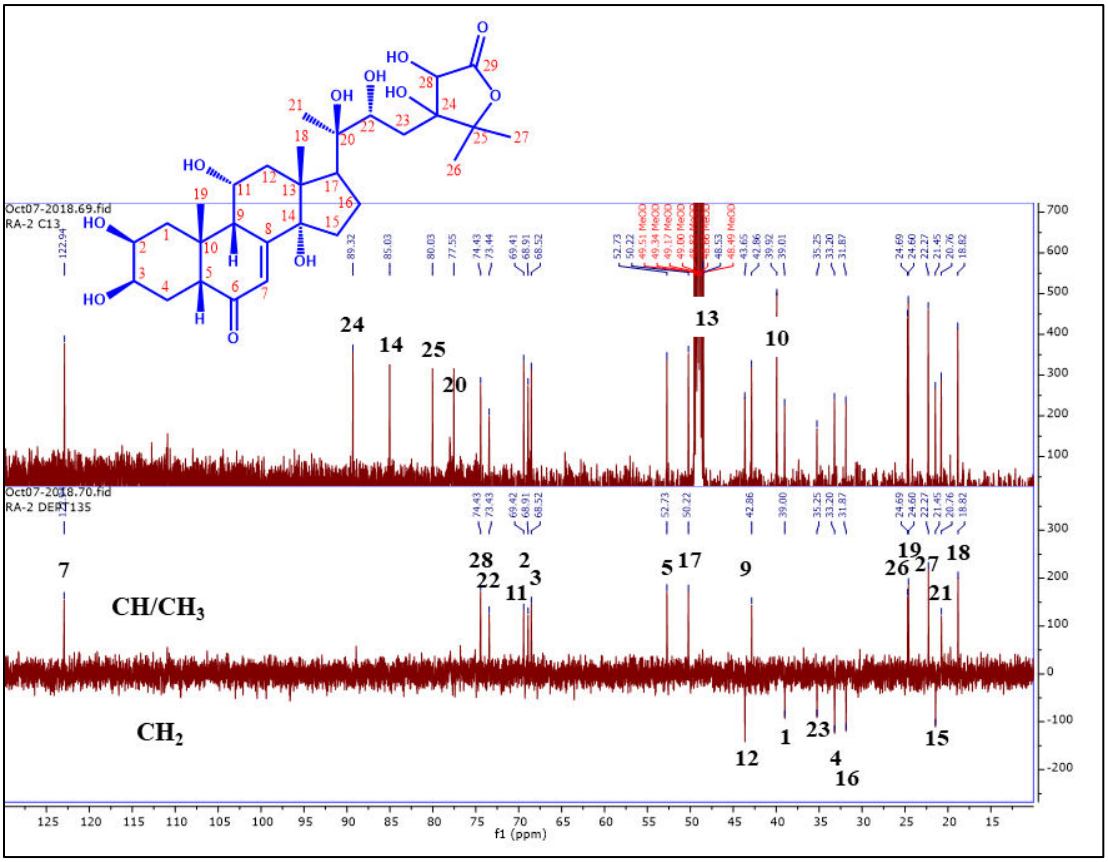

Spectrum 4.3.5. ^{13}C-NMR and DEPT-135 of RA-2 (Acaulesterone).

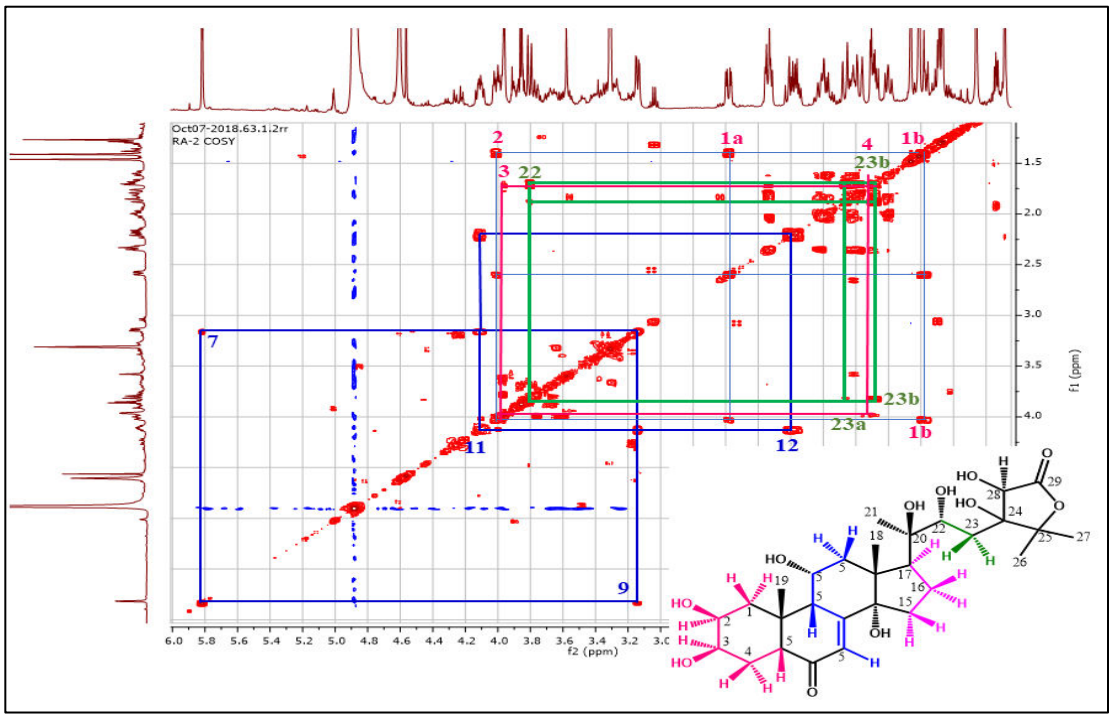

Spectrum 4.3.6.1. COSY of RA-2 (Acaulesterone).

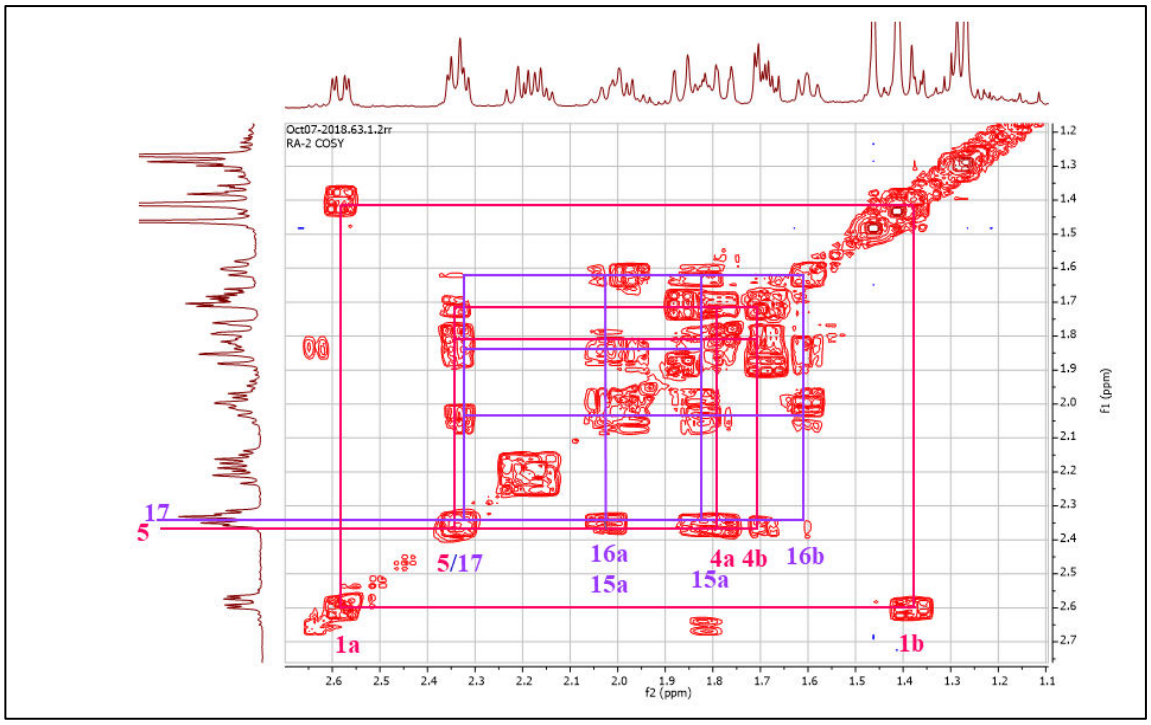

Spectrum 4.3.6.2. COSY of RA-2 (Acaulesterone) (1.1 – 2.7 ppm).

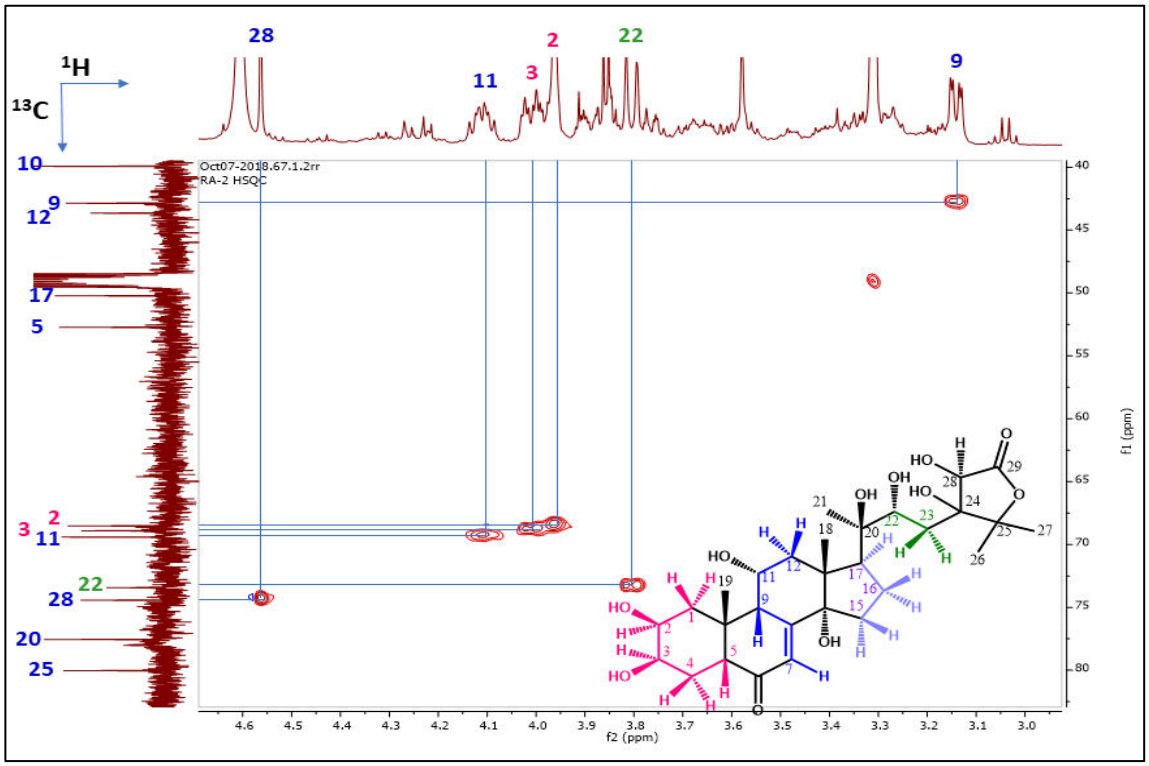

Spectrum 4.3.7.1. HSQC of RA-2 (Acaulesterone) (^{1}H: 2.9 – 4.7 ppm; ^{13}C: 40 – 85 ppm).

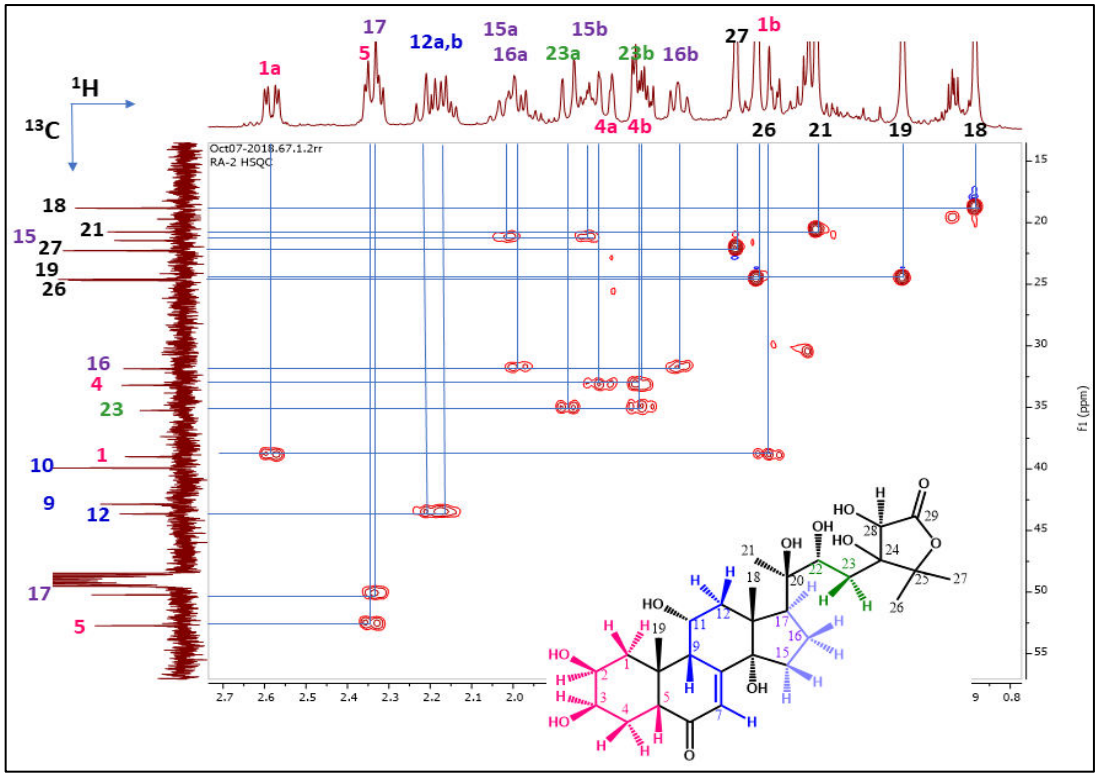

Spectrum 4.3.7.2. HSQC of RA-2 (Acaulesterone) (^{1}H: 0.8 – 2.7 ppm; ^{13}C: 15-55 ppm).

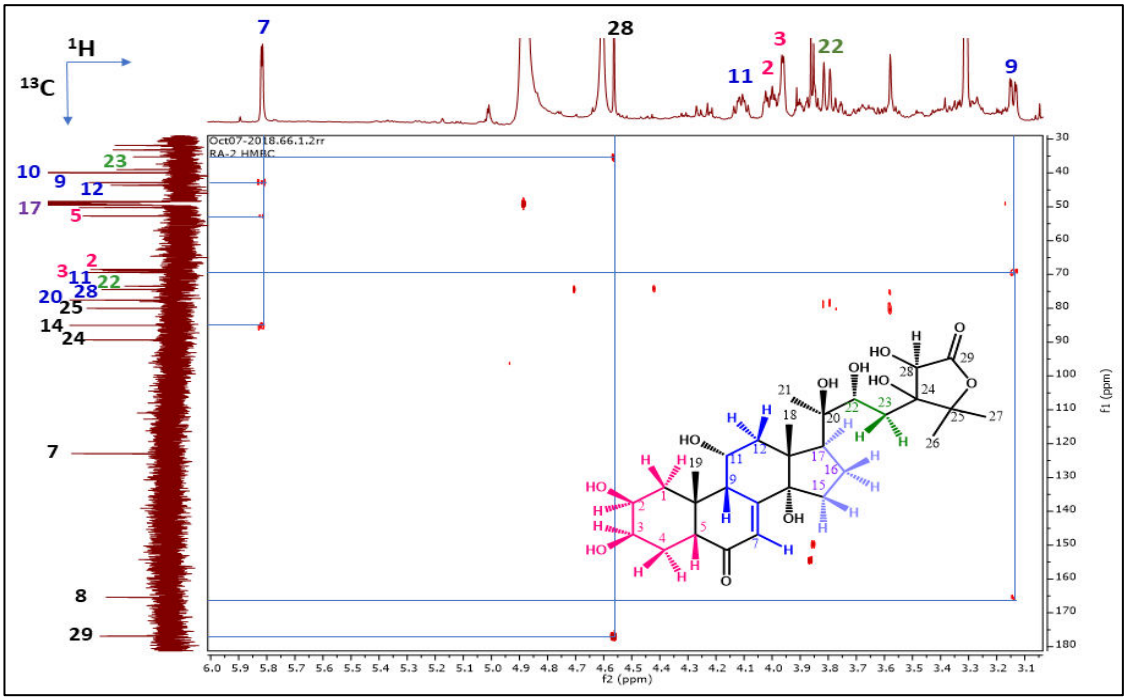

Spectrum 4.3.8.1. HMBC of RA-2 (Acaulesterone)(^{1}H: 3.0-6.0 ppm; ^{13}C: 30-180 ppm).

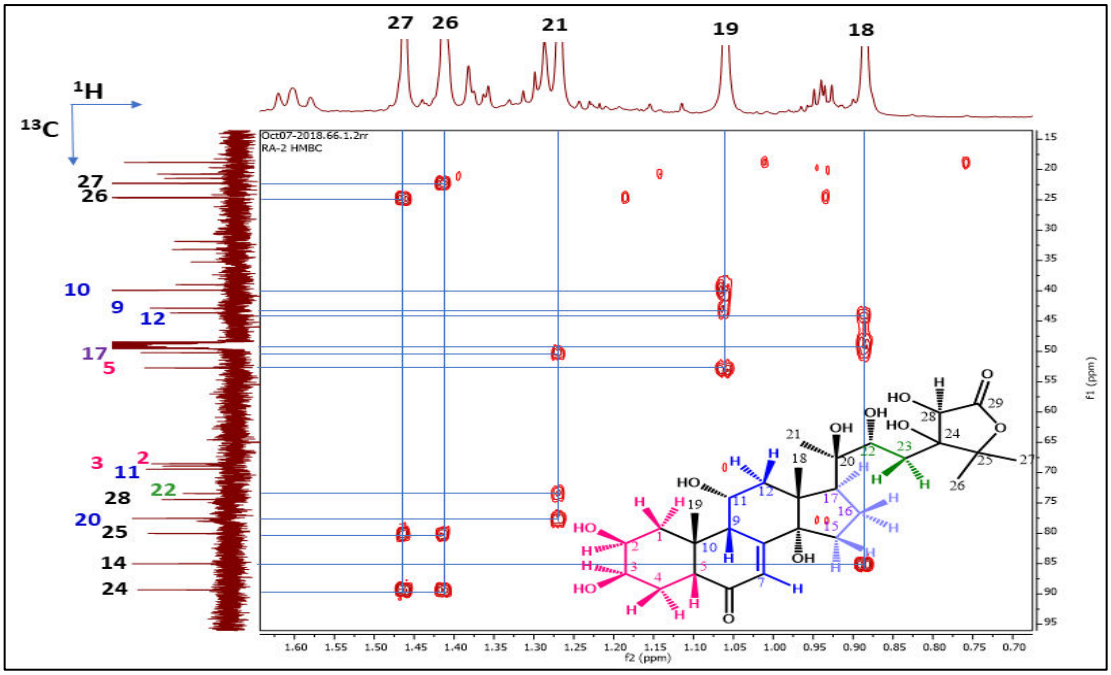

Spectrum 4.3.8.2. HMBC of RA-2 (Acaulesterone) (^{1}H: 0.7 – 1.7 ppm; ^{13}C: 15 – 95 ppm).

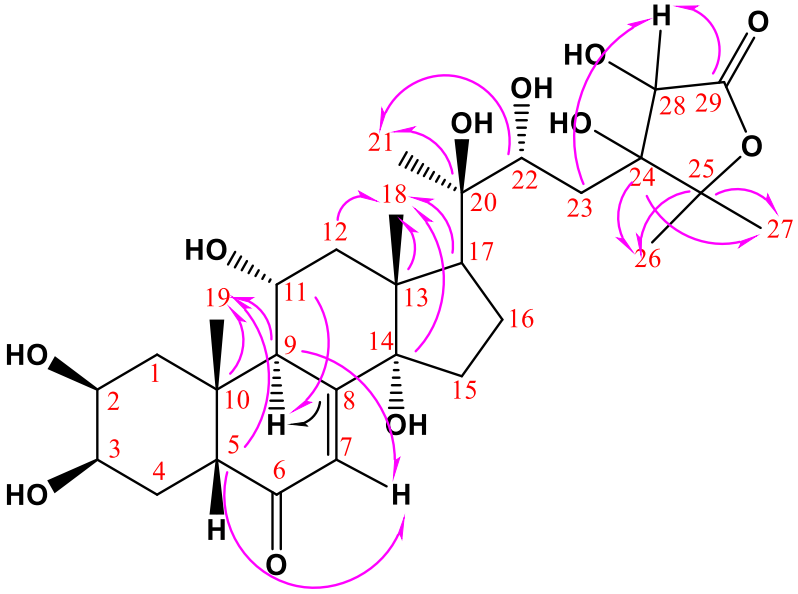

Figure 4. 5. HMBC Correlations observed for RA-2.

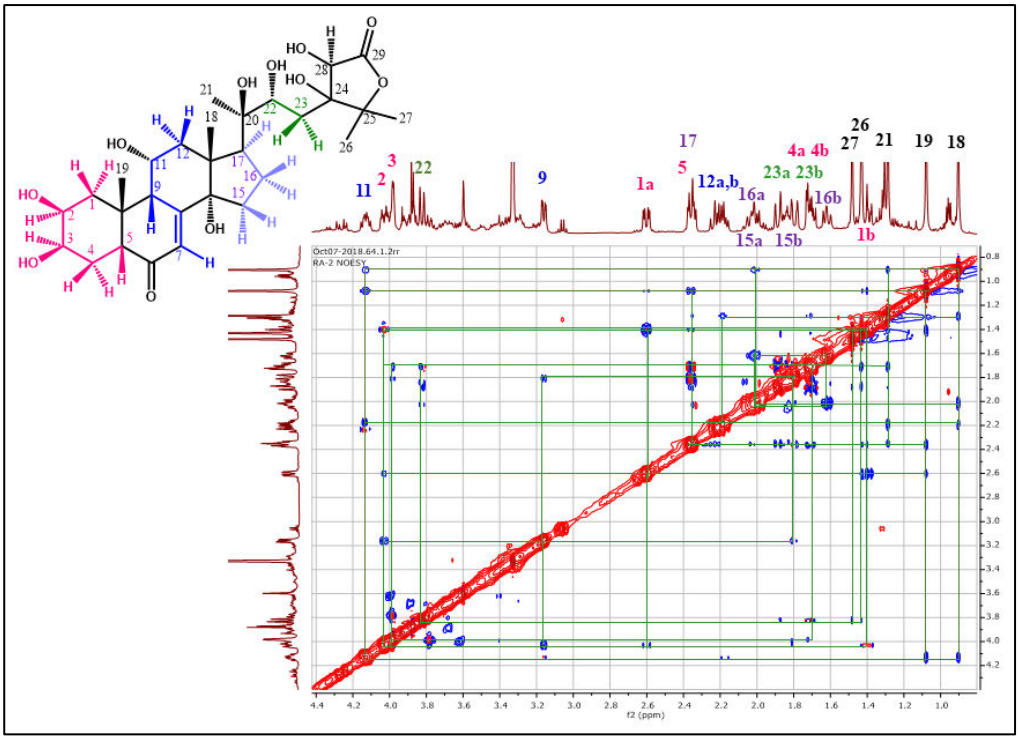

Spectrum 4.3.9. NOESY of RA-2 (Acaulesterone).

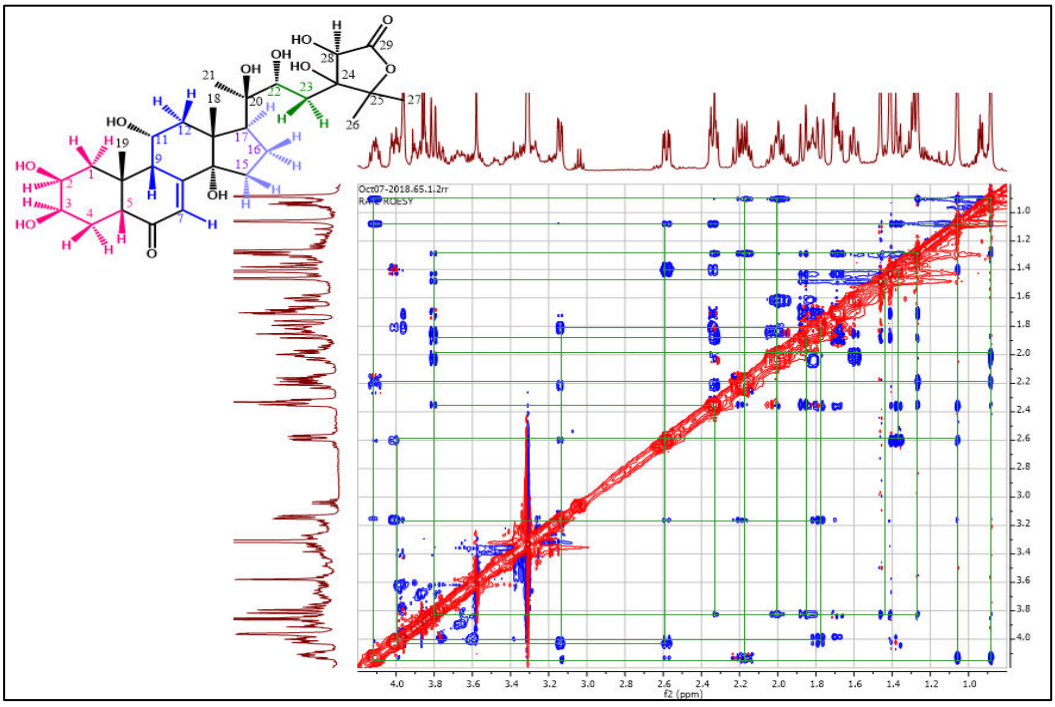

Spectrum 4.3.10.1. ROESY of RA-2 (Acaulesterone) (f1 & f2: 0.8 – 4.2 ppm).

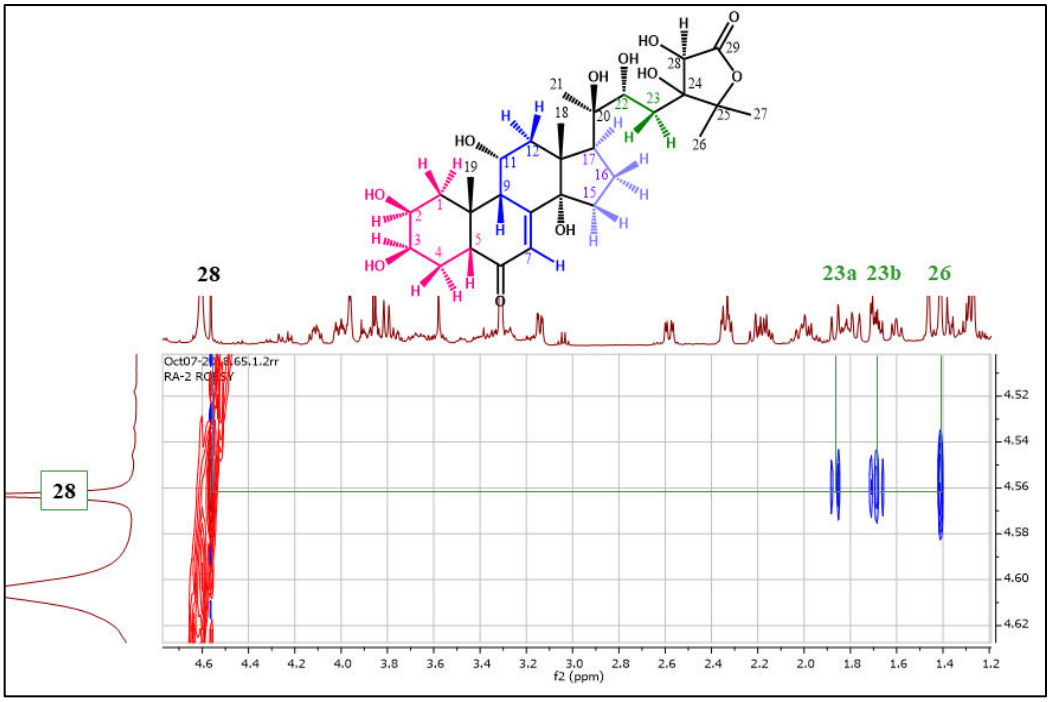

Spectrum 4.3.10.2. ROESY of RA-2 (Acaulesterone) (f1: 4.50 – 4.62; f2: 1.2 – 4.8 ppm).

4.3.2. RA-2Ac (2,3,11,22,28-pentaacetyl-acaulesterone)

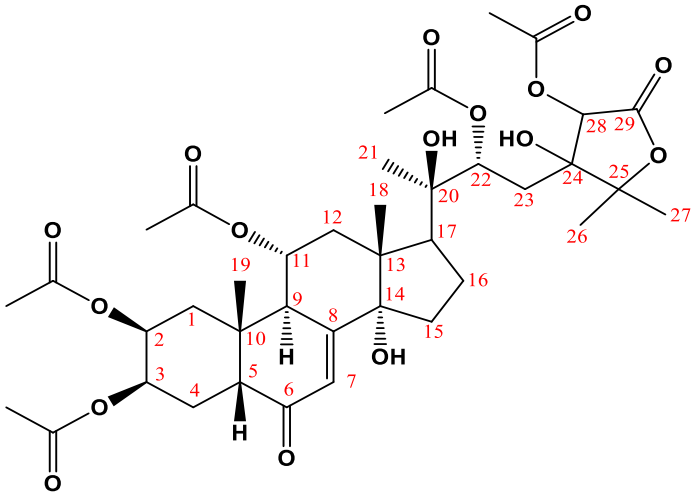

Chemical Formula: $C_{39}H_{54}O_{16}$
Exact Mass: 778,34
Molecular Weight: 778,85

RA-2 (Acaulesterone): $[\alpha]_D^{20}$ +35.0° (c 0.08, MeOH).

RA-2Ac=2,3,11,22,28-pentaacetyl-acaulesterone (3a): $[\alpha]_D^{20}$ +35.9° (c 0.117, MeOH).

In order to obtain more evidence to support the proposed structure, **RA-2** was acetylated. The mild acetylation of **RA-2** yielded a pentaacetate (**RA-2Ac**). Its molecular formula was determined as $C_{39}H_{54}O_{16}$ from the ion peaks at m/z 777.333 $[M-H]^-$ and 801.3293 $[M+Na]^+$ in the negative and positive ion HRMS (**Spectra 4.3.2.1 and 4.3.2.2**), respectively. The ^{1}H-NMR spectrum of **RA-2Ac** (Spectrum 4.3.2.4) displayed five acetoxy methyl resonances at δ 2.13, 2.04, 1.99, 1.92 and 1.89 ppm (all s). The acetylated positions have been recognized by the shift of the signals of the protons directly linked to the substituted positions. The five oxymethine protons assigned as H-2, H-3, H-11, H-22, and H-28 of **RA-2Ac** showed more than a 1.00 ppm down-field shift compared with those of compound 3 (δ 5.20, H-2; 5.31, H-3; 5.21, H-11; 5.04, H-22 and 5.53, H-28) due to the alpha effect of esterification, thereby confirming the sites of acetylation. The assignments of the remaining protons and carbon atoms in **RA-2Ac** (**Table 4.6**) were established with the help of ^{13}CNMR, DEPT135 (**Spectrum 4.3.2.5**) and 2D-NMR experiments (COSY, HSQC, HMBC NOESY and ROSY). The COSY experiment showed the presence of four molecular fragments (protons of rings A, B & C, D and side chain, H-22, and H_2-23) in addition to five methyl resonances and an isolated oxymethine resonance (H-28) (**Spectrum 4.3.2.6**). Intramolecular connectivities were established with the help of a HMBC experiment (**Spectra 4.3.2.8.1 and 4.3.2.8.2**), which revealed long-range correlations between the carbon atoms and the methyl signals of Me-18, Me-19, Me-21, Me-26, and Me-27. The presence of a hydroxylated five-membered lactone ring at the side chain was also established by the long-range correlations from C-29 (δ 170.09) and C-23 (δ 34.78) to H-28 (δ 5.53 s). Additional long-range correlations from C-24 (δ 88.34) and C-25 (δ 77.81) to Me-26 (δ 1.40 s) and Me-27 (δ 1.44 s) revealed the proposed structure. The HSQC (**Spectrum 4.3.2.7**) verified the attached protons to their carbon atoms, in meanwhile, NOESY (**Spectrum 4.3.2.9**) and ROESY experiments (Spectra 4.3.2.10.1 and 4.3.2.10.2) confirmed the close correlation between the unbonded protons through space. Based on these results, the structure of **RA-2** was established as 2β,3β,11β,20β,22β,24,28-heptahydroxy-6-oxo-stigmast-7-en-25,29-lactone. The trivial name Acaulestrone is proposed for this compound.

Table 4.6. The ^{1}H and ^{13}C-NMR Data for RA-2Ac.

C/H	DEPT	δ_C, ppm	δ_H ppm, *J* (Hz)	HMBC (from C to H)
1	CH_2	35.78	1.64 1.54 dd "t" (13.2)	
2	CH	68.53	5.20†	
3	CH	66.80	5.31 brs	H_2-4
4	CH_2	29.18	1.74†	
5	CH	51.57	2.30†	Me-19, H-7
6	C	201.29	-	
7	CH	122.98	5.86 br s	
8	C	160.72	-	
9	CH	38.23	3.36 brd (8.5)	
10	C	39.21	-	Me-19
11	CH	71.19	5.21†	
12	CH_2	37.33	2.27† 2.03†	
13	C	47.11	-	Me-18
14	C	83.89	-	H-7, Me-18
15	CH_2	20.49	2.02† 1.87†	
16	CH_2	31.17	1.99† 1.63†	
17	CH	48.56	2.27†	Me-21
18	CH_3	17.85	0.81 s	
19	CH_3	23.79	1.03 s	
20	C	77.3	-	Me-21
21	CH_3	20.29	1.13 s	
22	CH	73.37	5.04 br d (6.9)	Me-21
23	CH_2	34.78	1.80	Me-28
24	C	88.34	-	Me-26, Me-27
25	C	77.81	-	Me-26, Me-27
26	CH_3	21.19	1.40# s	Me-27
27	CH_3	25.09	1.38#s	Me-26
28	CH	72.67	5.53 s	
29	C	170.09	-	

Additional acetoxy signals ($\underline{\boldsymbol{C}}OCH_3$): δ 173.24, 170.55, 170.49, 170.28 and 169.94; ($CO\underline{\boldsymbol{C}}\mathbf{H_3}$): δ_C 21.35, 21.29, 21.11, 20.90 and 21.77; δ_H 2.13 s, 2.04 s, 1.99 s, 1.92 s and 1.89 s.
†) *J* values are not clear due to overlapping; #) Interchangeable.

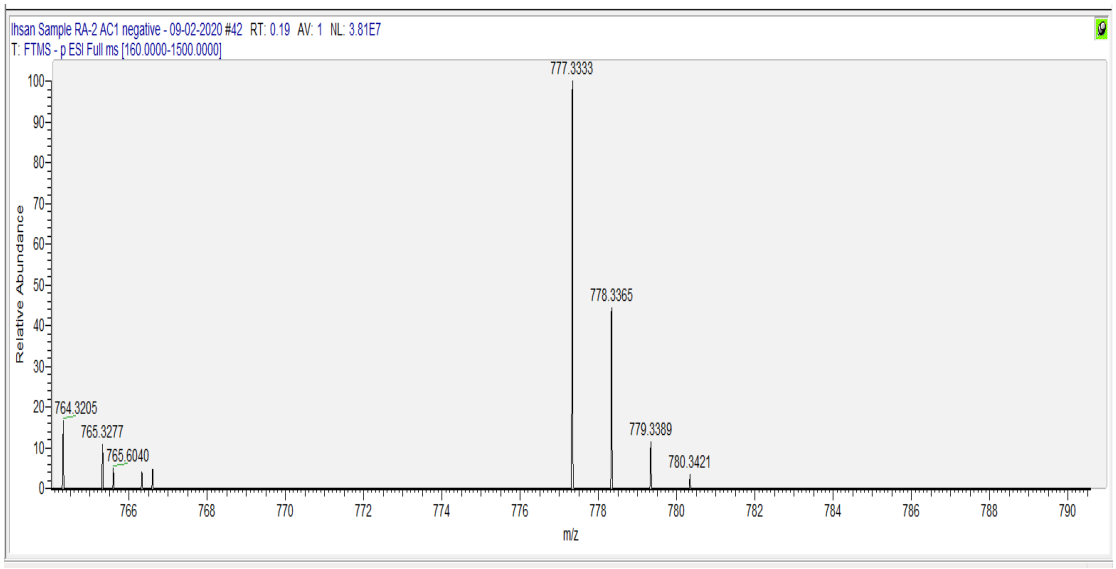

Spectrum 4.3.2 1. (-)-HRMS of RA-2Ac $[M-H]^-$ m/z 777.3333.

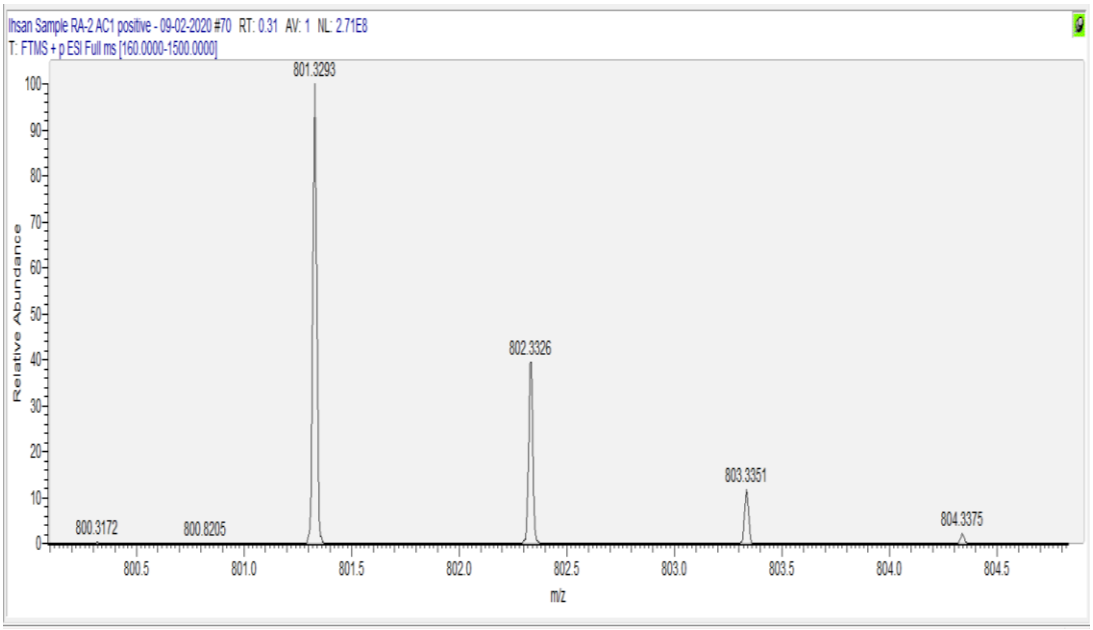

Spectrum 4.3.2.2. (+)-HRMS of RA-2Ac $[M+Na]^+$ m/z 801.3293.

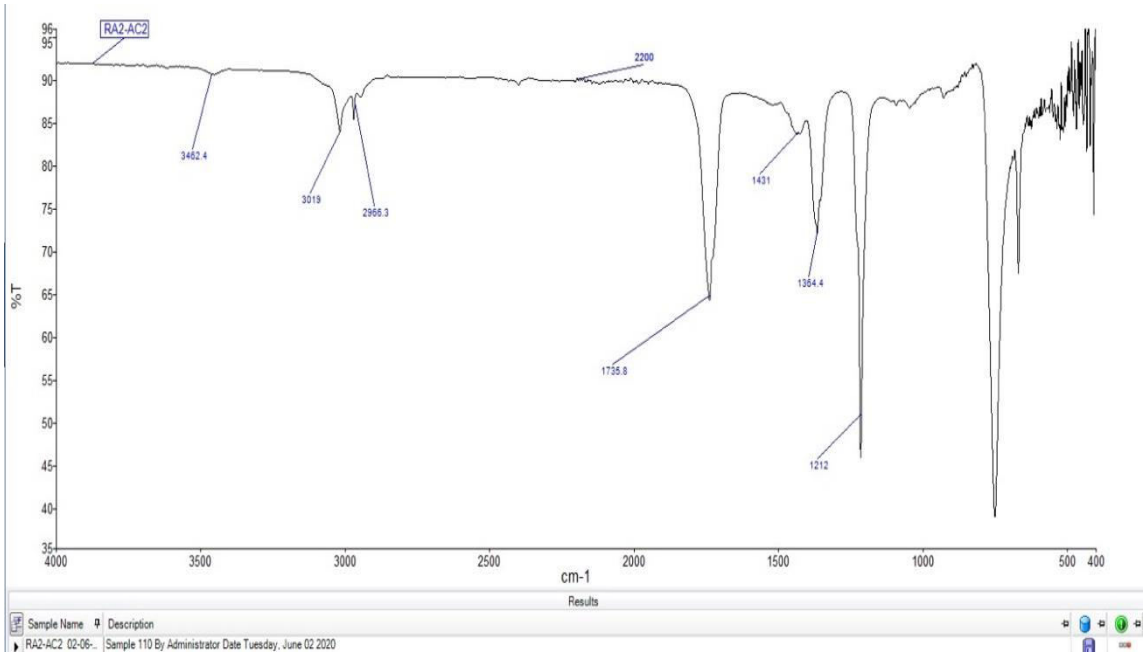

Spectrum 4.3.2.3. FT-IR of RA-2Ac.

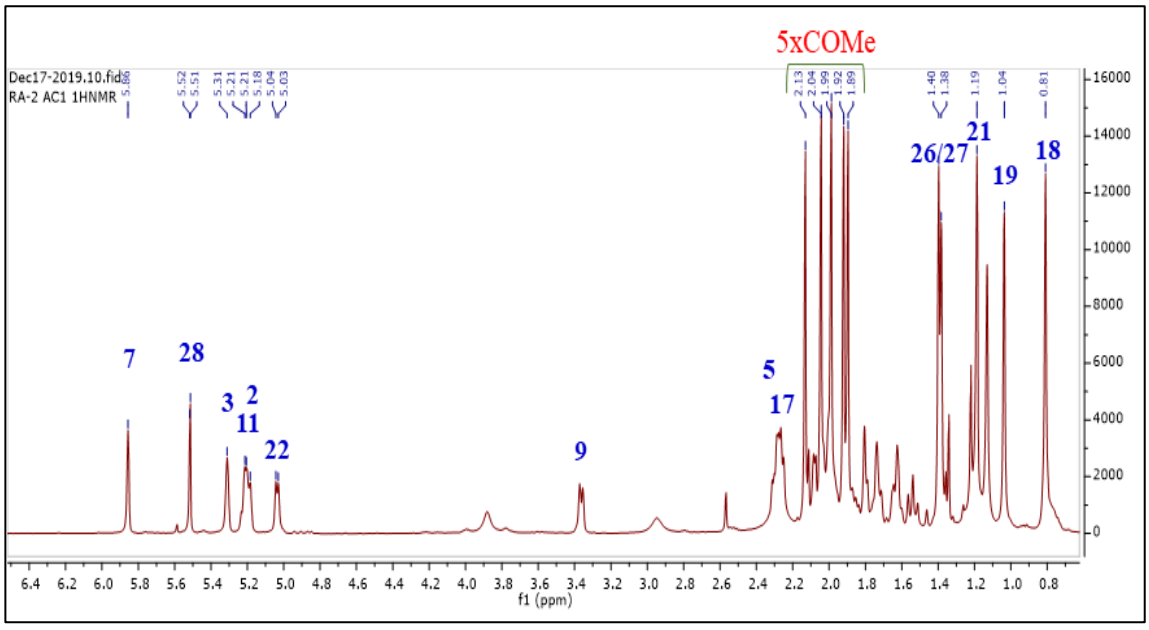

Spectrum 4.3.2.4. ^{1}H-NMR Spectrum of RA-2Ac (Pentaacetyl-Acaulesterone).

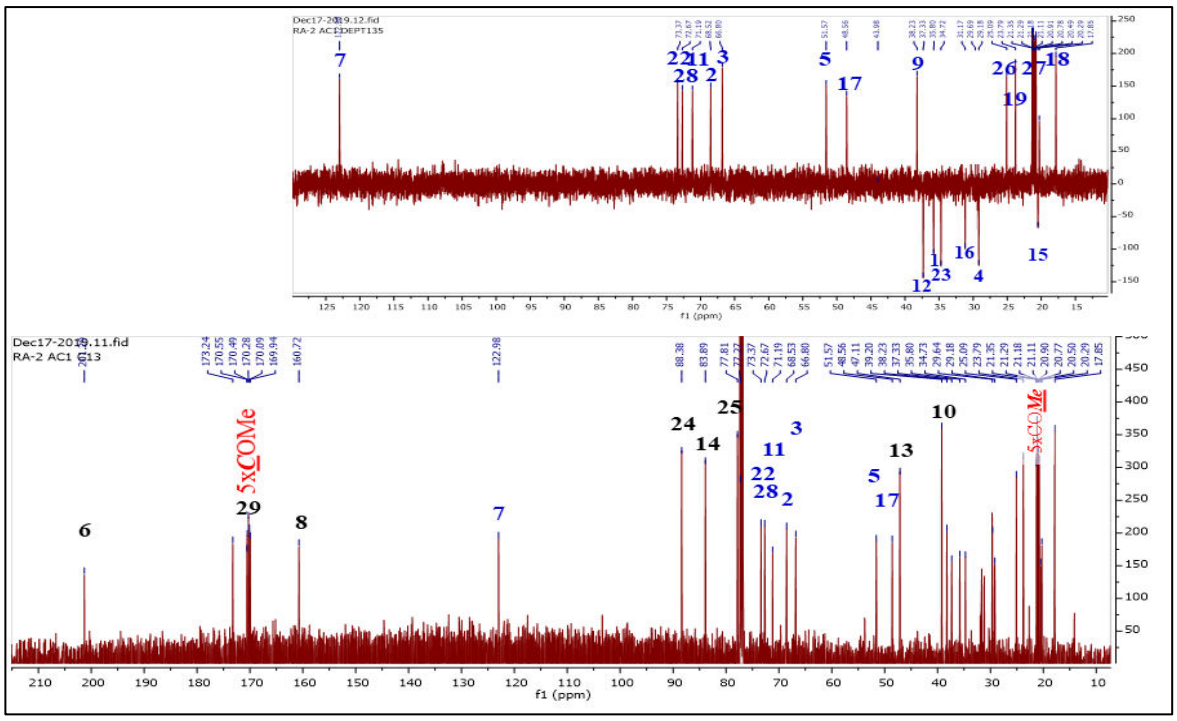

Spectrum 4.3.2.5. ^{13}C-NMR and DEPT-135 of RA-2Ac (Pentaacetyl-Acaulesterone).

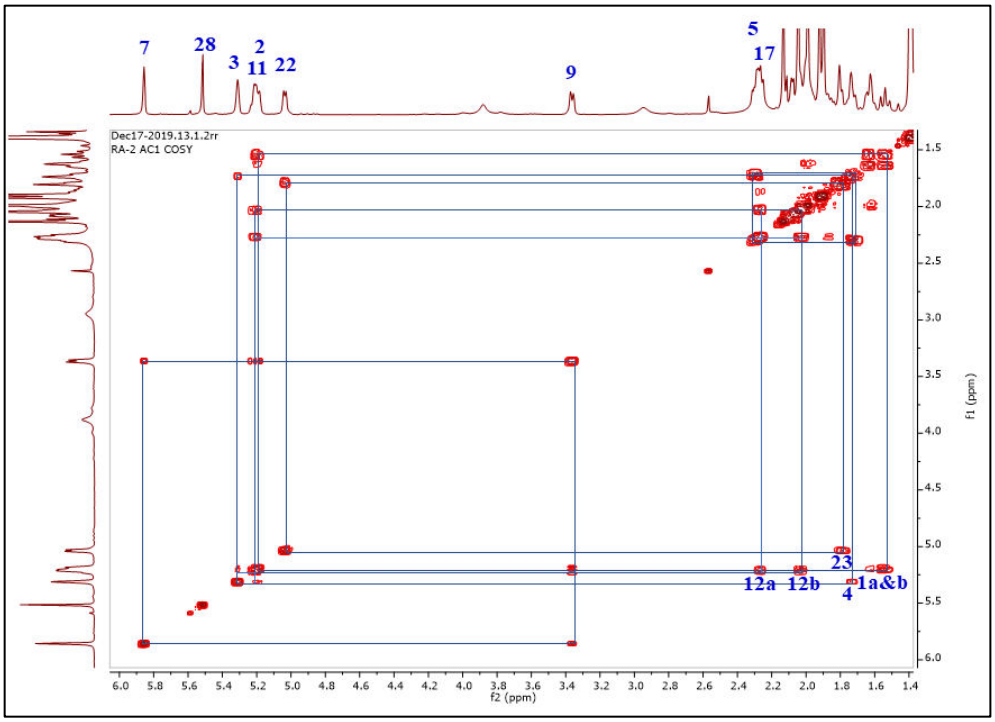

Spectrum 4.3.2.6. COSY of RA-2Ac (Pentaacetyl-Acaulesterone).

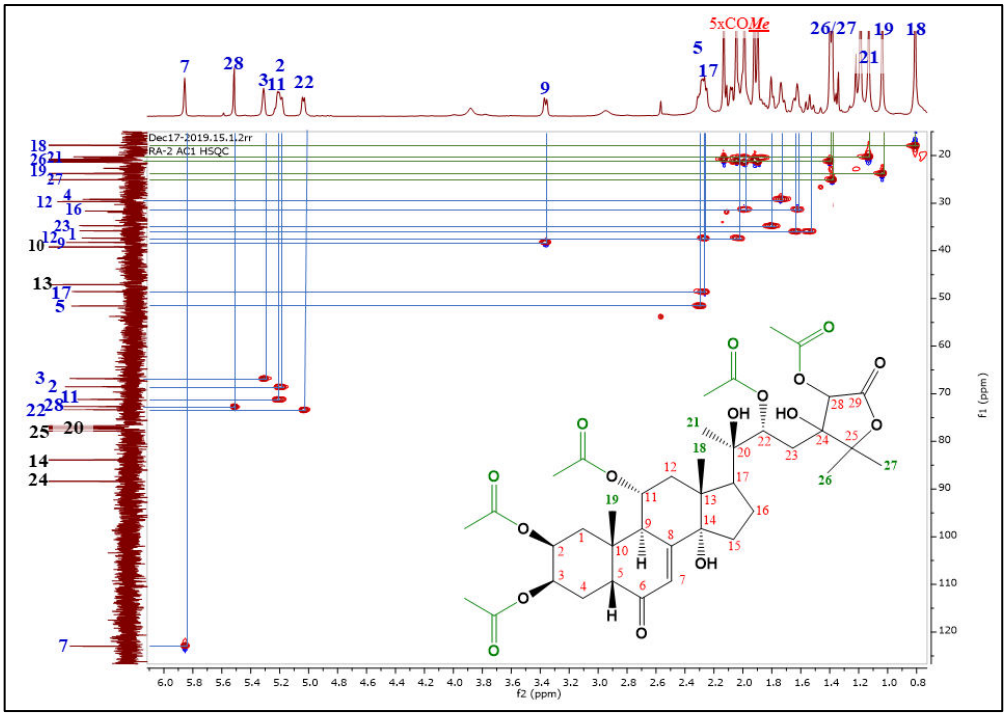

Spectrum 4.3.2.7. HSQC of RA-2Ac (Pentaacetyl-Acaulesterone) (^{1}H: 6.2– 0.7 ppm; ^{13}C: 15 – 125 ppm).

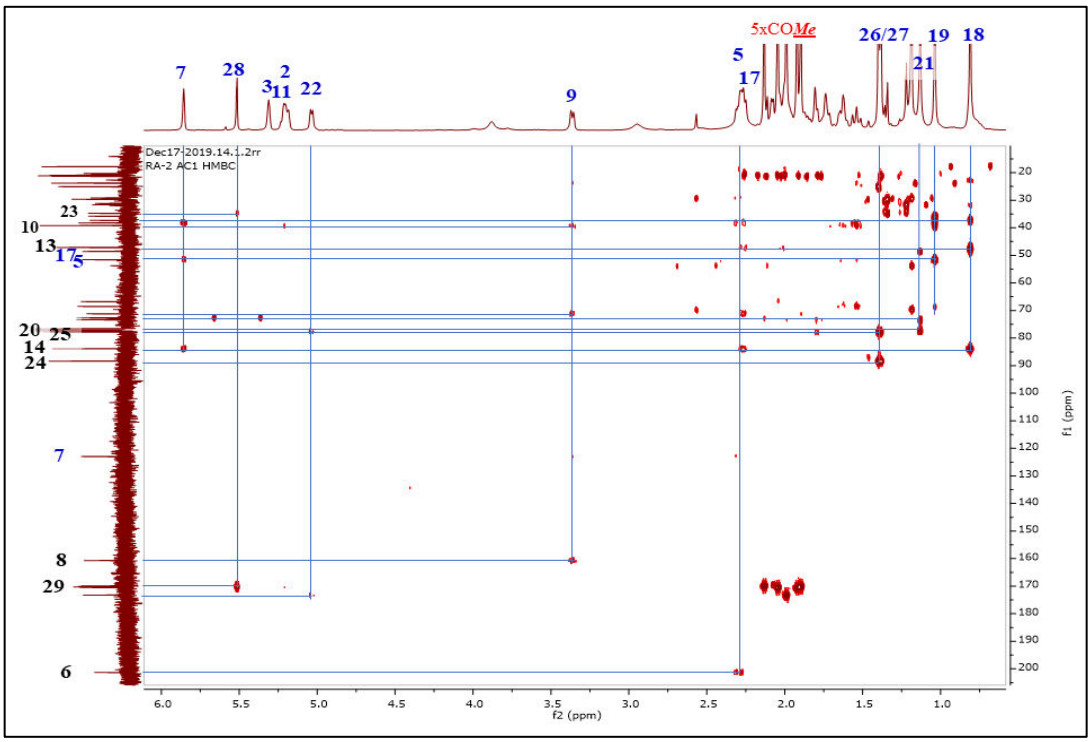

Spectrum 4.3.2.8. 1. HMBC of RA-2Ac (Pentaacetyl-Acaulesterone) (^{1}H: 0.5 – 6.0 ppm; ^{13}C: 10 – 210 ppm).

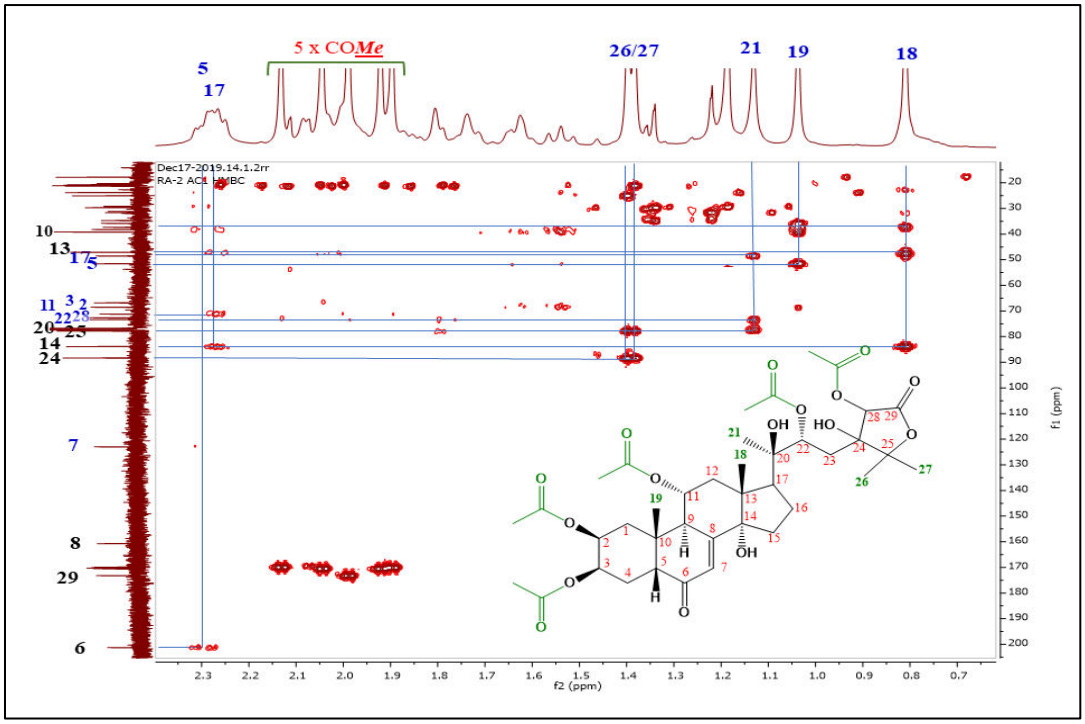

Spectrum 4.3.2.8. 2. HMBC of RA-2Ac (Pentaacetyl-Acaulesterone) (^{1}H: 0.6 – 2.4 ppm; ^{13}C: 10 – 205 ppm).

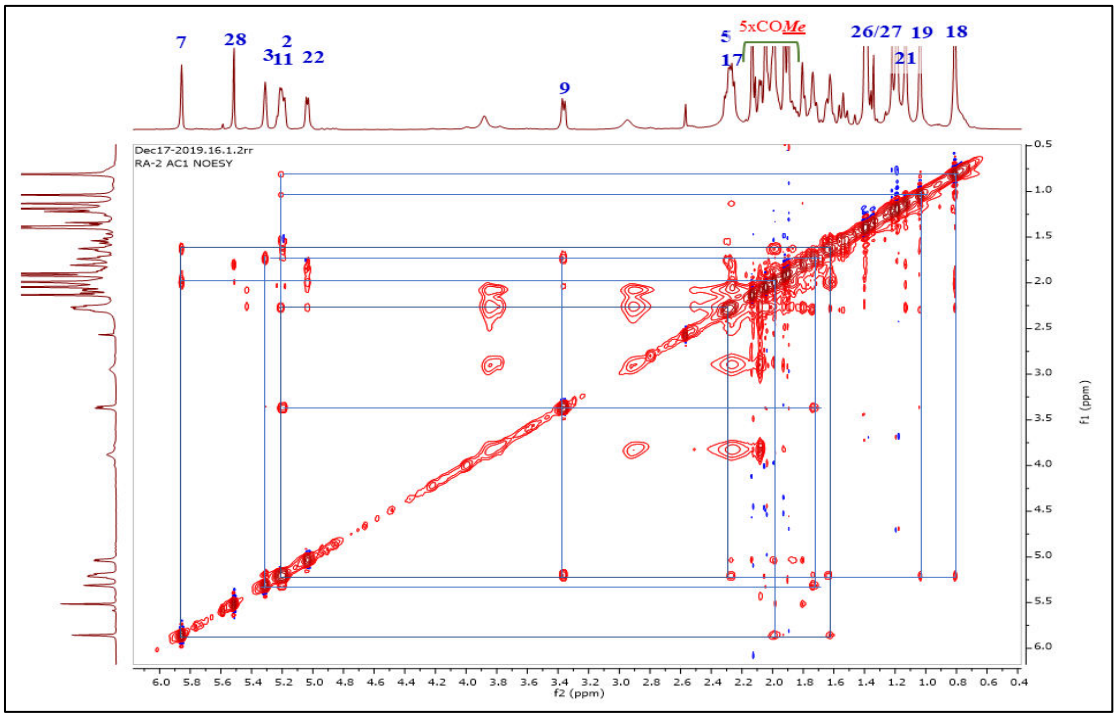

Spectrum 4.3.2.9. NOESY of RA-2Ac (Pentaacetyl-Acaulesterone).

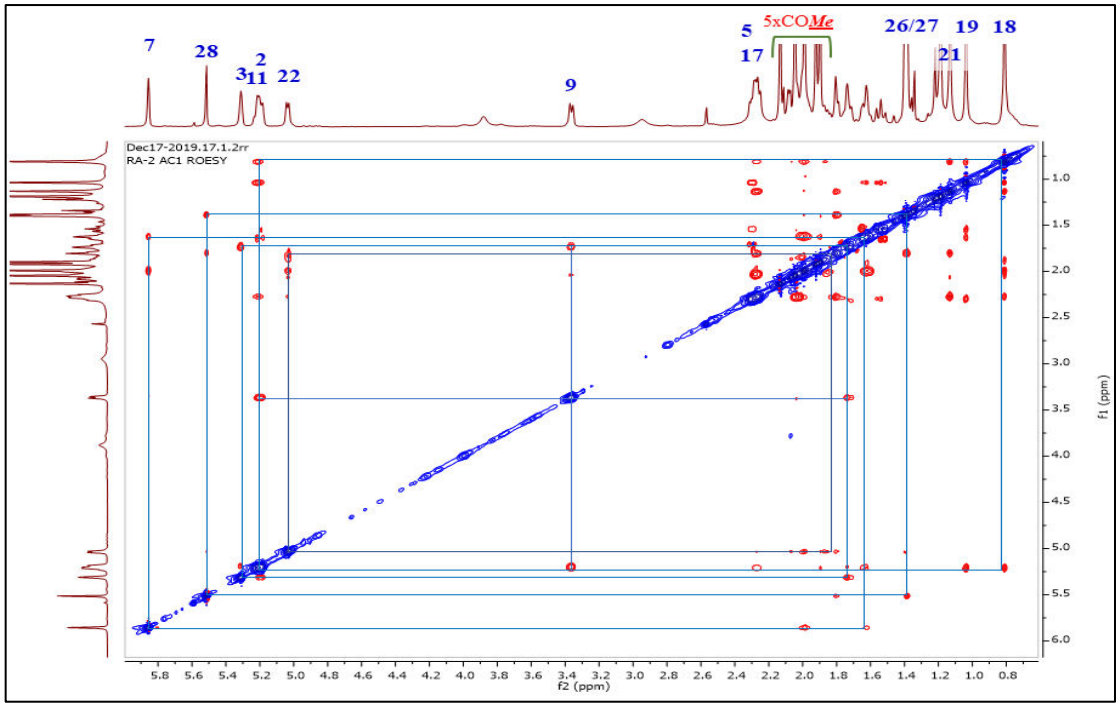

Spectrum 4.3.2.10. 1. ROESY of RA-2Ac (Pentaacetyl-Acaulesterone) (f1 & f2: 0.8 – 6.0 ppm).

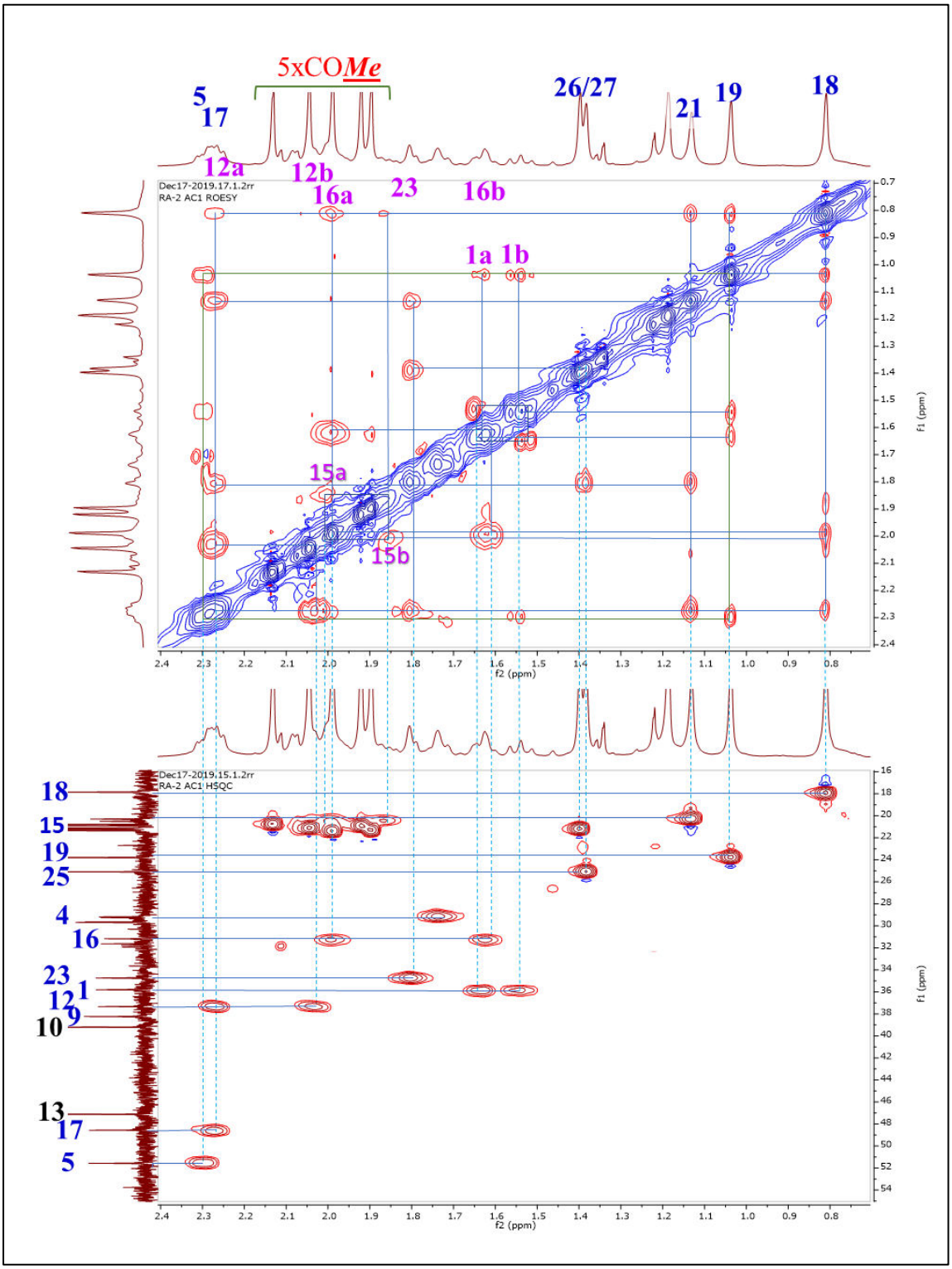

Spectrum 4.3.2.10.2. ROESY and HSQC of RA-2Ac (Pentaacetyl-Acaulesterone) (ROESY: f1: 0.7 – 2.4 ppm; f2: 0.7 – 2.4 ppm) (HSQC: f1: 16 – 54 ppm; f2: 0.7 – 2.4 ppm).

4.4. RA-6 = RA-8 (Mixture of 4a and 5a)

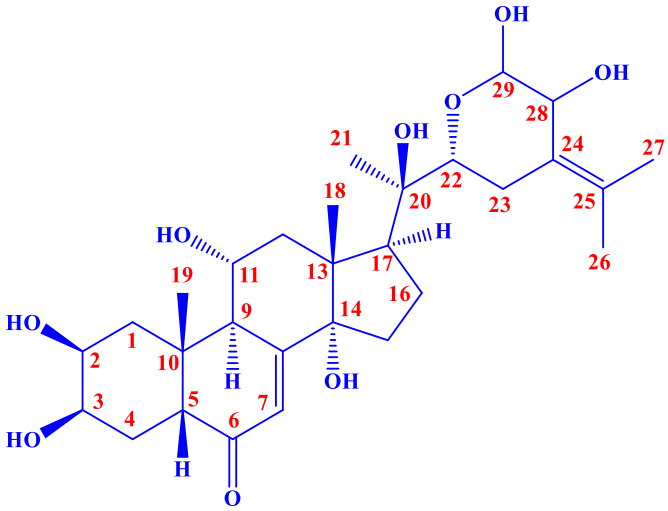

Chemical Formula: $C_{29}H_{44}O_9$
Exact Mass: 536,30
Molecular Weight: 536,66

Unsaturation Degree: (29x2)+2 -44/2 = 8

Rhapocasterones A and B (**RA-6** & **RA-8**)

RA-6 or 8 Mixture (**4a&4b**): $[\alpha]_D^{20}$ +32.3° (c 0.124, MeOH).

The mixture of compounds **RA-6** and **RA-8** was obtained as a white amorphous solid in which **RA-6** was the minor component. The negative and positive ion HRMS gave $[M-H]^-$, $[M+H]^+$ and $[M+Na]^+$ peaks at m/z 535.2901, 537.3053 and 559.2871, respectively (**Spectra 4.4.1 and 4.4.2**), which corresponds with the molecular formula $C_{29}H_{44}O_9$ (calc. 536,66) with eight degrees of unsaturation. The IR (**Spectrum 4.4.3**) exhibited absorption bands for hydroxy (3370 cm^{-1}), α,β-unsaturated ketone (1648 cm^{-1}) and ether (1032 cm^{-1}) functionalities.

The ^{13}C-NMR and DEPT-135 (**Spectra 4.4.5**) of the mixture of **4** and **5** showed signals at δ 206.7, 165.7 and 122.7, which were indicative of the presence of an α,β-unsaturated ketone system, as observed for **1**, **2** and **3**. A UV absorption band at δ_{max} 230 nm supported this proposal.

Table 4.7. The ^{1}H and ^{13}C-NMR Data for 4 (RA-6&8: Rhapocasterone A&B) Major.

C/H	DEPT	δ_C, ppm	δ_H ppm, *J* (Hz)	HMBC (from C to H)
1	CH_2	39.0	2.38 dd (12.7/5.0) H-1eq 1.39 dd (12.7/12.7) H-1ax	Me-19
2	CH	68.9	4.02 ddd (12.0/7.0/3.4)	H-3
3	CH	68.5	3.96 br s	H-5
4	CH_2	33.2	1.78† 1.70†	H-5
5	CH	52.7	2.34 dd (13.2/2.9)	H-7, Me-19
6	C	206.7	-	H-1eq, H-5
7	CH	122.7	5.81 d (2.2)	H-5, H-9
8	C	165.7	-	H-9
9	CH	42.8	3.16 dd (9.0/2.5)	H-5, H-7, Me-19
10	C	39.9	-	H-5, H-9, Me-19
11	CH	69.4	4.11 ddd (15.8/10.2/6.6)	H-9, H-7, Me-18
12	CH_2	43.6	2.22 dd "t" (12.0/12.0) 2.10 dd (12.0, 6.3)	Me-19
13	C	48.3	-	Me-18
14	C	84.9	-	H-7, H_2-12, Me-18
15	CH_2	31.8	1.97 m 1.60 m	H-17
16	CH_2	21.7	1.99† 1.75†	
17	CH	50.4	2.43 dd "t" (8.3)	Me-18, Me-21
18	CH_3	19.1	0.86 s	H_2-12
19	CH_3	24.6	1.06 s	H-5, H-9
20	C	77.1	-	Me-21, H-22
21	CH_3	21.7	1.33 s	H-22
22	CH	75.0	3.74 dd (12.0/2.0)	Me-21,
23	CH_2	26.4	2.14 dd 2.48 dd	
24	C	127.0	-	H-22, Me-26, Me-27
25	C	131.2	-	Me-26, Me-27
26	CH_3	20.10	1.79 d (1.3)	Me-27
27	CH_3	20.41	1.75 s	Me-26
28	CH	68.0	4.36 d (1.1)	
29	CH	96.5	5.16 d (1.1)	

†) *J* values are not clear due to overlapping.

The ^{1}H and ^{13}C-NMR data of **4** and **5** revealed the presence of an ecdysteroid skeleton showing the same hydroxylation pattern as that found for compounds **RA-5** and **RA-2** at C-2, C-3, C-11, and C-14. However, the double signals of proton and carbon resonances arising from the side chain suggested the presence of two stereoisomeric structures. The most significant differences were observed for C-22/H-22, C-23/H_2-23,

C-24, C-25, C-26/Me-26, C-27/Me-27, C-28/H-28, and C-29/H-29 (**Tables 4.7 and 4.8**). In the ^{1}H-NMR experiment (**Spectrum 4.4.4**), three tertiary methyl groups (Me-21, Me-26, and Me-27), and the protons of an ABX system (H-22 and H_2-23) and an AB system (H-28 and H-29) were observed. The proton resonances of the two isomers showed an approximately 2:1 (major: minor) ratio (**Spectrum 4.4.4.1**). The ^{13}C-NMR and DEPT-135 spectra (**Spectrum 4.4.5**) exhibited the corresponding carbon resonances, which were assigned to three methyl (C-21, C-26, and C-27), one methylene (C-23), three methine (all oxygenated, C-22, C-28, and C-29) and three quaternary (one oxygenated, C-20; two olefinic, C-24 and C-25) carbon atoms. By comparing signal intensities, as well as using 2D-NMR experiments such as COSY, HSQC and HMBC, it was possible to assign the proton and carbon resonances of both isomers. An HMBC experiment showed the long-range correlations between the olefinic carbon resonances (C-24 and C-25) at δ 127.0/131.2 and 129.4/130.4, and four methyl resonances (Me-26 and Me-27) at δ 1.79/1.75 and 1.80/1.75, respectively. These assignments assumed that both methyl groups are olefinic. The most significant differences were observed for the chemical shifts of the proton and carbon resonances assigned as H-22 ((δ3.19 dd, J = 12.1 and 2.0 Hz, **4** Minor; δ 3.74 dd, *J* = 12.0 and 2.0 Hz, **5** Major;) and C-22 (δ 81.8, **4** Minor; δ 75.0, **5** Major). These differences suggest that the isomerisation is a consequence of the stereochemistry of the substituent at C-22. Moreover, in the HMBC experiment, the long-range correlation between C-22 and H-29, as well as between C-24 and H-29, supported the ether linkage as being between C-22 and C-29. The chemical shift values assigned to H-29 (δ 5.16 d, *J* = 1.1 Hz, **5**; δ 4.51 d, *J* = 1.2 Hz, **4**) and C-29 (δ 96.5, **5**; δ 97.3, **4**) strongly support the presence of a cyclic hemiacetal functionality (Hu *et al*., 2014). This assumption, or in other words, the presence of a six-membered ring at the side chain was also revealed by the unsaturation degree being eight. On the other hand, in the ^{13}C-NMR spectrum, the chemical shift values(δ) attributed to C-22 (δ 75.0) and C-29 (δ 96.5) for major compound **5** were in good agreement with those of ajuga acetalsterone A (Coll *et al*., 2007), which supports the conclusion of a similar stereochemistry at C-22. Furthermore, the COS (**Spectrum 4.4.6**) correlation between the hemiacetal protons (H-29) and an oxygenated proton (H-28) as an AB system for both isomers supported the notion that the stereoisomerism arises from the side chain.

HMBC (**Spectra 4.4.8.1&2**) correlations between C-22 of both isomers (δ 81.5 and 75.0; **4** and **5**, resp.) and H-29 (δ 4.51 and 5.16; **4** and **5**, resp.), as well as between C-25 (δ 130.9 and 131.2; **4** and **5**, resp.) and H-28 (δ 4.41 and 4.36, **4** and **5**, resp.), strongly supported the conclusion that the these AB systems arise from the side chain of compounds **4** and **5**. Additional important observations for the AB systems assigned to compounds **4** and **5** were the small coupling constant values ($J_{28,29} = J_{AB}$ = 1.1 and 1.2 Hz), respectively. These results strongly suggest that the isomerization did not arise from the stereochemistry of the hemiacetal proton. The relative stereochemistry of the side chain of both isomers was studied by NOESY (**Spectrum 4.4.9 and Figure 4.6**), which showed correlation between H-22 (δ 3.19 dd, J = 12.1 and 2.0 Hz) of minor isomer (**4**) and H-29 (δ 4.51 d, J = 1.2Hz; minor, **4**), while H-22 (δ 3.74 dd, J = 12.0 and 2.0 Hz) of major isomer (**5**) showed NOESY correlation with one of the olefinic methyl groups, Me-26 (δ 1.79 d, J = 1.3 Hz). The NOESY experiment (Figure 4.6) displayed further correlations between H-2/H-9, H-11/Me-19 and H-11-Me-18 for the tetracyclic steroid skeleton. Based on these results, the isomeric structures of compounds **4** and **5** occurring in the isolated mixture are proposed to be 22*R* and 22*S* stigmast-7-en-29-al, 2β,3β,11α,20α,22,28-hexahydroxy-6-oxo, cyclic 22,29-hemiacetal, and the proposed trivial names are rhapocasterones A and B, respectively.

Table 4. 8. The ^{1}H and ^{13}C-NMR Data for 5 (RA-6&8: Rhapocasterone A&B) Minor.

C/H	DEPT	δ_C, ppm	δ_H ppm, J (Hz)	HMBC (from C to H)
1	CH_2	39.0	2.38 dd (12.7/5.0) H-1eq 1.39 dd (12.7/12.7) H-1ax	Me-19
2	CH	68.9	4.02 ddd (12.0/7.0/3.4)	H-3
3	CH	68.5	3.96 br s	H-5
4	CH_2	33.2	1.78† 1.70†	H-5
5	CH	52.7	2.34 dd (13.2/2.9)	H-7, Me-19
6	C	206.7	-	H-1eq, H-5
7	CH	122.7	5.81 d (2.2)	H-5, H-9
8	C	165.7	-	H-9
9	CH	42.8	3.16 dd (9.0/2.5)	H-5, H-7, Me-19
10	C	39.9	-	H-5, H-9, Me-19
11	CH	69.4	4.11 ddd (15.8/10.2/6.6)	H-9, H-7, Me-18

12	CH_2	43.6	2.22 dd “t” (12.0/12.0) 2.10 dd (12.0, 6.3)	Me-19
13	C	48.3	-	Me-18
14	C	84.9	-	H-7, H_2-12, Me-18
15	CH_2	31.8	1.97 m 1.60 m	H-17
16	CH_2	21.7	1.99† 1.75†	
17	CH	50.4	2.43 dd “t” (8.3)	Me-18, Me-21
18	CH_3	19.1	0.84 s	H_2-12
19	CH_3	24.6	1.06 s	H-5, H-9
20	C	77.1	-	Me-21, H-22
21	CH_3	21.6	1.33 s	H-22
22	CH	81.5	3.19 dd (12.1/2.0)	Me-21,
23	CH_2	26.1	2.48 dd 2.08 dd	
24	C	129.4	-	H-22, Me-26, Me-27
25	C	130.9	-	Me-26, Me-27
26	CH_3	20.06	1.80 d (1.6)	Me-27
27	CH_3	20.59	1.75 s	Me-26
28	CH	68.5	4.41 d (1.2)	
29	CH	97.3	4.51 d (1.2)	

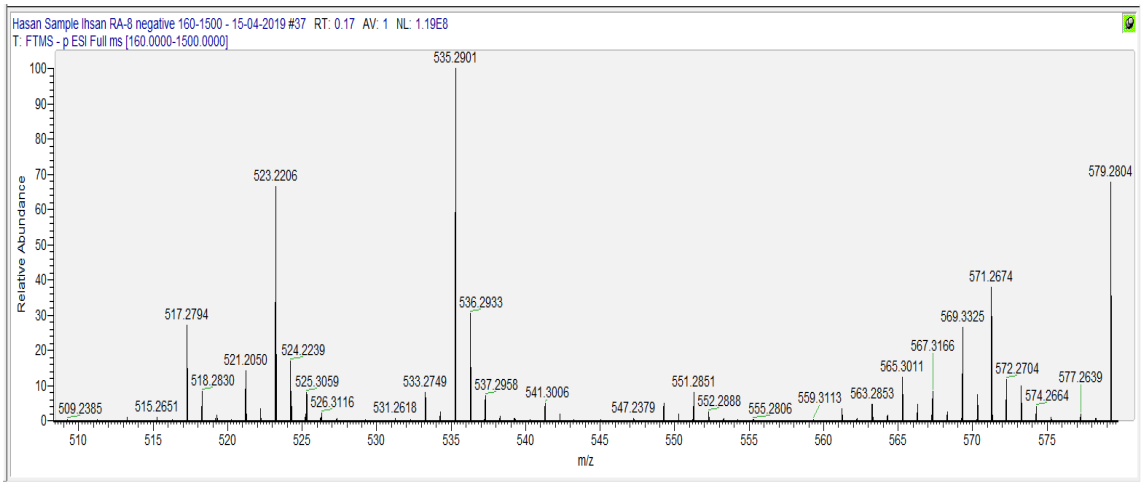

Spectrum 4.4.1. (-)-HRMS of isomeric mixture 4&5 $[M-H]^-$ m/z 535.2901.

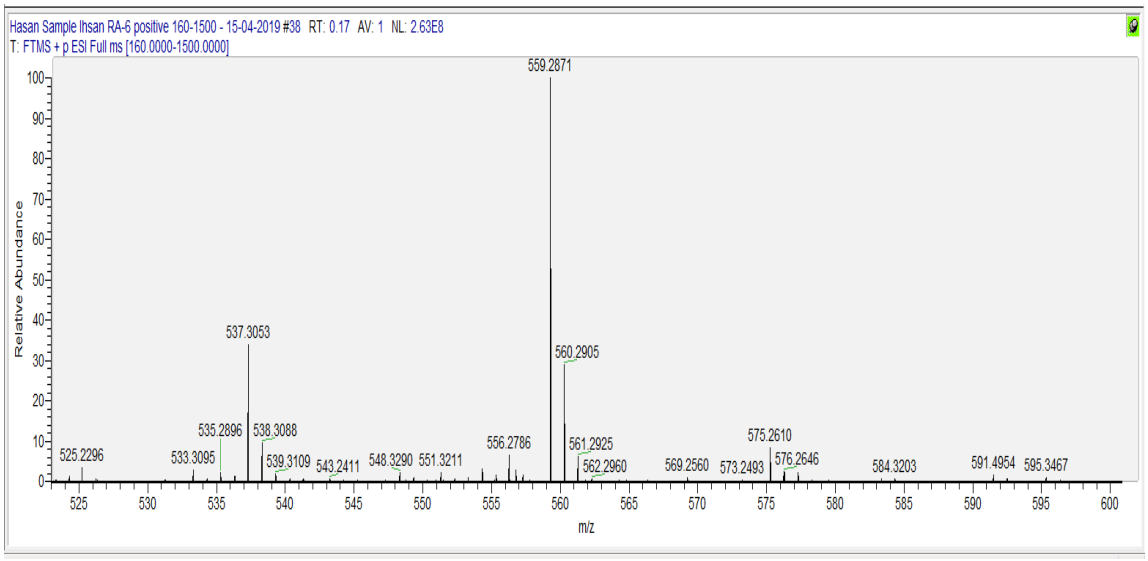

Spectrum 4.4.2. (+)-HRMS of isomeric mixture 4&5 $[M]^+$ m/z 537.3053; $[M+Na]^+$ m/z 559.2871.

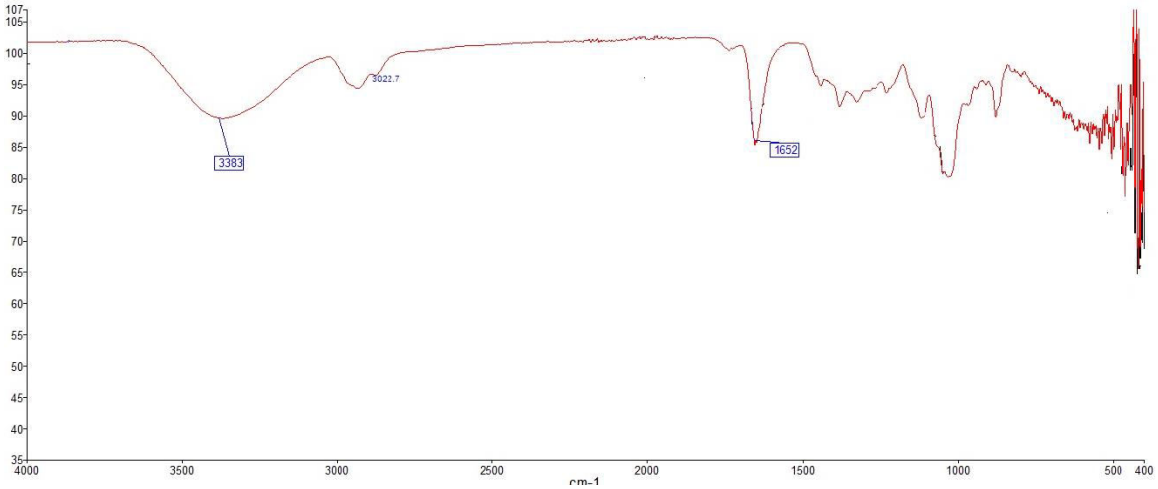

Spectrum 4.4.3. FT-IR of isomeric mixture 4&5.

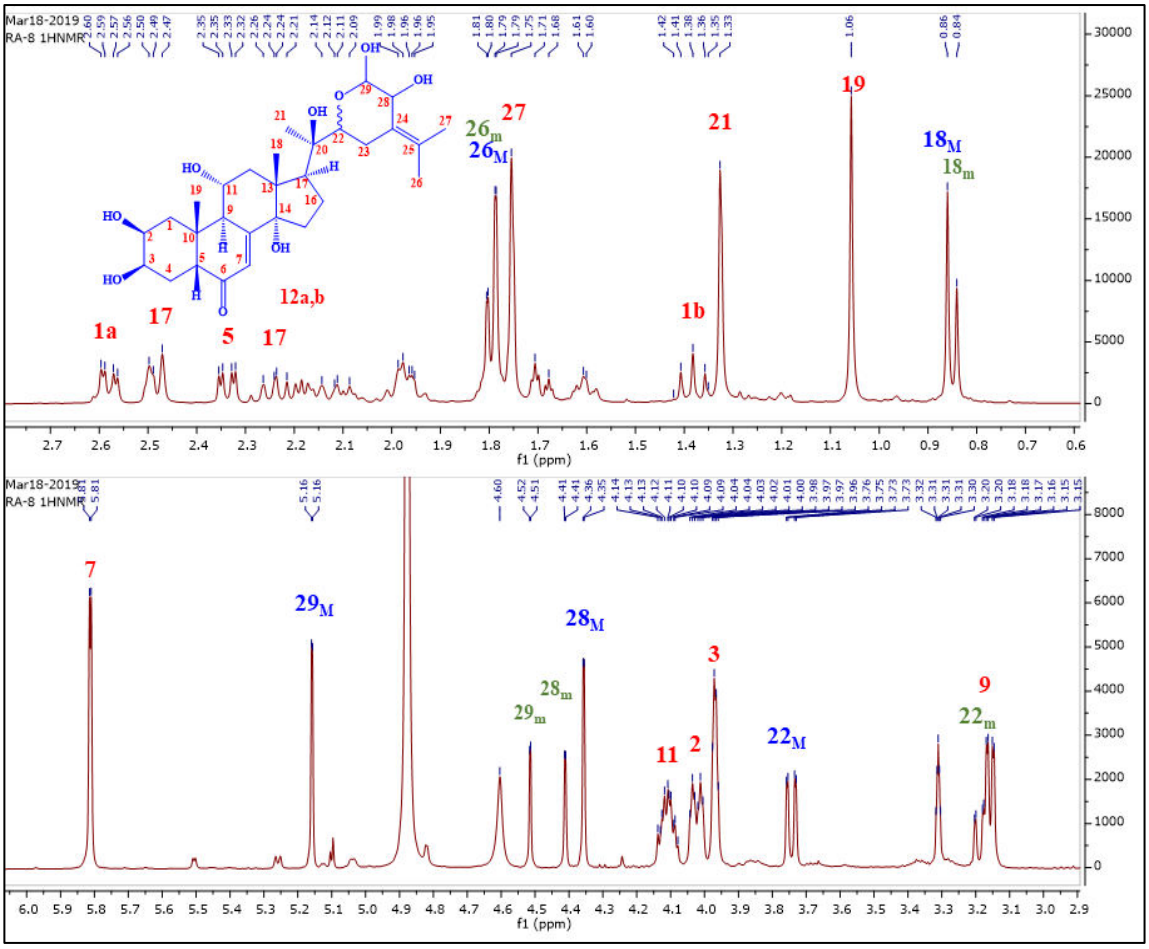

Spectrum 4.4.4. [1]H-NMR Spectrum of 4&5 (RA-6&8: Rhapocasterone A&B) (500 MHz, MeOD).

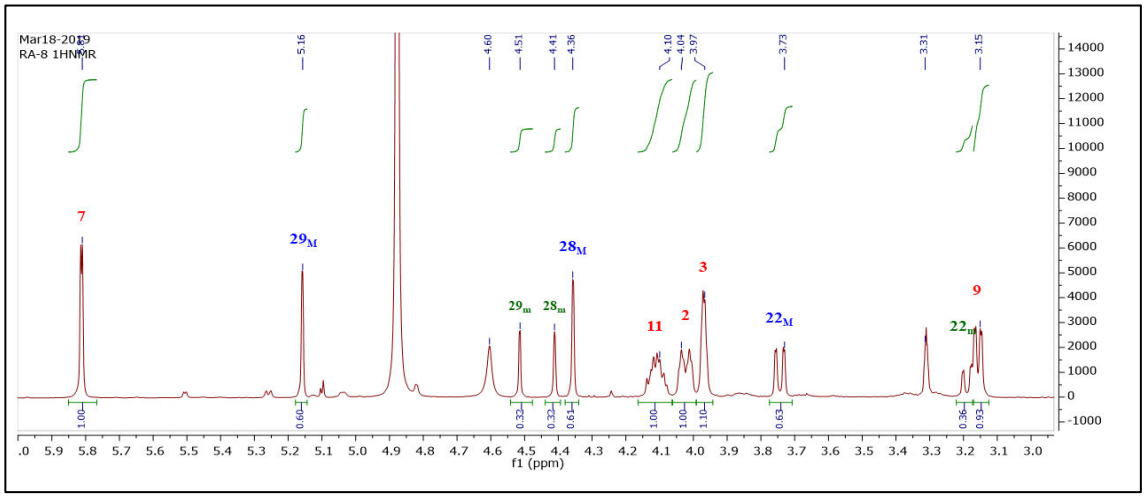

Spectrum 4.4.4.1. [1]H-NMR Spectrum of 4&5: Integration of the protons of the isomers.

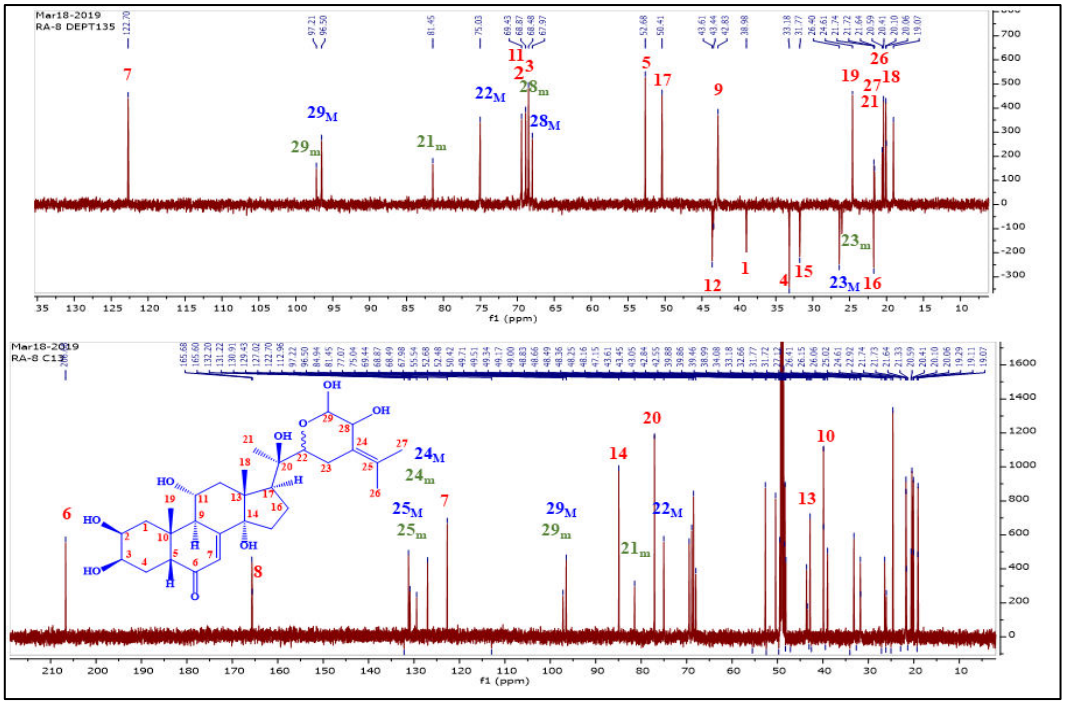

Spectrum 4.4.5. ^{13}C-NMR (A) and DEPT-135 (B) Spectra of 4&5 (RA-6&8: Rhapocasterone A&B) (125 MHz, MeOD).

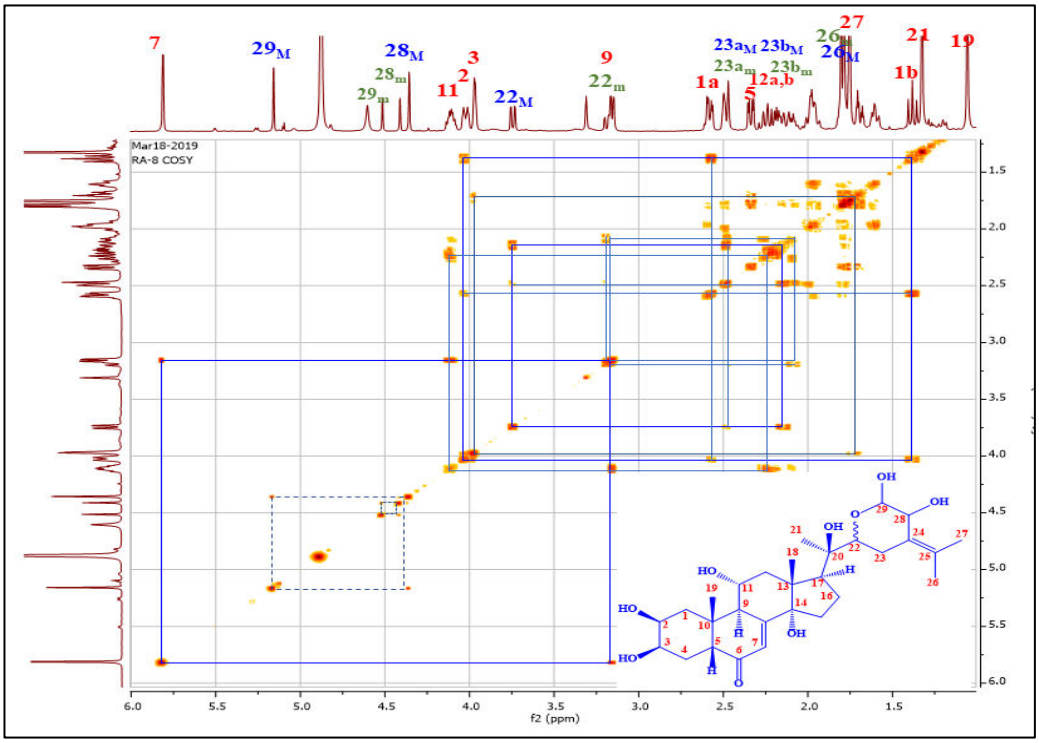

Spectrum 4.4.6. COSY of 4&5 (RA-6&8: Rhapocasterone A&B).

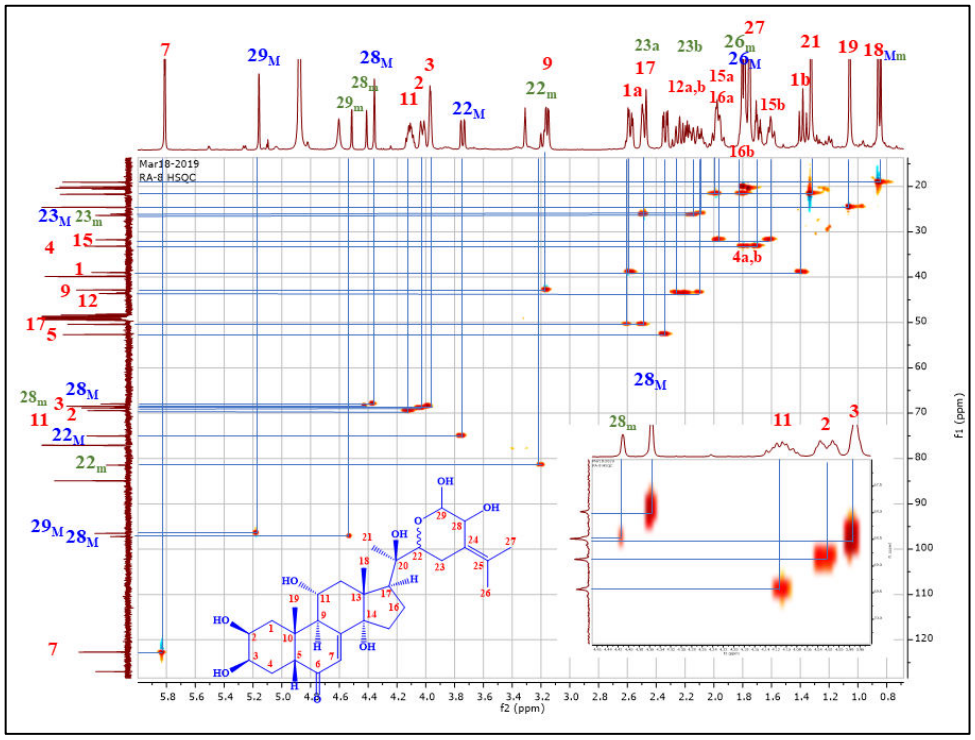

Spectrum 4.4.7. HSQC of 4&5 (RA-6&8: Rhapocasterone A&B).

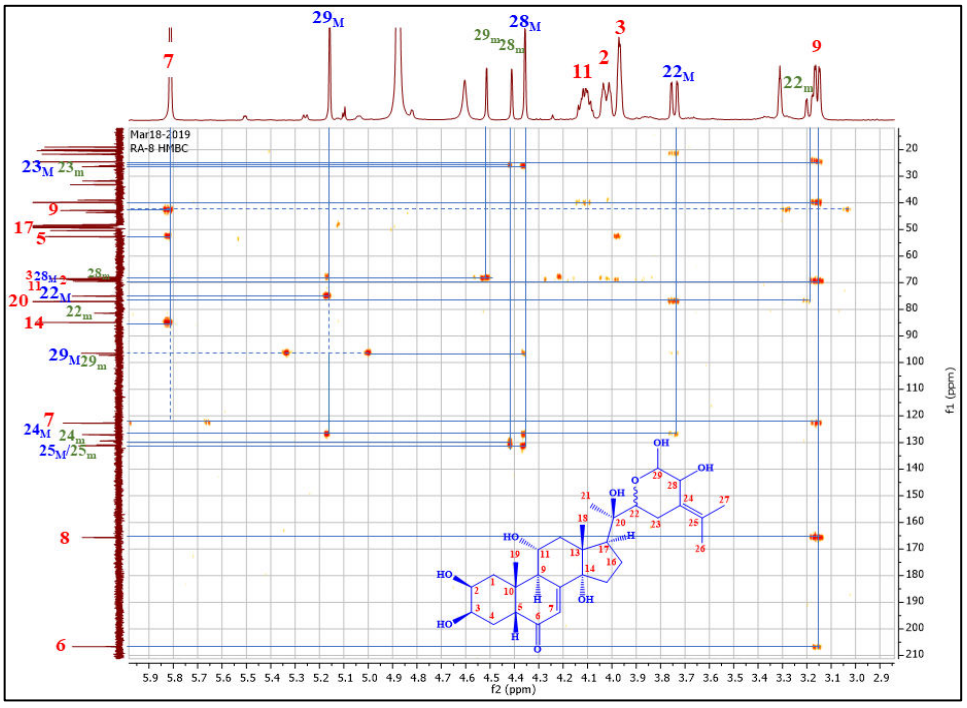

Spectrum 4.4.8.1. HMBC of 4&5 (RA-6&8: Rhapocasterone A&B) (^{1}H: 2.8 – 6.0 ppm; ^{13}C: 10 – 210 ppm).

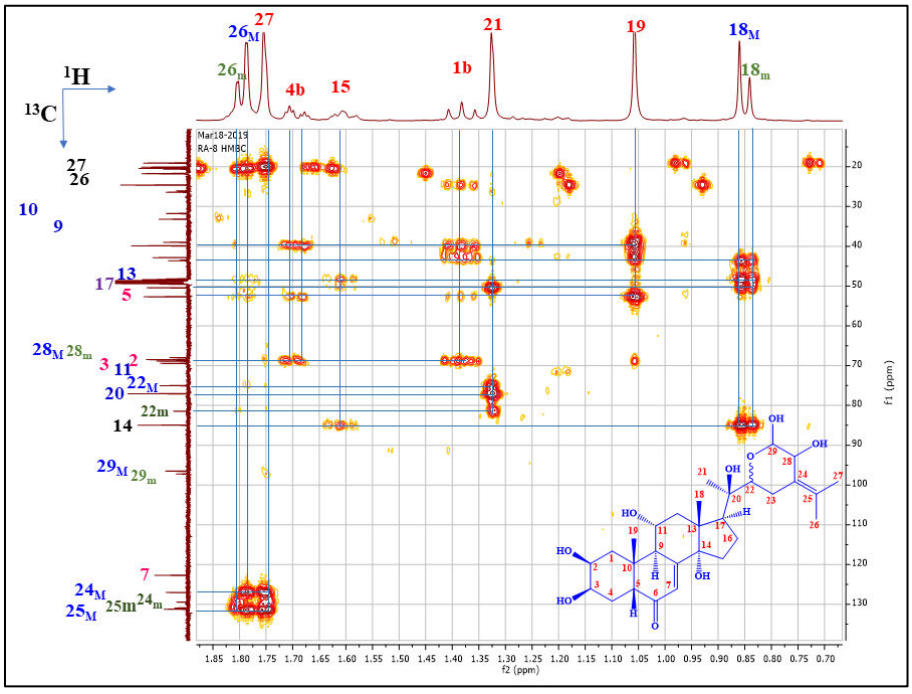

Spectrum 4.4.8. 2. HMBC of 4&5 (RA-6&8: Rhapocasterone A&B) (^{1}H: 0.6 – 1.90 ppm; ^{13}C: 10 – 140 ppm).

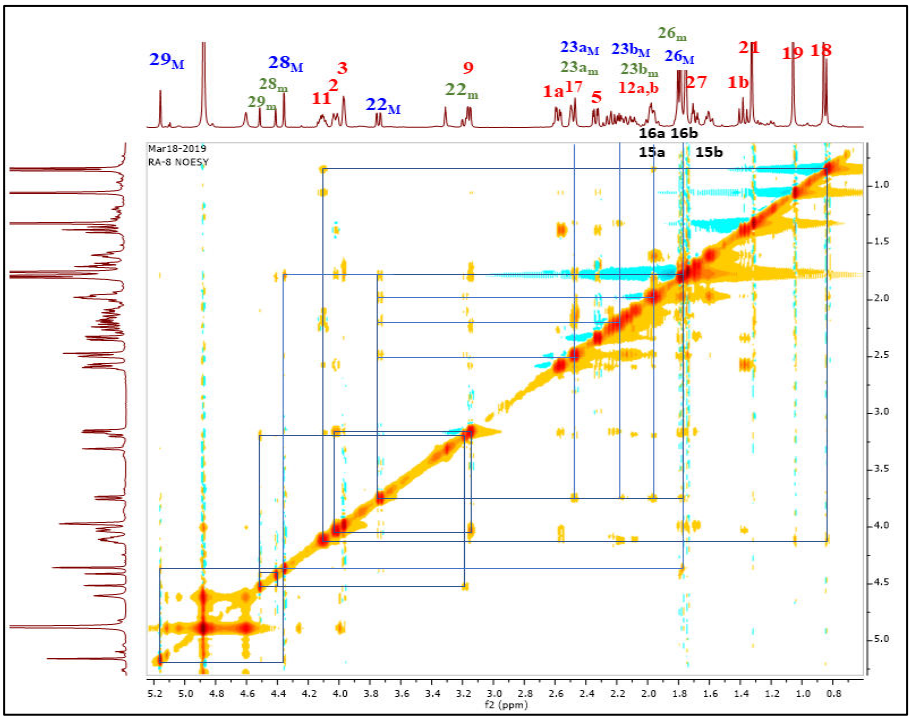

Spectrum 4.4.9. NOESY of 4&5 (RA-6&8: Rhapocasterone A&B).

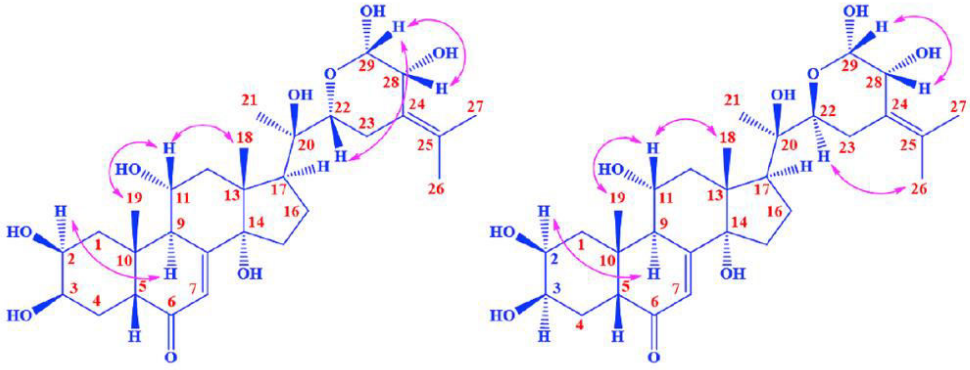

Compound **4** (minor)	Compound **5** (major)

Figure 4. 6. NOESY of 4&5 (Rhapocasterone A&B).

4.4.1. RA-6Ac1 (Pentaacetyl- Rhapocasterone A)

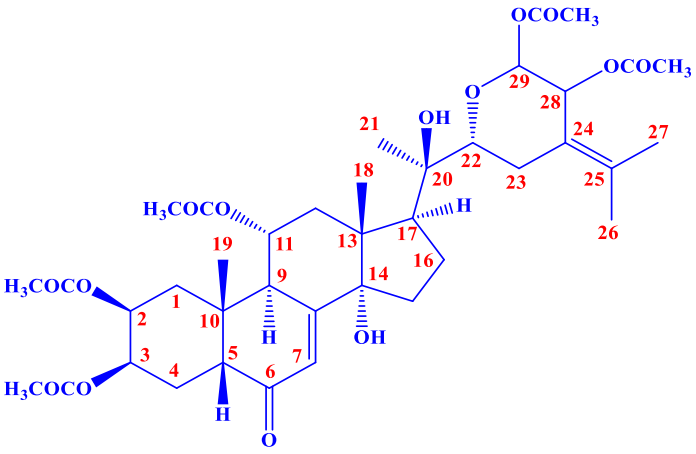

Chemical Formula: $C_{39}H_{54}O_{14}$
Exact Mass: 746,35
Molecular Weight: 746,85

Pentaacetyl-Rhapocasterone A (4a)

Unsaturation Degree: 13

RA-6Ac1 (**4**): $[\alpha]_D^{20}$ -11.8° (c 0.07, MeOH)

Acetylation of the mixture of **4** and **5** yielded two compounds, **4a** and **5a**. The mixture of **4a** and **5b** was separated by silica gel column chromatography using toluene-acetone (6:1) as the solvent system. The elucidation of the structures of the corresponding acetyl derivatives, **4a** and **5a** which are both pentaacetylated derivatives, was based on a comparison of the chemical shift values assigned to the C-22 resonances of both isomers and their acetyl derivatives (δ 81.5 and 81.24, for **4** and **4a**; δ 75.0 and 76.69, for **5** and **5a**; resp.). Thus, the more polar acetylated derivative is **4a** and the more lipophilic one is **5a**.

		d_C ppm		**d_C ppm**	
C Atom	**DEPT 135**	**4 RA-8m**	**4a RA-6Ac2**	**5 RA-8M**	**5a RA-6Ac1**
22	**CH**	**81.5**	**81.24**	**75.0**	**76.69**

The remaining ^{13}C-NMR resonances of **4a** and **5a** were in accordance with those of **4** and **5**, respectively (**Tables 4.9 and 4.10**). Their HRMS showed the same molecular weight for both confirming that the distinction between **4a** and **5a** lies only in their stereochemistry. Positive and negative ion HRMS of **4a** and **5a**, exhibited $[M+H]^+$ at m/z 747.3472 and 747.3392, $[M+Na]^+$ at m/z 769.3395 and 769.3396 and $[M-H]^-$ at m/z 745.3402 and 745.3438, respectively, corresponding with the same molecular formulae, $C_{39}H_{54}O_{13}$ (calc. Mol. wt. 746.35) with thirteen degrees of unsaturation. However, the optical rotation values were reversed {**4a**: $[\alpha]_D^{20}$ +42.7° (c 0.15, MeOH); **5a**: $[\alpha]_D^{20}$ -11.8° (c 0.07, MeOH)}.

Table 4. 9. The ^{1}H and ^{13}C-NMR Data of Compound 4a (RA-6Ac1 = Pentaacetyl-Rhapocasterone A) (500 MHz, CD3OD).

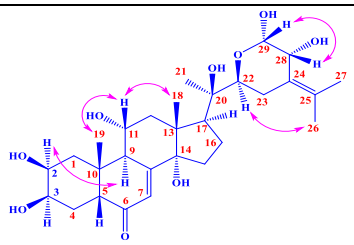

C/H	DEPT	δ_C, ppm	δ_H ppm, *J* (Hz)	HMBC (from C to H)
1	CH_2	35.78	1.62 m 1.54 m	Me-19
2	CH	68.49	5.22†	H-3
3	CH	66.75	5.34 br s	H-5
4	CH_2	29.21	1.76†, 1.73†	H-5
5	CH	51.56	2.32†	H-7, Me-19
6	C	201.27	-	H-1eq, H-5
7	CH	122.81	5.86 d (2.3)	H-5, H-9
8	C	161.35	-	H-9
9	CH	38.26	3.36 dd (9.0/2.5)	H-5, H-7, Me-19
10	C	39.34	-	H-5, H-9, Me-19
11	CH	71.24	5.24 m	H-9, H-7, Me-18
12	CH_2	37.43	2.33† 2.04†	Me-19
13	C	47.10	-	Me-18
14	C	84.03	-	H-7, H_2-12, Me-18
15	CH_2	31.67	2.00† 1.53†	H-17
16	CH_2	20.54	2.01 - 1.69†	
17	CH	48.96	2.27†	Me-18, Me-21
18	CH_3	18.07	0.86 s	H_2-12
19	CH_3	23.81	1.05 s	H-5, H-9
20	C	75.21	-	Me-21, H-22
21	CH_3	21.7	1.22 s	H-22
22	CH	76.69	3.51 brd (12.2)	Me-21,
23	CH_2	25.92	2.42 brd (13.6) 1.99†	
24	C	120.95	-	H-22, Me-26, Me-27
25	C	133.94	-	Me-26, Me-27
26	CH_3	20.53	1.72 s	Me-27
27	CH_3	20.36	1.76 s	Me-26
28	CH	67.36	5.46 br s	
29	CH	92.37	5.99 br s	

Additional acetoxy signals (***C***OCH_3): d 170.37, 170.23, 170.12, 169.88 and 169.11; ($CO\mathbf{\underline{C}H_3}$): d_C 21.29, 21.03, 21.00, 20.89 and 21.10; d_H 2.04 s, 2.01 s, 2.00 s, 1.92 s and 1.89 s.
†) *J* values are not clear due to overlapping.

The assignments of all proton and carbon resonances of **4a** and **5a** were based on 1D-NMR experiment ^{1}HNMR, ^{13}CNMR and DEPT-135 and 2D-NMRexperiments COSY, HMBC and the relative stereochemistry was studied by NOESY and ROESY experiments. The signals arising from the tetracyclic steroid skeleton agreed with the proposed parent structure oxygenated at C-2, C-3, C-6, C-11, and C-14, of which C-6 and C-14 are quaternary carbons (^{13}C& DEPT-135& HSQC, **Spectra 4.4.1.5, 4.4.1.6 and 4.4.2.5**). The ^{1}H NMR spectra of **4a** and **5b** (**Spectrum 4.4.1.4 and 4.4.2.4**) exhibited five acetoxymethyl resonances for each. The proton resonances attributed to H-2, H-3, H-11, H-28, and H-29 showed downfield shifts compared with those of **4** and **5** (**Tables 4.9 and 4.10**), thereby indicating the sites of the acetylation. Furthermore, the chemical shift values for the proton and carbon resonances, as well as the coupling constants of the corresponding protons of **4a** and **5a**, did not show any significant differences, which confirmed the similar substitution pattern and stereochemistry for the steroid skeleton depicted for **4** and **5**. As expected, the most substantial distinctions were observed for the signals arising from the side chain. In the ^{1}H-NMR spectra of **4a** and **5a**, the signals of H-28 and H-29 showed a downfield shift indicating acetylation at these positions (δ5.72 and 5.49 for **4a**: δ 5.46 and 5.99 for **5a**). Despite the lack of observable coupling constants, the proton signals of H-28 and H-29 were observed in the same spin system as the partners of the AB systems (Spectra 4.85 and 4.86), but the chemical shifts of the H-22 protons of **4a** and **5a** were not same as those observed for **4** and **5** (δ 3.29 brd, J = 12.0 Hz: 3.51 brd, J = 12.2 Hz), respectively.

In addition to the different chemical shift values noted for C-22, major differences were observed for the carbon resonances assigned to C-24, C-25, C-28, and C-29. Compared with those of the corresponding signals of **4** and **5**, the signals assigned to C-28 and C-29 of **4a** and **5a** are shifted by ca. 1.2 ppm and 4.0 ppm, respectively, to higher field (δ 67.64 and 67.36, C-28 of **4a** and **5a**, resp.; δ 93.19 and 92.37, C-29 of **4a** and **5a**, resp.). These observations can be explained by the acetylation of the hydroxy groups of the same parent carbon atoms. Additionally, similar effects were observed for the olefinic carbon atoms. Compared with those of the corresponding signals of 4 and 5, the chemical shifts of C-24 were shifted ca. 6.0 ppm to higher field, while C-25 shifted ca. 3.0 ppm downfield (δ 123.16 and 120.95, C-24 of **4a** and **5a**, resp.; δ 134.19 and

133.94, C-25 of **4a** and **5a**, resp.). In the HMBC experiment (**Spectra 4.4.1.9.1, 4.4.1.9.2 and 4.4.2.8**), the $^{13}C,^{1}H$-long-range correlations from C-24 and C-25 to Me-26 and Me-27, as well as between C-24 and H-22, confirmed the proposed structures depicted for **4/4a** and **5/5a**. In the NOESY and ROESY experiments, the only significant correlation was observed between H-22 and H-29 for **4a** (**Spectra 4.4.1.10 and 4.4.1.11**). However, this correlation was missing from the NOESY and ROESY analyses of **5a** (**Spectra 4.4.2.9 and 4.4.2.10**). These observations clearly support the different stereochemistry at C-22 in compounds **4** and **5**.

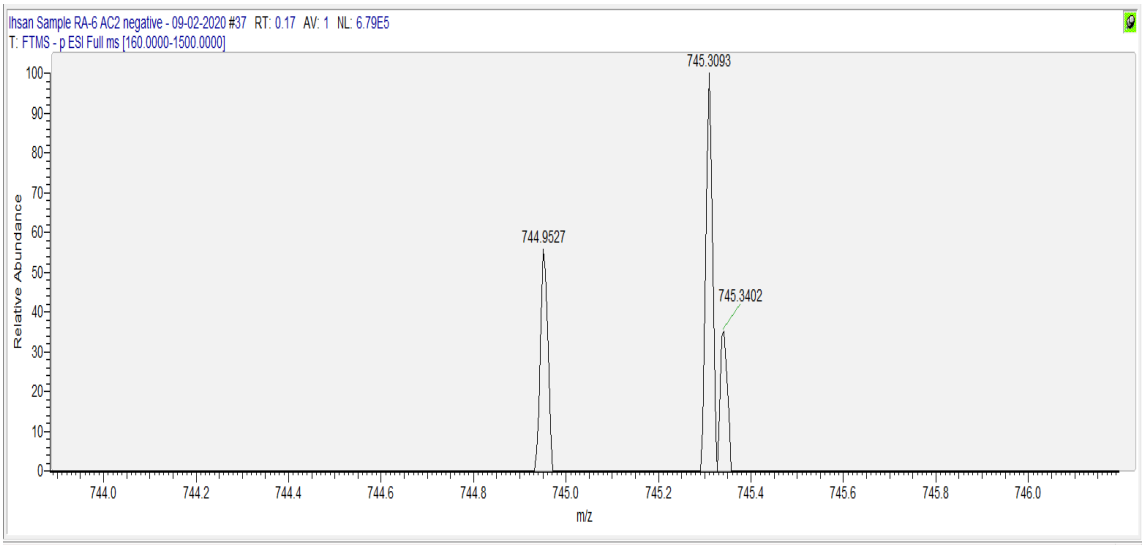

Spectrum 4.4.1.1. (-)-HRMS of Pentaacetyl-Rhapocasterone A (4a) $[M-H]^-$ m/z 745.3402.

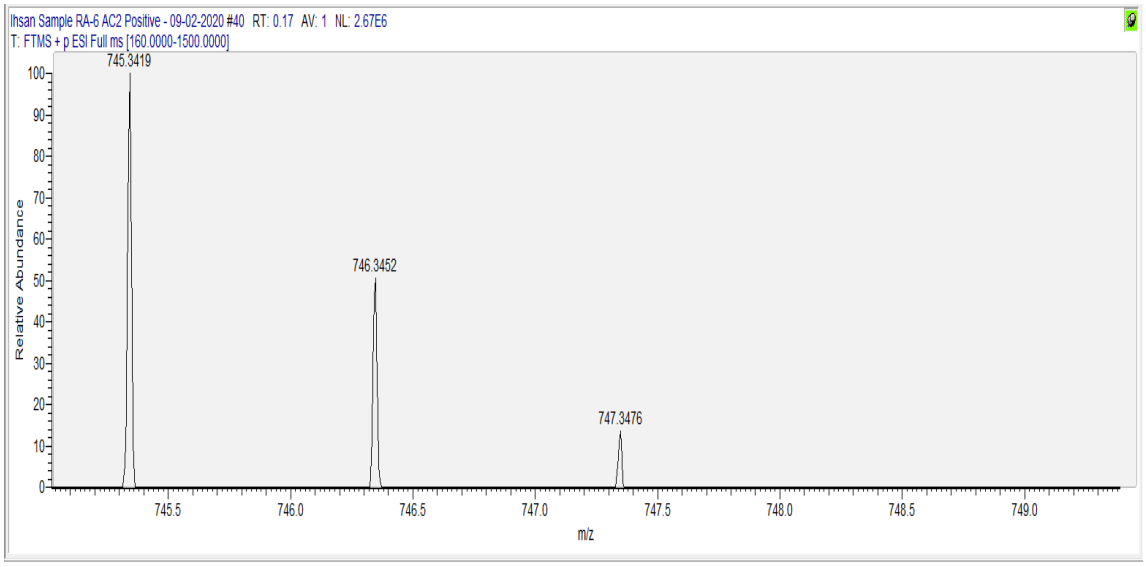

Spectrum 4.4.1.2. (-)-HRMS of Pentaacetyl-Rhapocasterone A (4a) $[M]^+$ m/z 746.3452, $[M+H]^+$ m/z 747.3472.

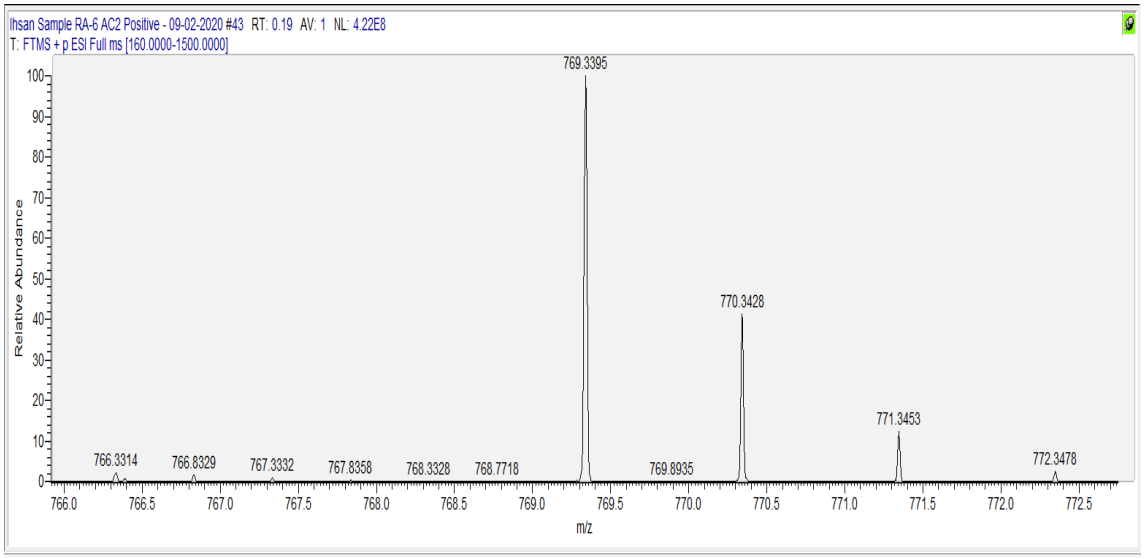

Spectrum 4.4.1.3. (+)-HRMS of Pentaacetyl-Rhapocasterone A (4a) [M+Na]+ m/z 769.3395.

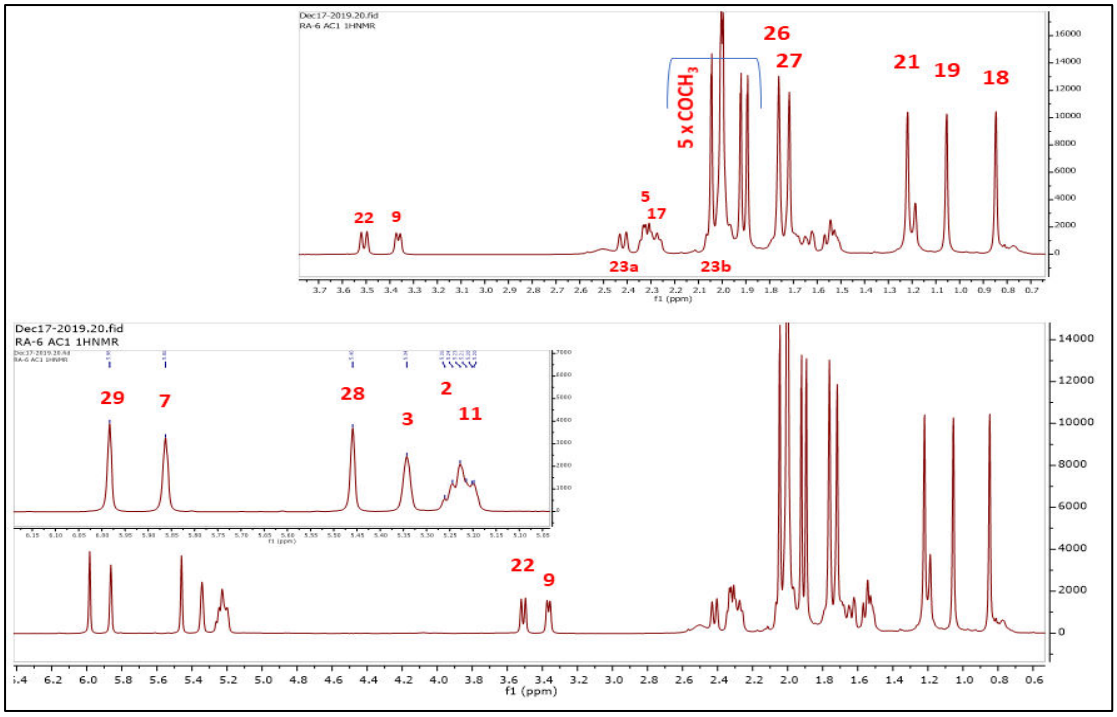

Spectrum 4.4.1.4. ^{1}H-NMR Spectrum of 4 (RA-6Ac1= Pentaacetyl-Rhapocasterone A) (500 MHz, CD_3OD).

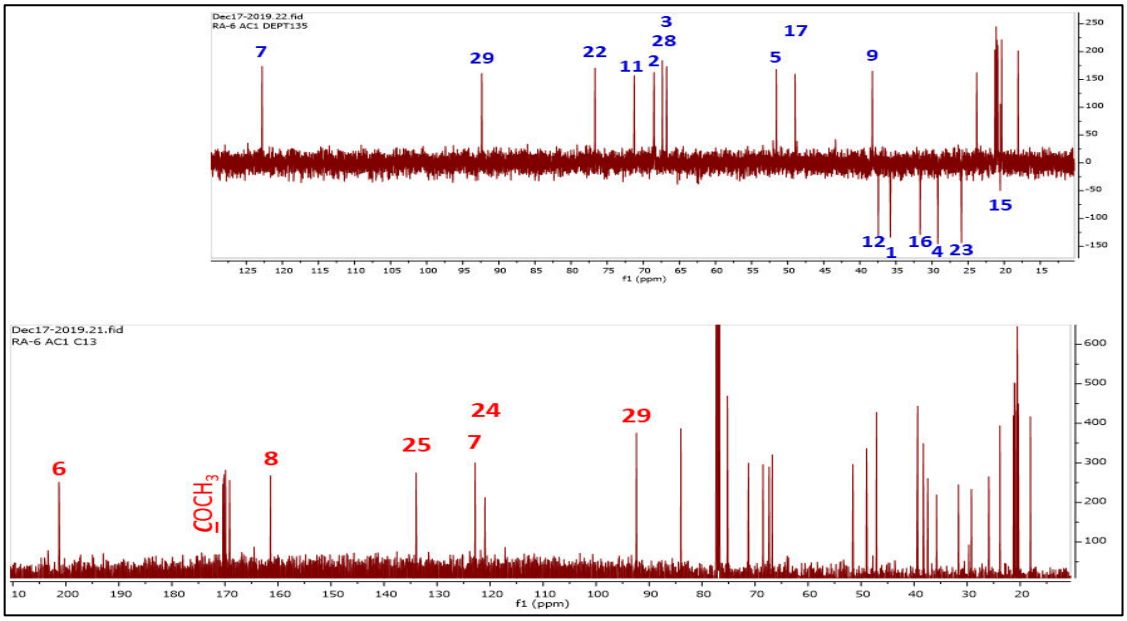

Spectra 4.4.1.5. ^{13}C-NMR Spectrum and DEPT-135 of 4 (RA-6Ac1= Pentaacetyl-Rhapocasterone A) (125 MHz, CD_3OD).

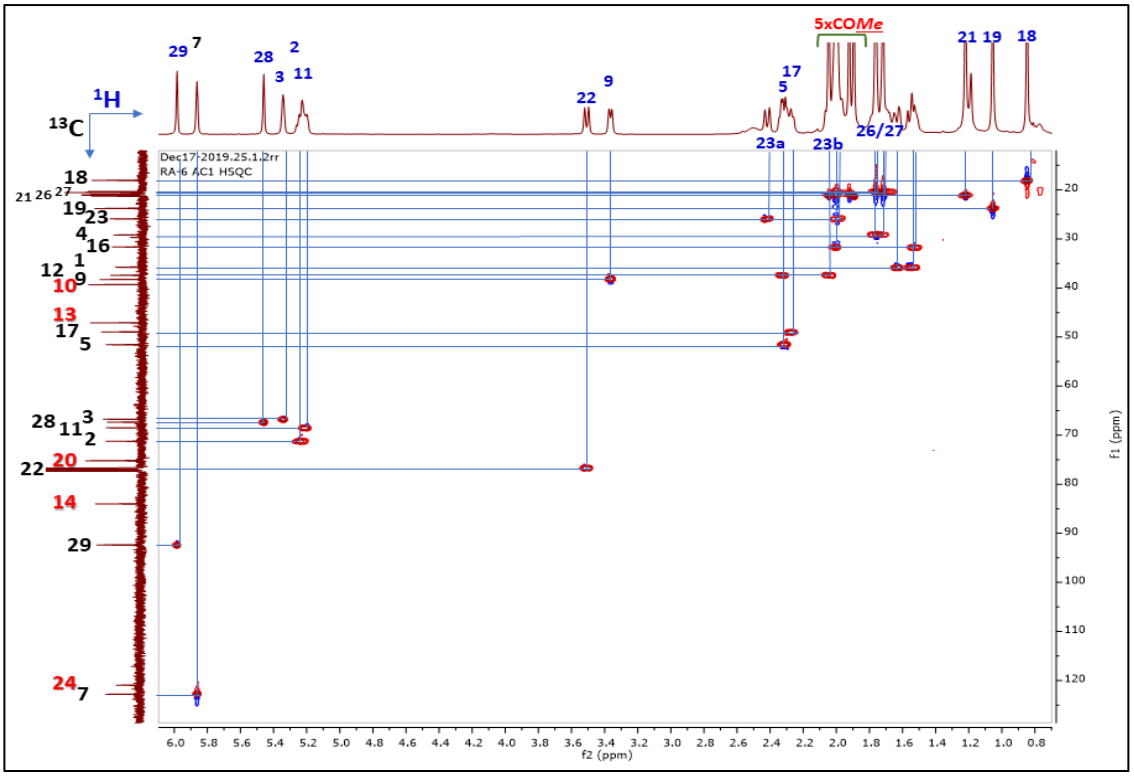

Spectrum 4.4.1.6. HSQC of 4 (RA-6Ac1= Pentaacetyl-Rhapocasterone A).

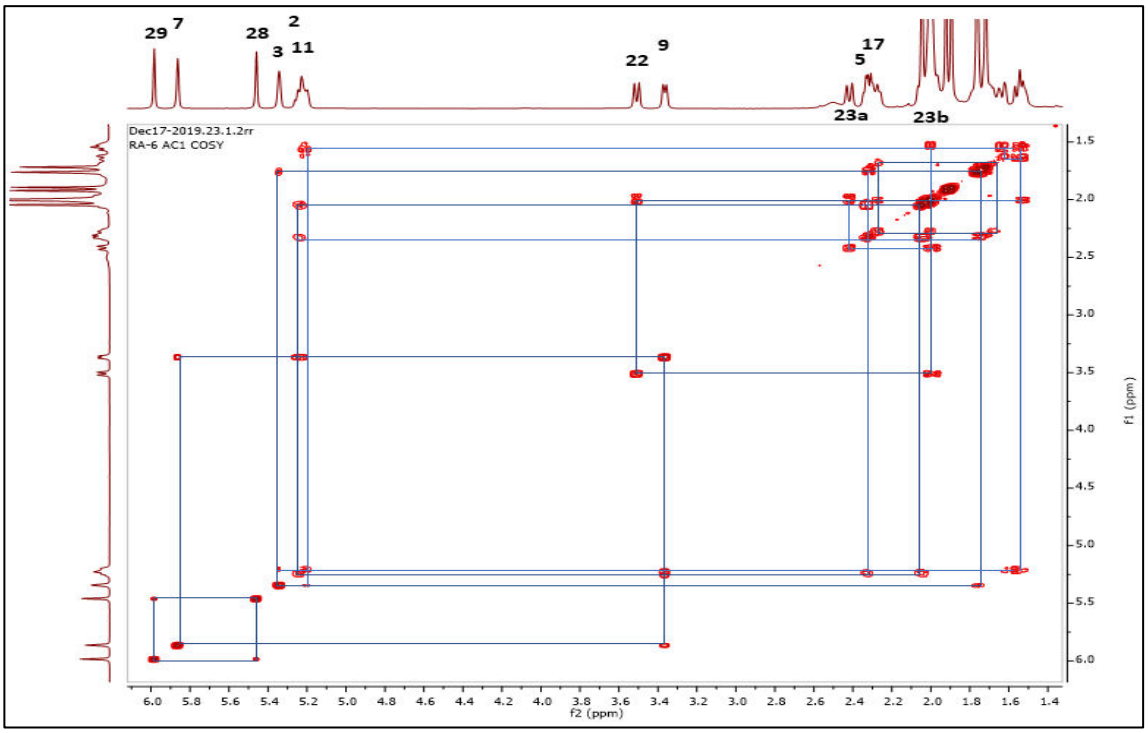

Spectrum 4.4.1.7. COSY of 4 (RA-6Ac1= Pentaacetyl-Rhapocasterone A).

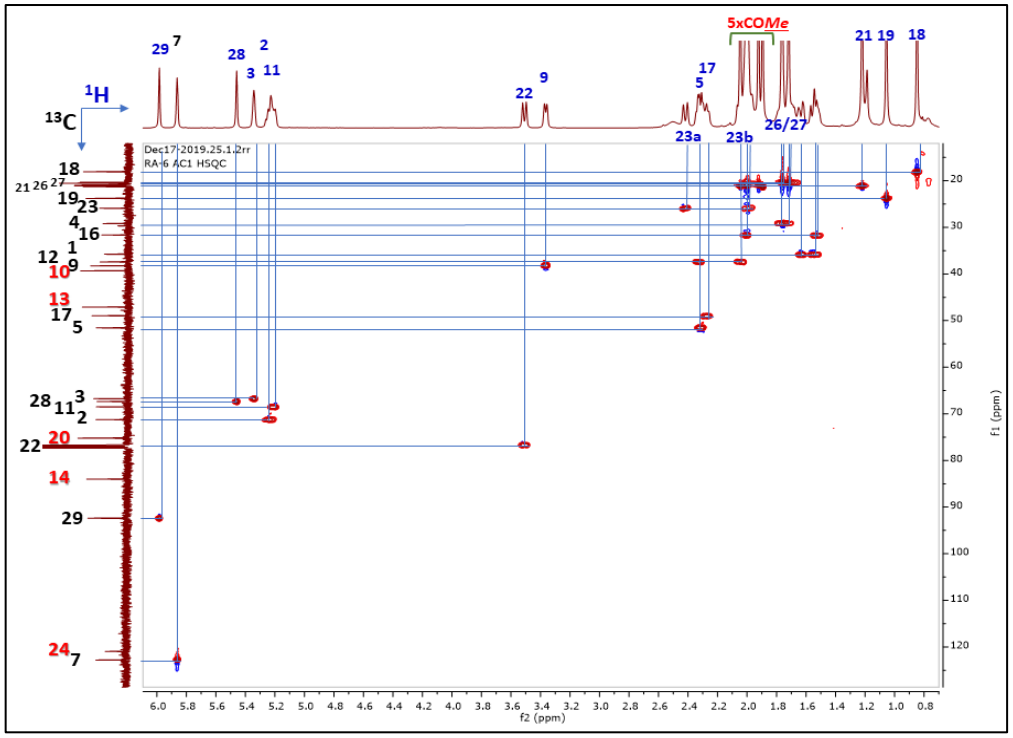

Spectrum 4.4.1.8.1. HSQC of 4 (RA-6Ac1= Pentaacetyl-Rhapocasterone A).

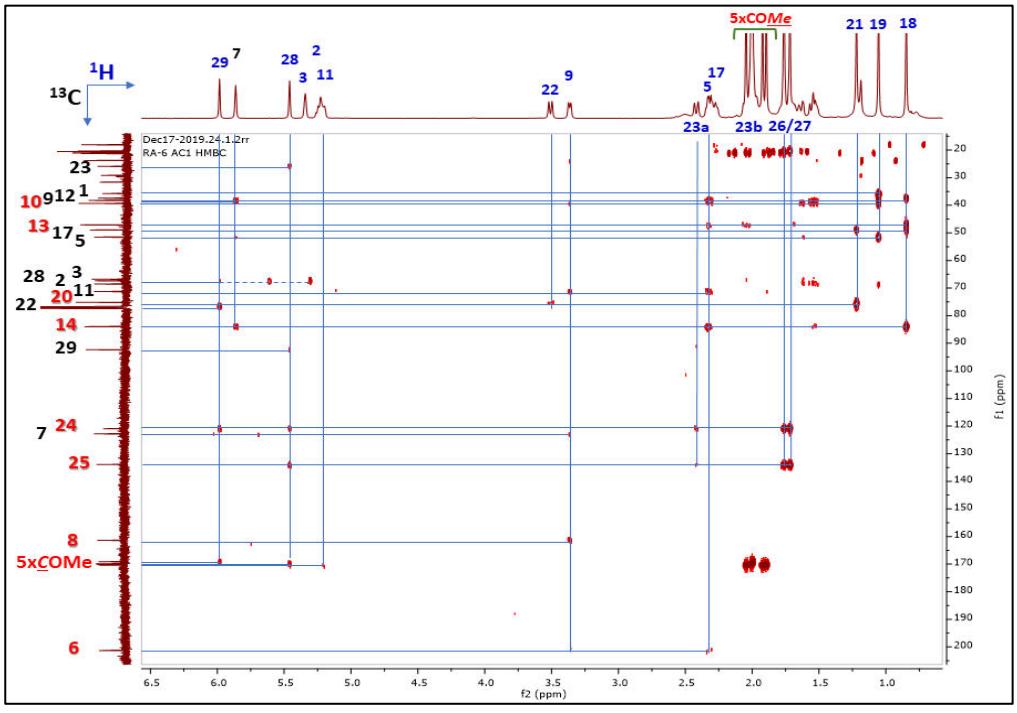

Spectrum 4.4.1.8.2. HSQC of 4 (RA-6Ac1= Pentaacetyl-Rhapocasterone A).

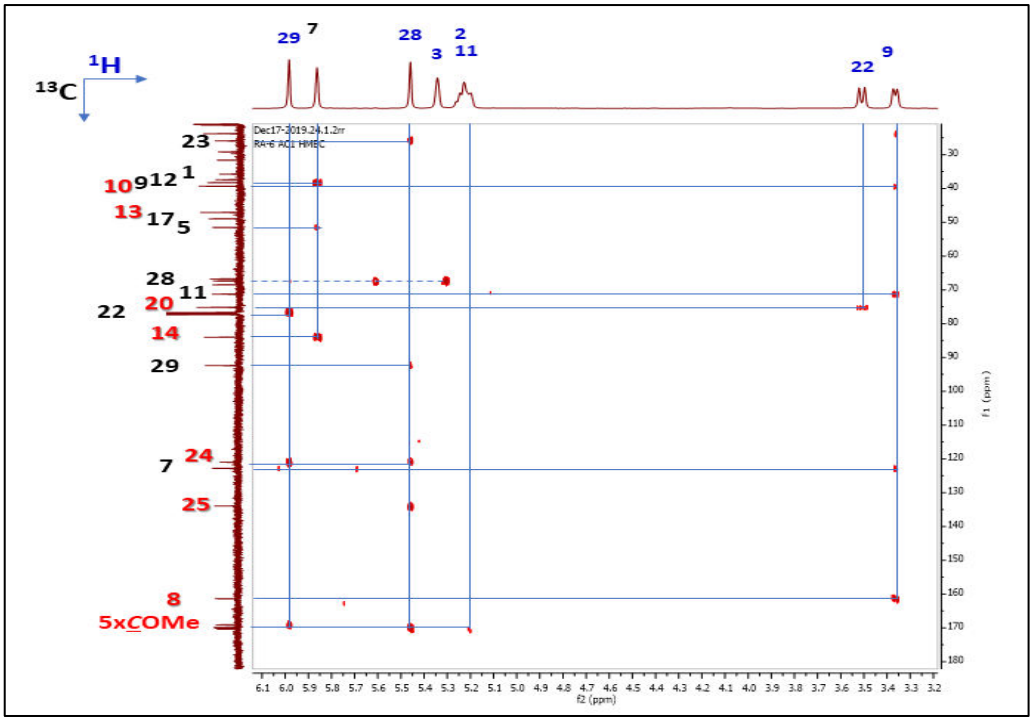

Spectrum 4.4.1.9.1. HMBC of 4 (RA-6Ac1= Pentaacetyl-Rhapocasterone A) (^{1}H: 6.10 – 3.2 ppm; ^{13}C: 20 – 180 ppm).

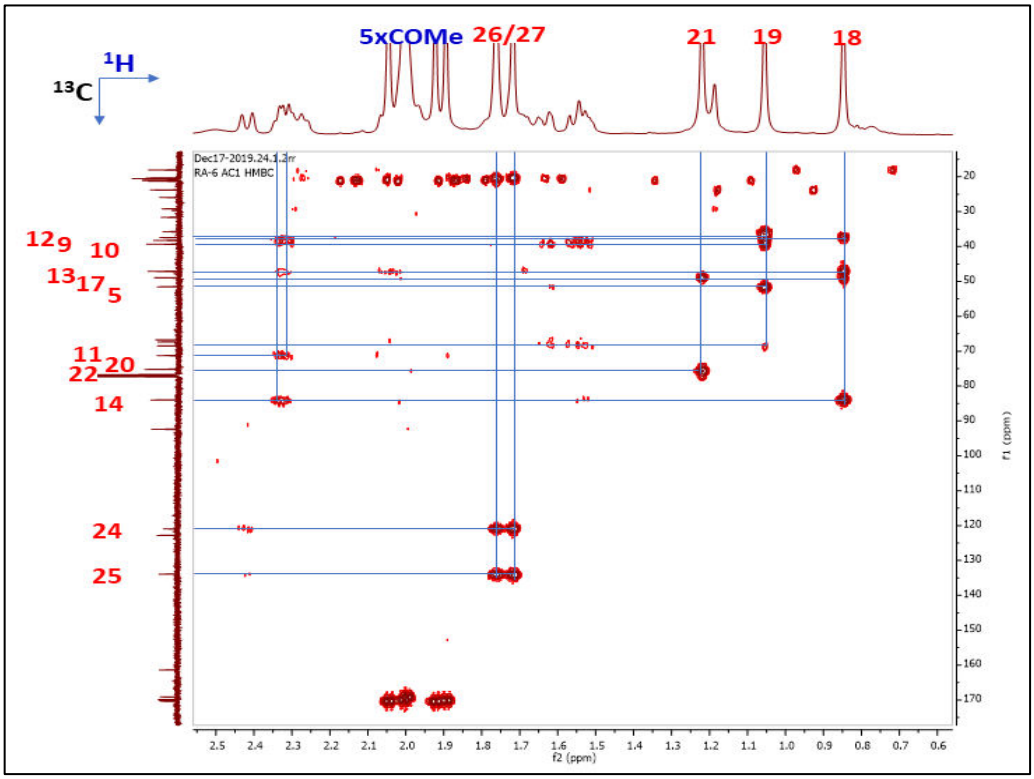

Spectrum 4.4.1.9.2. HMBC of 4 (RA-6Ac1= Pentaacetyl-Rhapocasterone A) (^{1}H: 3.0 – 0.5 ppm; ^{13}C: 10 – 180 ppm)

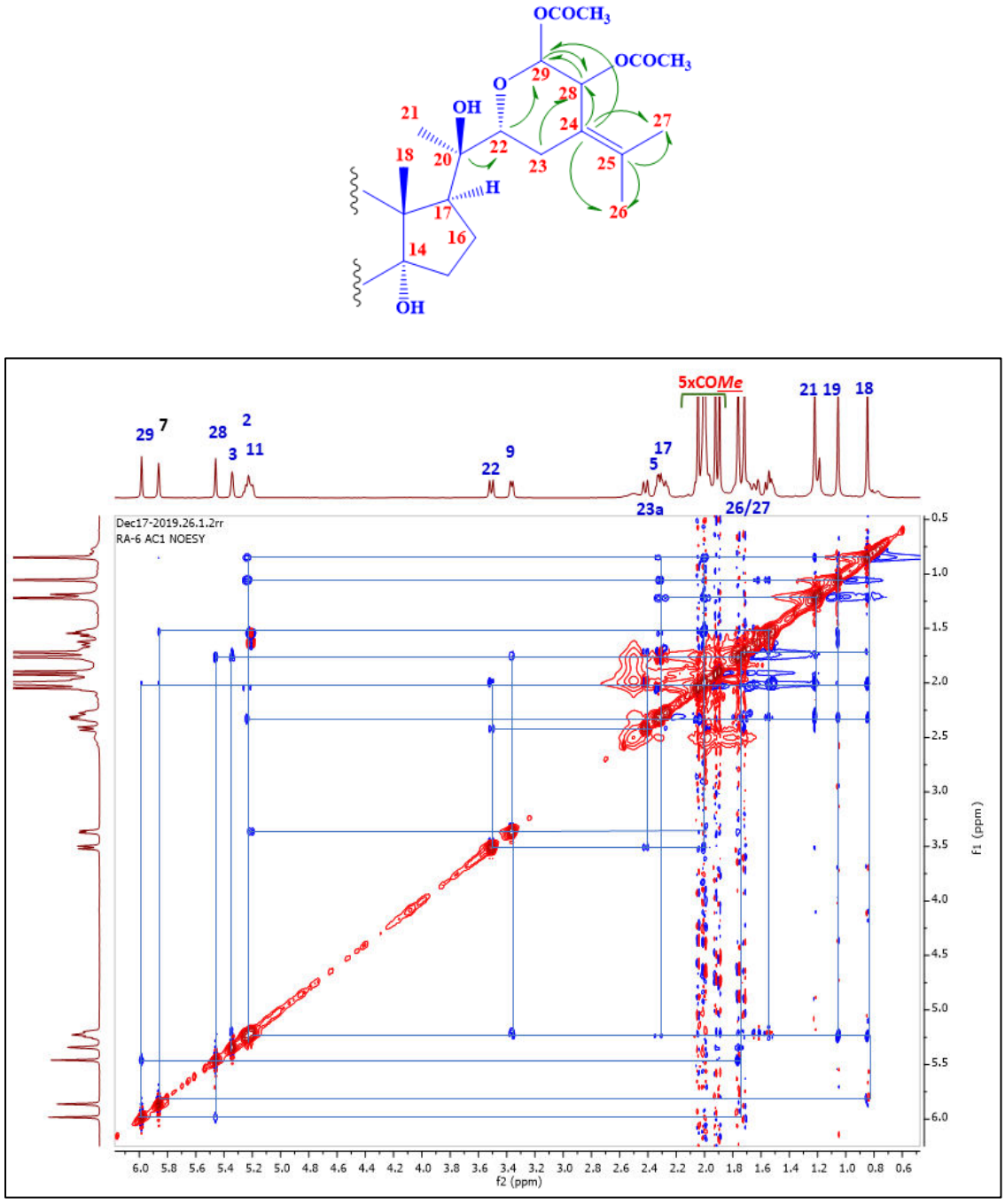

Spectrum 4.4.1.10. NOESY of 4 (RA-6Ac1= Pentaacetyl-Rhapocasterone A)

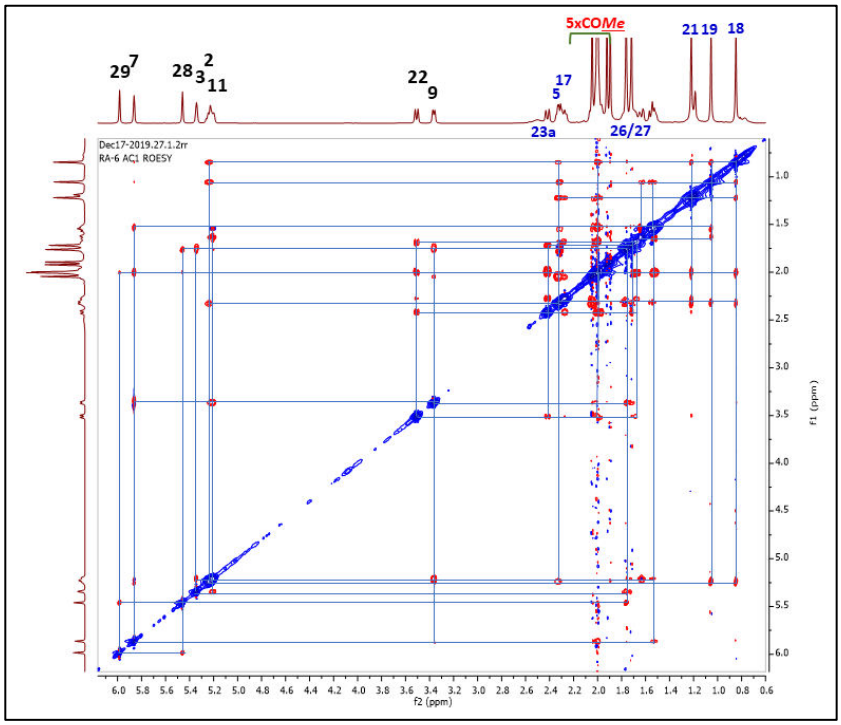

Spectrum 4.4.1.11. ROESY of 4 (RA-6Ac1= Pentaacetyl-Rhapocasterone A).

4.4.2. RA-6Ac2 (Pentaacetyl- Rhapocasterone B)

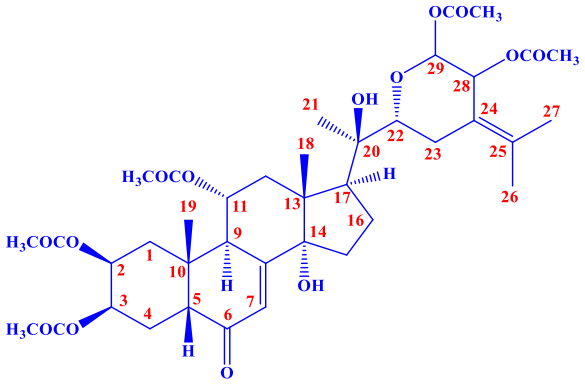

Chemical Formula: $C_{39}H_{54}O_{14}$
Exact Mass: 746,35
Molecular Weight: 746,85

Pentaacetyl-Rhapocasterone B (5a)

Unsaturation Degree: 13

RA-6Ac2 (**5**): $[\alpha]_D^{20}$ +42.7° (c 0.15, MeOH).

Table 4. 10. The ^{1}H and ^{13}C-NMR Data of Compound 5a (RA-6Ac2 = Pentaacetyl-Rhapocasterone B) (500 MHz, CD3OD).

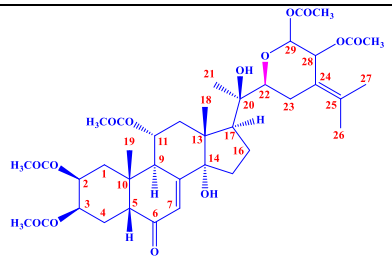

Chemical Formula: $C_{39}H_{54}O_{14}$
Exact Mass: 746,35

C/H	DEPT	δ_C, ppm	δ_H ppm, *J* (Hz)	HMBC (from C to H)
1	CH_2	35.77	1.61 m 1.55†	Me-19
2	CH	68.51	5.20†	H-3
3	CH	66.78	5.34 br s	H-5
4	CH_2	29.12	1.76†	H-5
5	CH	51.58	2.31 dd (11.8/5.8)	H-7, Me-19
6	C	201.30	-	H-1eq, H-5
7	CH	122.75	5.85 d (2.1)	H-5, H-9
8	C	161.41	-	H-9
9	CH	38.23	3.37 dd (8.5/2.4)	H-5, H-7, Me-19
10	C	39.33	-	H-5, H-9, Me-19
11	CH	71.14	5.21†	H-9, H-7, Me-18
12	CH_2	37.21	2.23 dd (12.2/6.5), 2.04†	Me-19
13	C	46.34	-	Me-18
14	C	83.99	-	H-7, H_2-12, Me-18
15	CH_2	31.55	1.98†, 1.57 †	H-17
16	CH_2	20.85	2.06†, 1.75†	
17	CH	49.36	2.43 dd “t” (8.7)	Me-18, Me-21
18	CH_3	18.18	0.80 s	H_2-12
19	CH_3	23.79	1.05 s	H-5, H-9
20	C	75.33	-	Me-21, H-22
21	CH_3	21.13	1.22 s	H-22
22	CH	81.24	3.29 brd (12.0)	Me-21,
23	CH_2	25.47	2.40 brd (12.0), 2.02†	
24	C	123.16	-	H-22, Me-26, Me-27
25	C	134.19	-	Me-26, Me-27
26	CH_3	20.56	1.78 s	Me-27
27	CH_3	20.70	1.68 s	Me-26
28	CH	67.64	5.72 br s	
29	CH	93.19	5.49 br s	

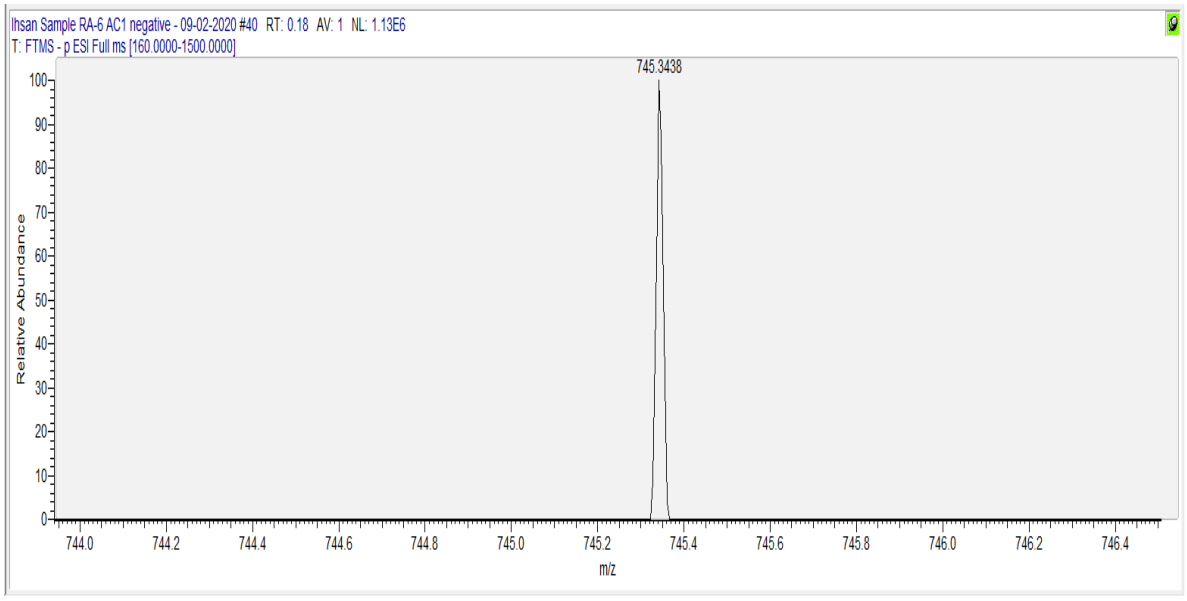

Spectrum 4.4.2. 1. (-)-HRMS of Pentaacetyl- Rhapocasterone B (5a) $[M-H]^-$ m/z 745.3438.

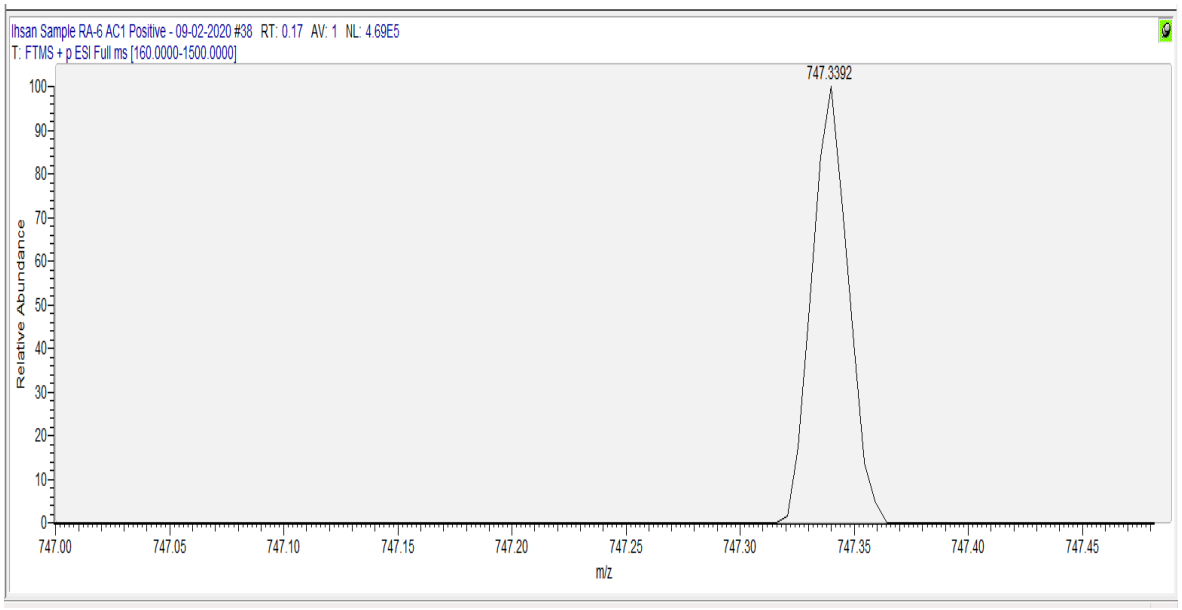

Spectrum 4.4.2.2. (+)-HRMS of Pentaacetyl- Rhapocasterone B (5a) $[M+H]^+$ m/z 747.3392.

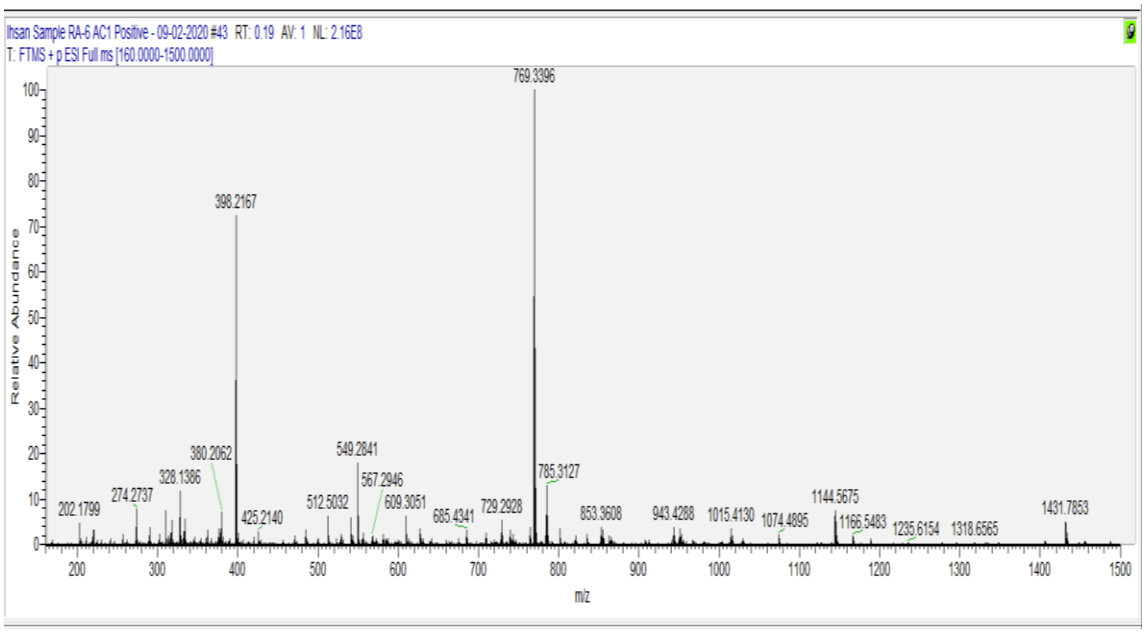

Spectrum 4.4.2.3. (+)-HMRS of Pentaacetyl-Rhapocasterone B (5a) [M+Na]+ m/z 769.3396.

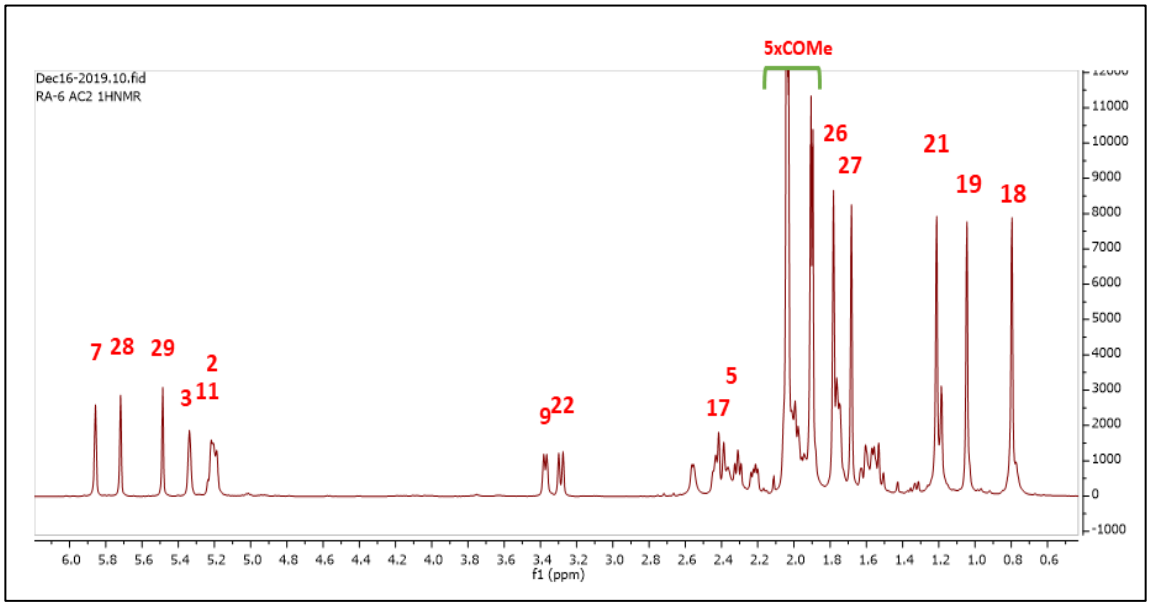

Spectrum 4.4.2.4. ^{1}H-NMR Spectrum of 5 (RA-6Ac2= Pentaacetyl-Rhapocasterone B) (500 MHz, CD_3OD).

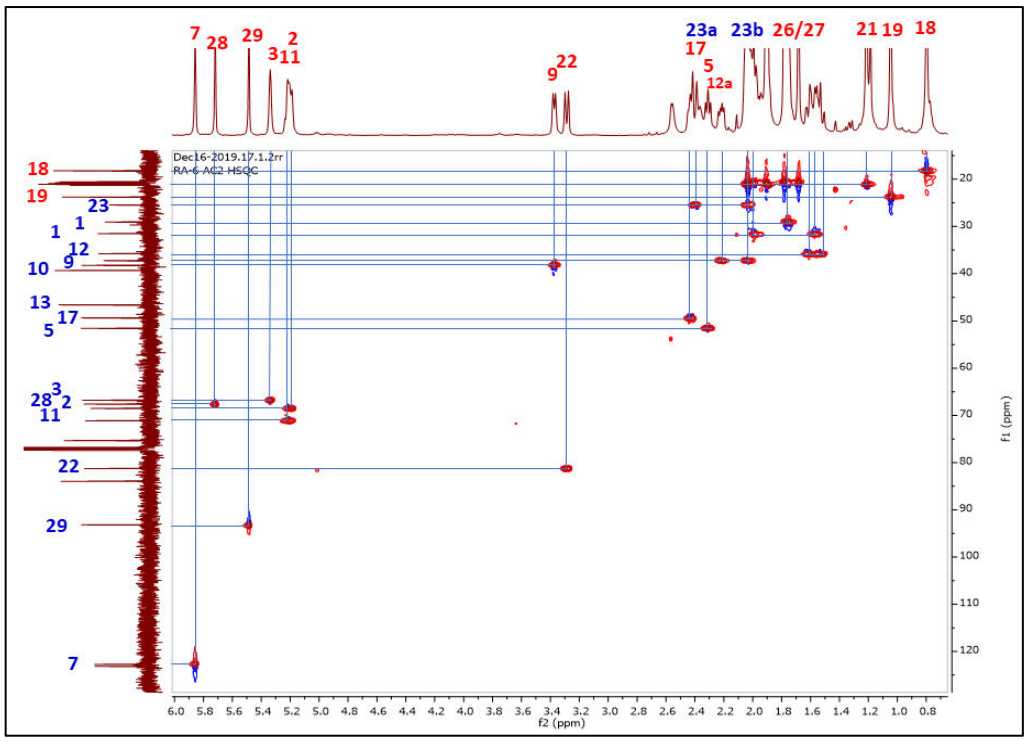

Spectrum 4.4.2.5. HSQC of 5 (RA-6Ac2= Pentaacetyl-Rhapocasterone B).

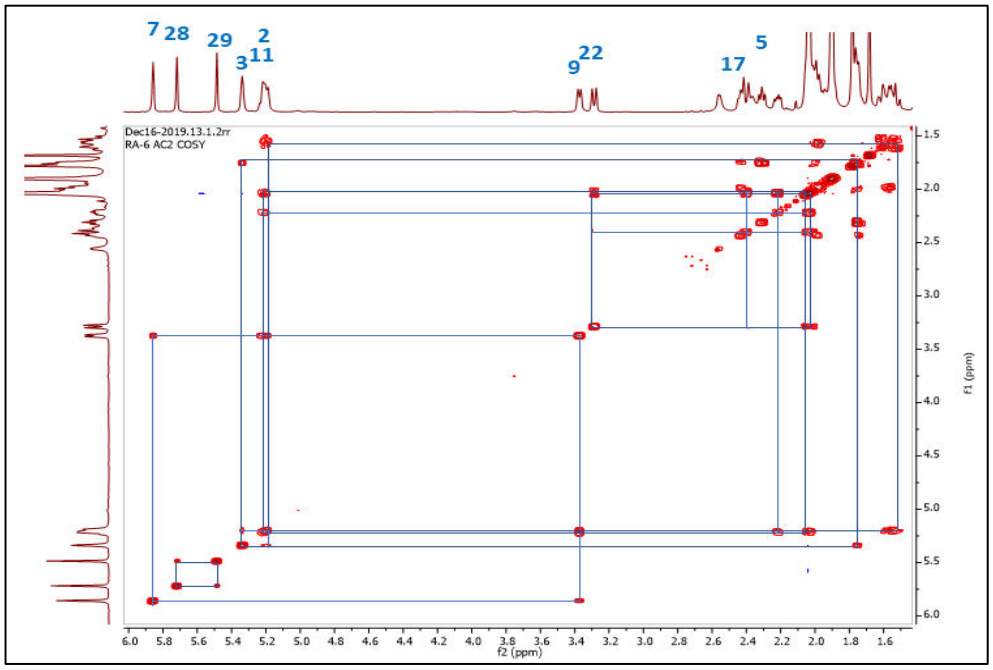

Spectrum 4.4.2.6. COSY of 5 (RA-6Ac2= Pentaacetyl-Rhapocasterone B).

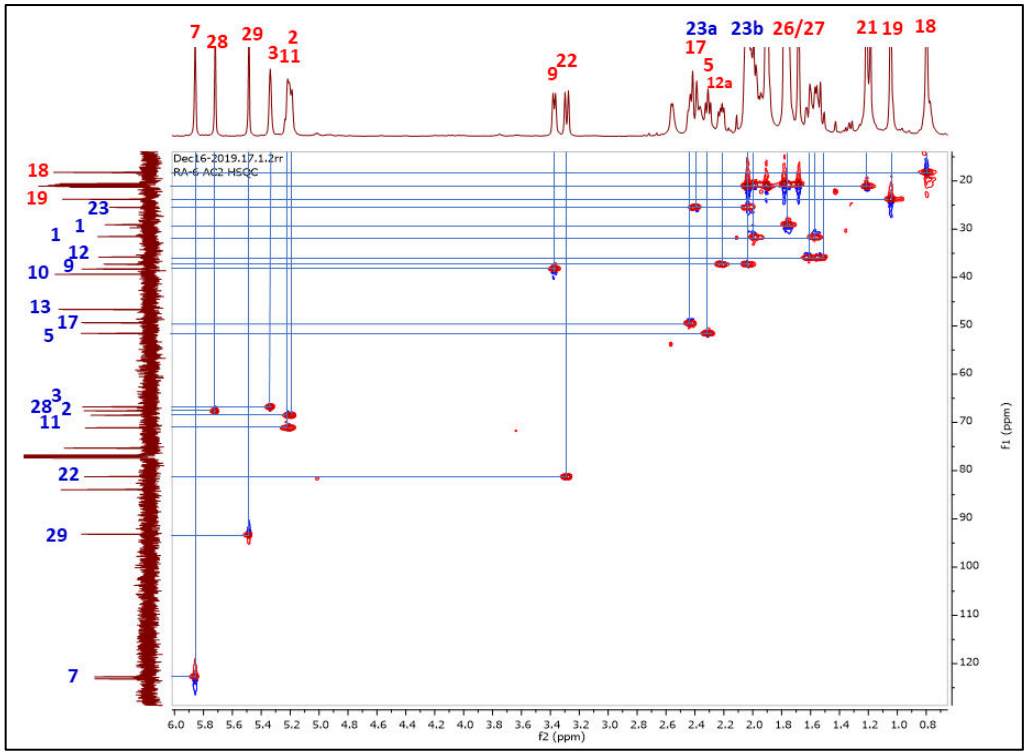

Spectrum 4.4.2.7. HSQC of 5 (RA-6Ac2= Pentaacetyl-Rhapocasterone B)

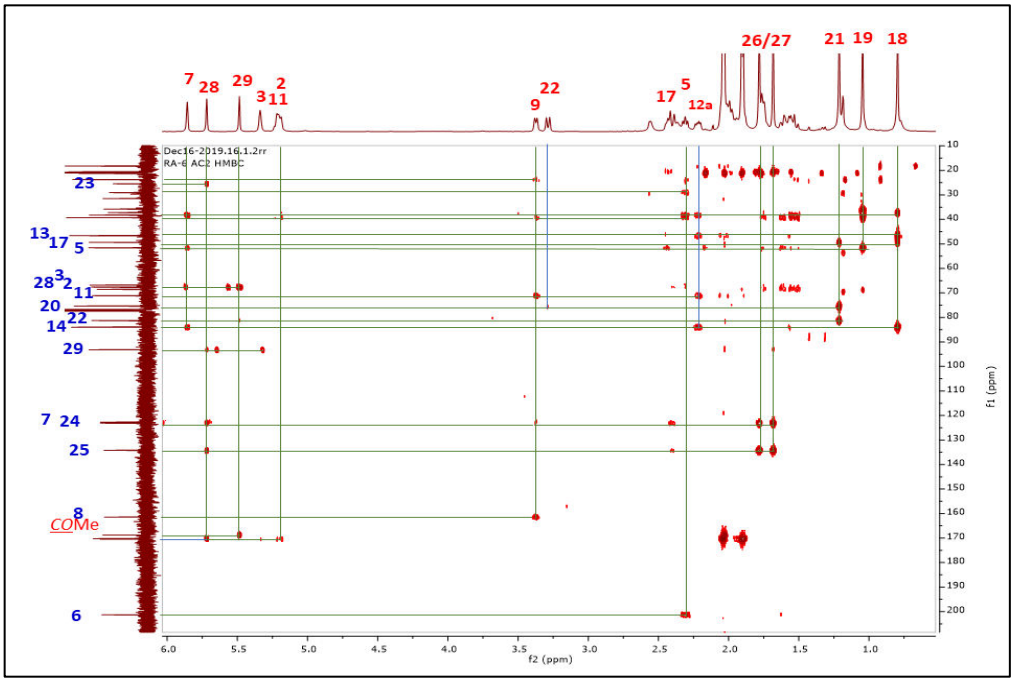

Spectrum 4.4.2.8. HMBC of 5 (RA-6Ac2= Pentaacetyl-Rhapocasterone B)

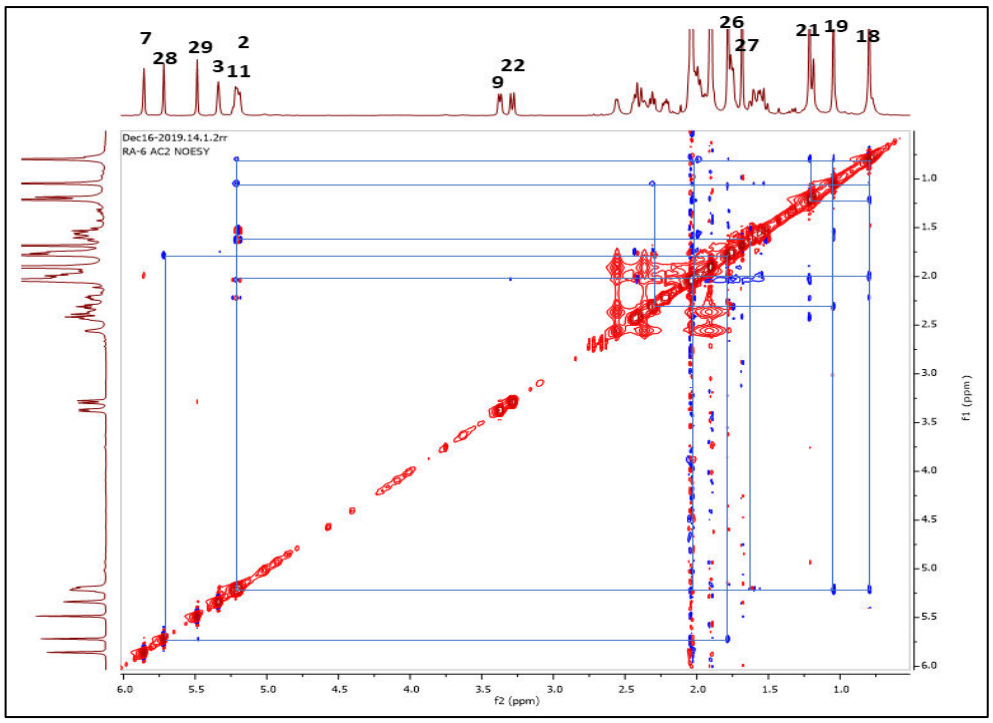

Spectrum 4.4.2.9. NOESY of 5 (RA-6Ac2= Pentaacetyl- Rhapocasterone B)

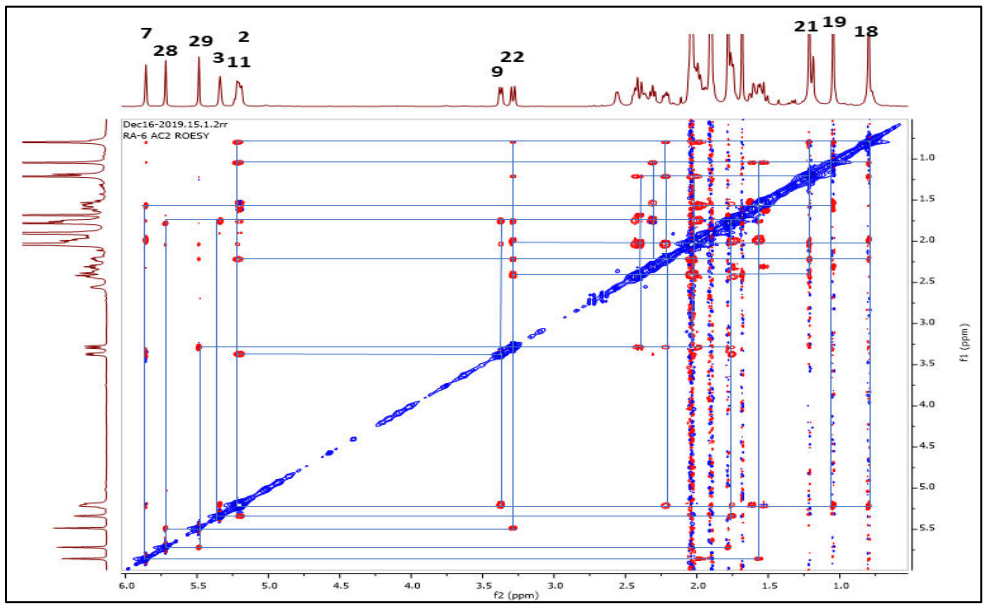

Spectrum 4.4.2.10. ROESY of 5 (RA-6Ac2= Pentaacetyl- Rhapocasterone B).

In order to confirm the structure and absolute stereochemistry of compounds **4** and **5**, attempts were made to grow single-crystals of the acetylated derivatives, **4a** and **5a**, for an X-ray crystal-structure determination; this was only successful for **4a**, which

crystalized from MeOH/H_2O as colourless plate-like crystals with composition **4a**·H_2O. The asymmetric unit contains one molecule of the steroid and two partially occupied sites for a water molecule. The acetyl substituent at C-11 is disordered over two equally occupied conformations. The water molecule is similarly disordered over its two sites as a consequence, with one site being further disordered about a two-fold axis. Refinement of the absolute structure parameter (Parsons *et al*., 2013) yielded a value of 0.00(3), which confidently confirms that the refined model represents the true enantiomorph with the 2*S*, 3*R*, 5*R*, 9*R*, 10*S*, 13*R*, 14*S*,17*S*, 20*R*, 22*R*, 28*R*, 29*R* -configuration.

In the molecular structure of **4a** (**Figure 4.7**), rings A–D have very similar conformations, and the same ring-junction configurations and positions of substituents as those described for the structure of **1a**; the additional C-11 acetyl group is in an equatorial position. The oxane ring, E, has a chair conformation with the acetyl substituents at C-28 and C-29 in *cis*-disposed axial and equatorial positions, respectively. The linkage *via* C-22–C-20 to the rest of the molecule is also equatorial. The approximate plane of the oxane ring lies perpendicular to the mean plane of the central section of the molecule defined by rings B, C and D.

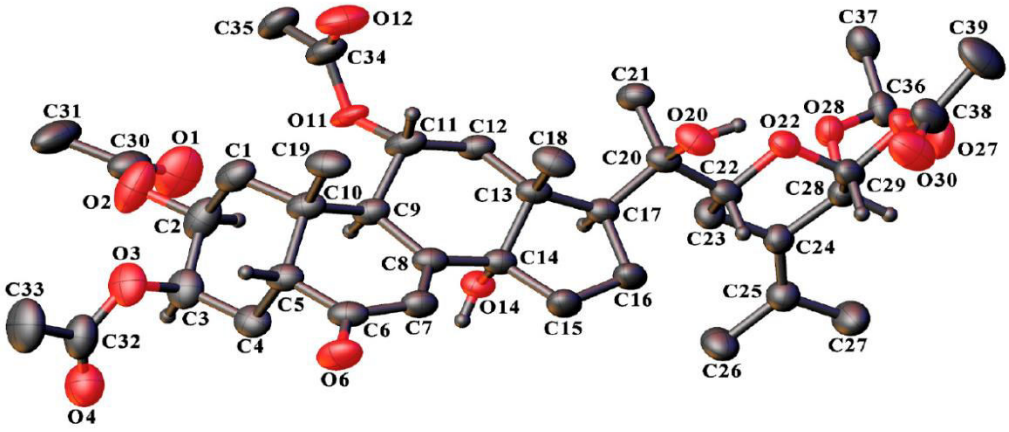

Figure 4.7. Displacement ellipsoid plot of the molecular structure of 4a (50% probability ellipsoids; only the major disorder conformation of the acetyl substituent at C- 11 is shown)

Intermolecular O–H···O hydrogen bonds link the steroid and water molecules into thick sheets which lie parallel to the (0 0 1) plane (**Figure 4.8**). The hydroxy substituent at C-14 interacts with the carbonyl O-atom of the acetyl substituent at C-28 in a neighbouring steroid molecule. This interaction links the steroid molecules into extended chains which run parallel to the [0 1 0] direction and have a graph set motif (Bernstein *et al*., 1995) of C (13). The hydroxy substituent at C-20 interacts weakly with the carbonyl O-atom of the acetyl substituent at C-2 in a different neighbouring steroid molecule. This interaction links the steroid molecules into extended chains which run parallel to the [1 -1 0] direction and have a graph set motif of C(14). The hydroxy substituent at C-20 also forms an intramolecular O–H···O hydrogen bond with the ether O-atom of the neighbouring oxane ring to give a loop with a graph set motif of S(5). The water molecules interact with the carbonyl O-atom of the disordered acetyl group, with the other water molecule sites and with the keto O-atom of another steroid molecule; these water molecules are thus bridging two steroid molecules and the interactions cross-link the tohick sheets formed by the other hydrogen-bonding interactions to give a three-dimensional supramolecular framework overall.

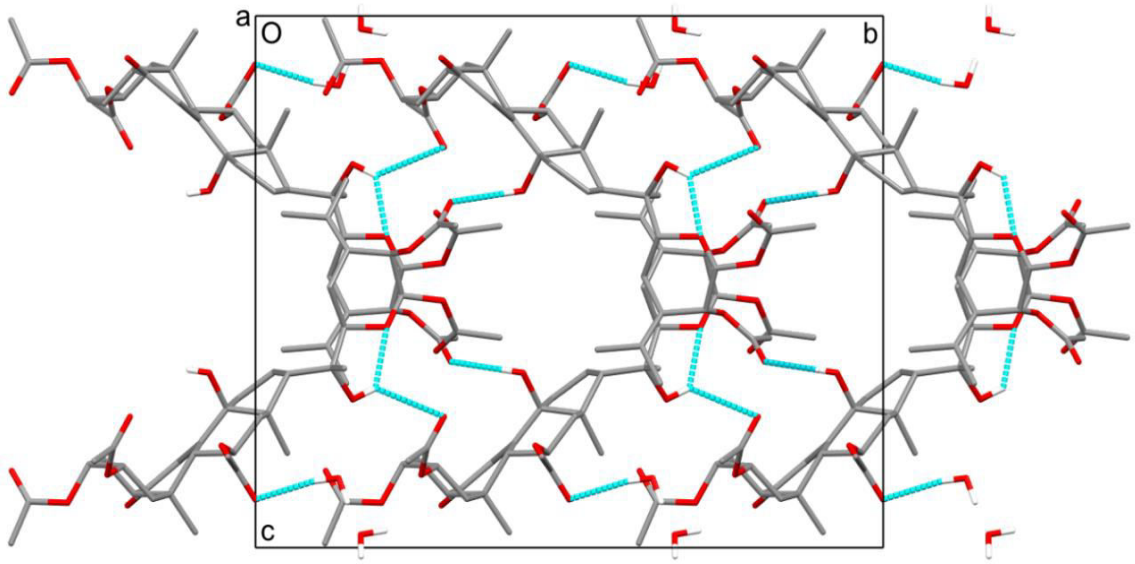

Figure 4.8. The packing of 4a·H2O viewed down the a-axis and showing the hydrogen-bonding network (uninvolved H-atoms have been omitted for clarity)

CHAPTER 5

5. CONCLUSION

As mentioned in the Introduction, the knowledge of traditional medicinal plants and the long history of ethnomedical applications have proven to be a rich source of therapeutic compounds in the field of drug discovery.

Rhaponticum acaule (Tafgha), an endemic plant in the family Asteraceae, has been widely used as a traditional medicine remedy in the countries of North Africa. The traditional use of *R. acaule* as an anti-inflammatory and analgesic agent in Libya has prompted us to investigate the chemical components of the underground parts of *R. acaule*.

This study was performed on the roots of *Rhaponticum acaule* which was collected from a specific region of the northwest Libya, Tarhunah city, during its flowering stage (March-April 2016). Essential oil of rhizomes was analyzed by GC-FID and GC-MS. Aplotaxene (1,8,11,14-heptadecatetraene) (34.6%), carvacrol (11.1%), amylfurane (6%), limonene (4.5%) were the main constituents of rhizomes of *R. acaule.*

In addition, result of the extraction and isolation studies five ecdysteroids were obtained and their structures were established by chemical (acetylation) and spectroscopic methods including UV, IR, HRMS, 1D-NMR: ^{1}H-NMR, ^{13}C-NMR, DEPT-135 and 2D-NMR: COSY, NOESY, HSQC, HMBC. In order to obtain more evidence to support the proposed structures, three compounds (RA1, RA2, RA4&RA5) were acetylated and subjected to spectroscopic studies. Additionally, in order to confirm the structure and to prove absolute stereochemistry, attempts were made to grow single crystals of the acetylated derivatives for an X-ray crystal-structure determination, this was successful for RA-6Ac1.

20-hydroxyecdysone (**1**) and turkesterone (**2**) have been isolated from *Rhaponticum carthamoides* (Willd.) Iljin, which is known as a Maral Root or Russian *Leuzea* (*Leuzea carthamoides* DC.) and commonly used in eastern parts of Russia for its biological properties (Buděšínský et al., 2008; Vokáč et al., 2002). We found that the ecdysteroid content of the roots of *Rhaponticum acaule* correlates closely with that of *Rhaponticum carthamoides*, which is a remarkable medicinal plant. In addition to 20-

hydroxyecdysterone (RA-1) and Turkesterone (RA-5), three new compounds (RA2, RA4 and RA5) were identified as 2β, 3β,11α, 20β, 22α, 24, 28-heptahydroxy-6-oxo-stigmast-7-en-25, 29-lactone, and the cyclic 22, 29-hemiacetals 22R and 22S stigmast-7-en-29- al, 2β, 3β,11α, 20α, 22, 28-hexahydroxy-6-oxo, respectively (Zughdani et al, 2020).

Since ecdysteroids are important group of hormones regulating molting, there is a growing interest in the pharmaceutical and medical applications of these compounds, particularly 20-hydroxyecdysone. Studies have revealed beneficial effect of this molecule in mammals: anabolic, hypolipidemic, anti-diabetic, anti-inflammatory, etc. Therefore, the significance of the isolated compounds warrants further bioactivity studies to uncover their biological and clinical potential.

REFERENCES

Abdelkader, H. Ben, Salah, K. B. H., Liouane, K., & Boussaada, O. (2010). Antimicrobial activity of Rhaponticum acaule and Scorzonera undulata growing wild in Tunisia. *African Journal of Microbiology Research*, *4*(19), 1954–1958.

Abuhadra, M. N., & Essokne, M. H. M. R. S. (2017). A New Record Artemisia vulgaris L.(Asteraceae) for the Flora of Libya. *American Journal of Life Science Researches*, *5*(3), 83–88.

Achan, J., Talisuna, A. O., Erhart, A., Yeka, A., Tibenderana, J. K., Baliraine, F. N., … D'Alessandro, U. (2011). Quinine, an old anti-malarial drug in a modern world: role in the treatment of malaria. *Malaria Journal*, *10*(1), 144.

Al Naggar, Y., Ghorab, M., & Mohamed, K. (2017). Phytoecdysteroids: isolation and biological applications. *American Journal of Life Sciences*, *5*(1), 7–10.

B. A. C. I. S. (1999). *ESO 2000, The Complete Database of Essential Oils*. Leffingwell and Associates publisher Georgia, USA.

Bakhtaoui, F.-Z., Lakmichi, H., Chait, A., & Gadhi, C. A. (2014). In vivo Gastro-Protective Effects of Five Moroccan Medicinal Plants against Gastric Ulcer. *American Journal of Phytomedicine and Clinical Therapeutics*, *2*(11), 1262–1276.

Baltaev, U. A. (1991). Phytoecdysteroids of Rhaponticum carthamoides. II. Rhapisterone B. *Chemistry of Natural Compounds*, *27*(6), 712–713.

Baltaev, U. A. (1992). Phytoecdysteroids of Rhaponticum carthamoides III. Rhapisterone C. *Chemistry of Natural Compounds*, *28*(2), 198–200.

Baltaev, U. A. (2000). Phytoecdysteroids: structure, sources, and biosynthesis in plants. *Russian Journal of Bioorganic Chemistry*, *26*(12), 799–831.

Baltaev, U., Gorovits, M. B., Abdullaev, N. D., IAgudaev, M. R., & Abubakirov, N. K. (1977). Phytoecdysones of Rhaponticum integrifolium. II. Integristeron A. *Khimiia Prirodnykh Soedinenii*.

Baltaev, U., Gorovits, M. B., Rashkes, Y. V, & Abubakirov, N. K. (1978). Phytoecdysones of Rhaponticum integrifolium IV. 24 (28)-Dehydromakisterone A. *Chemistry of Natural Compounds*, *14*(4), 393–395.

Barra, A. (2009). Factors affecting chemical variability of essential oils: a review of recent developments. *Natural Product Communications*, *4*(8), 1934578X0900400827.

Baser, K. H. C., & Buchbauer, G. (2009). *Handbook of Essential Oils: Science, Technology, and Applications*. CRC press.

Bathori, M., Toth, N., Hunyadi, A., Marki, A., & Zador, E. (2008). Phytoecdysteroids and Anabolic-Androgenic Steroids - Structure and Effects on Humans. *Current Medicinal Chemistry*, *15*(1), 75–91. https://doi.org/10.2174/092986708783330674

Ben Ismail, H. (2013). Edible wild vegetables used in North West of Tunisia. *Indian Journal of Research*, *2*, 9–11.

Benabdesselam, S., Guechi, E.-K., & Izza, H. (2018). Antioxidant, Antibacterial and Anticoagulant Activities of the Methanolic Extract of Rhaponticum acaule Fruit Growing Wild in Eastern Algeria. *Der Pharmacia Lettre*, *10*(1), 1–10.

Bendimerad-Mouttas, F., Beghdad, M. C., El Haci, I. A., Soualem, Z., Belarbi, M., & Bekkara, F. A. (2018). Bioactive compounds and antioxidant activity of Rhaponticum acaule (L.) DC. *Natural Product Research*, 1–5.

Bennett, J. W., & Chung, K.-T. (2001). *Alexander Fleming and the discovery of penicillin*.

Benyelles, B., Allali, H., Dib, M. E. A., Djabou, N., Tabti, B., & Costa, J. (2014). Essential oil from Rhaponticum acaule L. roots: Comparative study using HS-SPME/GC/GC–MS and hydrodistillation techniques. *Journal of Saudi Chemical Society*, *18*(6), 972–976.

Berdin, A. G., Raldugin, V. A., Shakirov, M. M., Bagryanskaya, I. Y., Gatilov, Y. V, Druganov, A. G., … Tolstikov, G. A. (2001). 15-O-Deacetylrhaposerin and rhaserin--new components of a lactone mixture from Rhaponticum serratuloides. *Russian Chemical Bulletin*, *50*(3), 537–542.

Bernstein, J., Davis, R. E., Shimoni, L., & Chang, N. (1995). Patterns in hydrogen bonding: functionality and graph set analysis in crystals. *Angewandte Chemie International Edition in English*, *34*(15), 1555–1573.

Biskup, E., Golebiowski, M., Borsuk, K., Stepnowski, P., & Lojkowska, E. (2009). Analysis of Rhaponticum carthamoides (Willd.) Iljin crude extracts composition and ability to simulate cell proliferation. *Planta Medica*, *75*(09), PI3.

Boussaada, O., Ammar, S., Saidana, D., Chriaa, J., Chraif, I., Daami, M., … Mighri, Z. (2008). Chemical composition and antimicrobial activity of volatile components from capitula and aerial parts of Rhaponticum acaule DC growing wild in Tunisia. *Microbiological Research*, *163*(1), 87–95. https://doi.org/10.1016/j.micres.2007.02.010

Bruno, M., Bancheva, S., Rosselli, S., & Maggio, A. (2013). Sesquiterpenoids in subtribe Centaureinae (Cass.) Dumort (tribe Cardueae, Asteraceae): Distribution, 13C NMR spectral data and biological properties. *Phytochemistry*, *95*, 19–93.

Budĕšínský, M., Vokáč, K., Harmatha, J., & Cvačka, J. (2008). Additional minor ecdysteroid components of Leuzea carthamoides. *Steroids*, *73*(5), 502–514.

Butenandt, A., & Karlson, P. (1954). Über die isolierung eines metamorphose-hormons der insekten in kristallisierter form. *Zeitschrift Für Naturforschung B*, *9*(6), 389–391.

Calcagno, M.-P., Camps, F., Coll, J., Melé, E., & Sánchez-Baeza, F. (1996). New phytoecdysteroids from roots of Ajuga reptans varieties. *Tetrahedron*, *52*(30), 10137–10146.

Chaturvedi, D. (2011). Sesquiterpene lactones: structural diversity and their biological activities, In-Opportunity, Challanges and Scope of Natural Products in Medicinal Chemistry. *ISBN: 978-81-308-0448-4, Research Signpost, Trivandrum*, 313–334.

Chaubey, M. K. (2018). Role of phytoecdysteroids in insect pest management: A review. *Journal of Agronomy*, *17*(1), 1–10.

Chen, H., Wang, C., Qi, M., Ge, L., Tian, Z., Li, J., … Tang, X. (2017). Anti-tumor effect of Rhaponticum uniflorum ethyl acetate extract by regulation of peroxiredoxin1 and epithelial-to-mesenchymal transition in oral cancer. *Frontiers in Pharmacology*, *8*, 870.

Chen, T., Diao, Q.-Y., Yu, H.-Z., Jiao, C.-L., & Ruan, J. (2018). Phytochemical, cytotoxic and chemotaxonomic study on Ajuga forrestii Diels (Labiatae). *Natural Product Research*, *32*(8), 977–981.

Cis, J., Nowak, G., & Kisiel, W. (2006). Antifeedant properties and chemotaxonomic implications of sesquiterpene lactones and syringin from Rhaponticum pulchrum. *Biochemical Systematics and Ecology*, *34*(12), 862–867. https://doi.org/10.1016/j.bse.2006.05.019

Coll, J., Tandrón, Y. A., & Zeng, X. (2007). New phytoecdysteroids from cultured plants of Ajuga nipponensis Makino. *Steroids*, *72*(3), 270–277.

Cragg, G. M., & Newman, D. J. (2013). Natural products: a continuing source of novel drug leads. *Biochimica et Biophysica Acta (BBA)-General Subjects*, *1830*(6), 3670–3695.

Das, N., Mishra, S. K., Bishayee, A., Ali, E. S., & Bishayee, A. (2020). The phytochemical, biological, and medicinal attributes of phytoecdysteroids: an updated review. *Acta Pharmaceutica Sinica B*.

Dinan, L., Bourne, P., Whiting, P., Tsitsekli, A., Saatov, Z., Dhadialla, T. S., … Coll, J. (2003). Synthesis and biological activities of turkesterone 11α-acyl derivatives. *Journal of Insect Science*, *3*(1).

Dioh, W., Chabane, M., Tourette, C., Azbekyan, A., Morelot-Panzini, C., Hajjar, L. A., … Mariani, J. (2021). Testing the efficacy and safety of BIO101, for the prevention of respiratory deterioration, in patients with COVID-19 pneumonia (COVA study): a structured summary of a study protocol for a randomised controlled trial. *Trials*, *22*(1), 1–5.

Elpel, T. J. (2004). *Botany in a day: the patterns method of plant identification*. Hops Press.

Elsebai, M. F., Mocan, A., & Atanasov, A. G. (2016). Cynaropicrin: A comprehensive research review and therapeutic potential as an anti-hepatitis C virus agent. *Frontiers in Pharmacology*, *7*, 472.

Fábián, L., Argay, G., Kálmán, A., & Báthori, M. (2002). Crystal structures of ecdysteroids: the role of solvent molecules in hydrogen bonding and isostructurality. *Acta Crystallographica Section B: Structural Science*, *58*(4), 710–720.

Fabricant, D. S., & Farnsworth, N. R. (2001). The value of plants used in traditional medicine for drug discovery. *Environmental Health Perspectives*, *109*(suppl 1), 69–75.

Funk, V. A., Susanna, A., Steussy, T. F., & Robinson, H. E. (2009). Classification of compositae. *Systematics, Evolution, and Biogeography of Compositae*.

Gawhari, A. M. H., Jury, S. L., & Culham, A. (2018). Towards an updated checklist of the Libyan flora. *Phytotaxa*, *338*(1), 1–16.

Girault, J-P, Lafont, R., Varga, E., Hajdu, Z., Herke, I., & Szendrei, K. (1988). Ecdysteroids from Leuzea carthamoides. *Phytochemistry*, *27*(3), 737–741.

Girault, J. P., & Lafont, R. d. (1988). The complete 1H-NMR assignment of ecdysone and 20-hydroxyecdysone. *Journal of Insect Physiology*, *34*(7), 701–706.

Girault, Jean-Pierre, Bathori, M., Varga, E., Szendrei, K., & LaFont, R. (1990). Isolation and identification of new ecdysteroids from the Caryophyllaceae. *Journal of Natural Products*,

53(2), 279–293.

Głazowska, J., Kamiński, M. M., & Kamiński, M. (2018). Chromatographic separation, determination and identification of ecdysteroids: Focus on maral root (Rhaponticum carthamoides, Leuzea carthamoides). *Journal of Separation Science*, *41*(23), 4304–4314.

Greuter, W. (2003). The Euro Med treatment of Cardueae (Compositae)—generic concepts and required new names. *Willdenowia*, *33*(1), 49–61.

Greuter, W., & von Raab-Straube, E. (2008). *Med-checklist: a critical inventory of vascular plants of the circum-mediterranean countries. 2. Dicotyledones (Compositae)*. OPTIMA Secretariat.

Guibout, L., Mamadalieva, N., Balducci, C., Girault, J., & Lafont, R. (2015). The minor ecdysteroids from Ajuga turkestanica. *Phytochemical Analysis*, *26*(5), 293–300.

Havlik, J., Budesinsky, M., Kloucek, P., Kokoska, L., Valterova, I., Vasickova, S., & Zeleny, V. (2009). Norsesquiterpene hydrocarbon, chemical composition and antimicrobial activity of Rhaponticum carthamoides root essential oil. *Phytochemistry*, *70*(3), 414–418.

Heinrich, M., Barnes, J., Prieto-Garcia, J., Gibbons, S., & Williamson, E. M. (2017). *Fundamentals of Pharmacognosy and Phytotherapy E-Book*. Elsevier Health Sciences.

Horn, D. H. S., & Bergamasco, R. (1985). *Comprehensive Insect Physiology, Biochemistry and Pharmacology, edited by GA Kerkut & L. Gilbert*. Oxford: Pergamon Press.

Ifantis, T. M., Solujić, S., Pavlović-Muratspahić, D., & Skaltsa, H. (2013). Secondary metabolites from the aerial parts of Centaurea pannonica (Heuff.) Simonk. from Serbia and their chemotaxonomic importance. *Phytochemistry*, *94*, 159–170.

Jafri, S. M., & Elgadi, A. (1986). Flora of Libya, vol: 25-144. *Department of Botany, Al Faateh University-Tripoli*.

Jafri, S. M. H., & El-Gadi, A. (1983). Al Faateh University. Faculty of Science, Department of Botany, Tripoli. *Flora of Libya*, *107*.

Jeong, Y. H., Oh, Y.-C., Cho, W.-K., Yim, N.-H., & Ma, J. Y. (2016). Anti-inflammatory effect of rhapontici radix ethanol extract via inhibition of NF-κB and MAPK and induction of HO-1 in macrophages. *Mediators of Inflammation*, *2016*.

Ji, H., Song, N., Ren, J., Li, W., Zhang, L., Xu, B., … Li, H. (2020). Systems toxicology approaches reveal the mechanisms of hepatotoxicity induced by diosbulbin B in male mice. *Chemical Research in Toxicology*.

Joulain, D., & König, W. A. (1998). The atlas of spectral data of sesquiterpene hydrocarbons. Hamburg. *Verlag: EB-Verlag, Hamburg, Germany*.

Kaur, N., Chaudhary, J., Jain, A., & Kishore, L. (2011). Stigmasterol: a comprehensive review. *International Journal of Pharmaceutical Sciences and Research*, *2*(9), 2259.

Khan, M. A., Ahmad, M., Zafar, M., Sultana, S., Marwat, S. K., Shaheen, S., … Nazir, A. (2011). Medico-botanical and chemical standardization of pharmaceutically important plant of Tricholepis chaetolepis (Boiss) Rech. F. *Journal of Medicinal Plants Research*, *5*(8), 1471–1477.

Kokoska, L., & Janovska, D. (2009a). Chemistry and pharmacology of Rhaponticum carthamoides: a review. *Phytochemistry*, *70*(7), 842–855.

Kokoska, L., & Janovska, D. (2009b). Chemistry and pharmacology of Rhaponticum carthamoides: A review. *Phytochemistry*, *70*(7), 842–855. https://doi.org/10.1016/j.phytochem.2009.04.008

Kubo, I., Matsumoto, A., & Hanke, F. J. (1985). The 1H-NMR assignment of 20-hydroxyecdysone. *Agricultural and Biological Chemistry*, *49*(1), 243–244.

Le Bizec, B., Antignac, J.-P., Monteau, F., & Andre, F. (2002). Ecdysteroids: one potential new anabolic family in breeding animals. *Analytica Chimica Acta*, *473*(1–2), 89–97.

Lotocka, B., & Geszprych, A. (2004). Anatomy of the vegetative organs and secretory structures of Rhaponticum carthamoides (Asteraceae). *Botanical Journal of the Linnean Society*, *144*(2), 207–233.

Mahdi, J. G., Mahdi, A. J., Mahdi, A. J., & Bowen, I. D. (2006). The historical analysis of aspirin discovery, its relation to the willow tree and antiproliferative and anticancer potential. *Cell Proliferation*, *39*(2), 147–155.

Mamadalieva, N. Z., Zibareva, L. N., & Saatov, Z. (2002). Phytoecdysteroids of Silene linicola. *Chemistry of Natural Compounds*, *38*(3), 268–271.

McLafferty, F. W., & Stauffer, D. B. (1989). *The Wiley/NBS registry of mass spectral data* (Vol. 1). Wiley New York.

Mosbah, H., Chahdoura, H., Kammoun, J., Hlila, M. B., Louati, H., Hammami, S., … Selmi, B. (2018). Rhaponticum acaule (L) DC essential oil: chemical composition, in vitro antioxidant and enzyme inhibition properties. *BMC Complementary and Alternative Medicine*, *18*(1), 1–12.

Nakanishi, K., Koreeda, M., Sasaki, S., Chang, M. L., & Hsu, H. Y. (1966). Insect hormones. The structure of ponasterone A, insect-moulting hormone from the leaves of Podocarpus nakaii Hay. *Chemical Communications (London)*, (24), 915–917.

Olennikov, D N. (2019). Guaiane-Type Sesquiterpenes from Rhaponticum uniflorum. *Chemistry of Natural Compounds*, *55*(1), 157–159.

Olennikov, Daniil N, Gadimli, A. I., Isaev, J. I., Kashchenko, N. I., Prokopyev, A. S., Kataeva, T. N., … Vennos, C. (2019). Caucasian Gentiana species: Untargeted LC-MS metabolic profiling, antioxidant and digestive enzyme inhibiting activity of six plants. *Metabolites*, *9*(11), 271.

Özbek, M. U., Koç, M., & Hamzaoğlu, E. (2017). Rhaponticum pulchrum (Asteraceae), a new record for the Turkish Flora. *Gazi University Journal of Science*, *30*(4), 43–47.

Parsons, S., Flack, H. D., & Wagner, T. (2013). Use of intensity quotients and differences in absolute structure refinement. *Acta Crystallographica Section B: Structural Science, Crystal Engineering and Materials*, *69*(3), 249–259.

Petkov, V., Roussinov, K., Todorov, S., Lazarova, M., Yonkov, D., & Draganova, S. (1984). Pharmacological investigations on Rhaponticum carthamoides. *Planta Medica*, *50*(03), 205–209.

Ramawat, K. G., & Mérillon, J.-M. (2008). *Bioactive molecules and medicinal plants*. Springer.

Ramazanov, N. S., Makshimov, E. S., Saatov, Z., Mamatkhanov, A. U., & Abdullaev, N. D. (1997). Phytoecdysteroids of plants of the genus Rhaponticum I. Carthamosterone a from

Rh. carthamoides. *Chemistry of Natural Compounds*, *33*(3), 301–302.

Rastogi, S., Pandey, M. M., & Rawat, A. K. S. (2016). Traditional herbs: a remedy for cardiovascular disorders. *Phytomedicine*, *23*(11), 1082–1089.

Rele, S., Banerji, A., Chintalwar, G., Kumar, V., & Yadava, V. (2003). A new conformer of 20-hydroxyecdysone from Sesuvium portulacastrum: an X-ray crystallographic study. *Natural Product Research*, *17*(2), 103–108.

Rimbau, V., Cerdan, C., Vila, R., & Iglesias, J. (1999). Antiinflammatory activity of some extracts from plants used in the traditional medicine of North-African countries (II). *Phytotherapy Research: An International Journal Devoted to Pharmacological and Toxicological Evaluation of Natural Product Derivatives*, *13*(2), 128–132.

Rimbau, V., Risco, E., Canigueral, S., & Iglesias, J. (1996). Antiinflammatory activity of some extracts from plants used in the traditional medicine of North-African countries. *Phytotherapy Research*, *10*(5), 421–423.

Saleem, M., Musaddiq, S., Riaz, N., Zubair, M., Ashraf, M., Nasar, R., & Jabbar, A. (2013). Ecdysteroids from the flowers of Aerva javanica. *Steroids*, *78*(11), 1098–1102.

Schwalbe, H. (2014). *Applied NMR Spectroscopy for Chemists and Life Scientists. By Oliver Zerbe and Simon Jurt.* Wiley Online Library.

Seigler, D. S. (2012). *Plant secondary metabolism*. Springer Science & Business Media.

Sena Filho, J. G., Duringer, J., Maia, G. L. A., Tavares, J. F., Xavier, H. S., Sobral da Silva, M., … Barbosa-Filho, J. M. (2008). Ecdysteroids from Vitex Species: Distribution and Compilation of Their 13C-NMR Spectral Data. *Chemistry & Biodiversity*, *5*(5), 707–713.

Skała, E., Picot, L., Bijak, M., Saluk-Bijak, J., Szemraj, J., Kicel, A., … Sitarek, P. (2019). An efficient plant regeneration from Rhaponticum carthamoides transformed roots, enhanced caffeoylquinic acid derivatives production in pRi-transformed plants and their biological activity. *Industrial Crops and Products*, *129*, 327–338.

Skała, E., Rijo, P., Garcia, C., Sitarek, P., Kalemba, D., Toma, M., … Śliwiński, T. (2016). The essential oils of Rhaponticum carthamoides hairy roots and roots of soil-grown plants: chemical composition and antimicrobial, anti-inflammatory, and antioxidant activities. *Oxidative Medicine and Cellular Longevity*, *2016*.

Sokolov, S. Y. (2000). Phytotherapy and Phytopharmacology: The Manual for Doctors. *Moscow: Medical News Agency*, 197–199.

Speranza, A. (2010). Into the world of steroids: A biochemical “keep in touch” in plants and animals. *Plant Signaling & Behavior*, *5*(8), 940–943.

Srivastava, A., Srivastava, P., Pandey, A., Khanna, V. K., & Pant, A. B. (2019). Phytomedicine: A potential alternative medicine in controlling neurological disorders. In *New Look to Phytomedicine* (pp. 625–655). Elsevier.

Suksamrarn, A., Kumpun, S., & Yingyongnarongkul, B. (2002). Ecdysteroids of Vitex s cabra Stem Bark. *Journal of Natural Products*, *65*(11), 1690–1692.

Tadesse, M. (2014). How to study the Asteraceae (compositae) with special reference to the Asteraceae of fee. *Ethiopian Journal of Biological Sciences*, *13*(Supp.)), 91–101.

Taylor, J. L. S., Rabe, T., McGaw, L. J., Jäger, A. K., & Van Staden, J. (2001). Towards the

scientific validation of traditional medicinal plants. *Plant Growth Regulation*, *34*(1), 23–37.

Thiem, B., Kikowska, M., Maliński, M. P., Kruszka, D., Napierała, M., & Florek, E. (2017). Ecdysteroids: production in plant in vitro cultures. *Phytochemistry Reviews*, *16*(4), 603–622.

Todorov, I. N., Mitrokhin, Y. I., Efremova, O. I., & Sidorenko, L. I. (2000). Effect of extract from Rhaponticum carthamoides on RNA and protein biosynthesis in mice. *Pharmaceutical Chemistry Journal*, *34*(9), 479–481.

Usmanov, B. Z., Gorovits, M. B., & Abubakirov, N. K. (1973). Phytoecdysones of Ajuga turkestanica. II. *Chemistry of Natural Compounds*, *9*(1), 125–126.

Usmanov, B. Z., Gorovits, M. B., & Abubakirov, N. K. (1975). Phytoecdysones of Ajuga turkestanica. III. The structure of turkesterone. *Chemistry of Natural Compounds*, *11*(4), 484–487.

Vokáč, K., Budějínský, M., & Harmatha, J. (2002). Minor ecdysteroid components of Leuzea carthamoides. *Collection of Czechoslovak Chemical Communications*, *67*(1), 124–139.

Wei, H. X., Gao, W. Y., Tian, Y. J., Guan, Y. K., Huang, M. H., & Cheng, D. L. (1997). *New eudesmane sesquiterpene and thiophene derivatives from the roots of Rhaponticum uniflorum*.

Winston, D., & Maimes, S. (2007). Adaptogens: Herbs for Strength. *Stamina, and Stress Relief*, 226–227.

, Y., JI, X., , X., , H., , X., LI, X., & , L. (2005). Experimental Study on Improving Learning and Memory Abilities of Total Steron e-extracts of Rhaponticum uniflorum [J]. *Traditional Chinese Drug Research & Clinical Pharmacology*, *6*.

Yan, X., Zhao, H., Guan, Y., Song, Y., & Meng, J. (2013). A study on the effect of ethanol extract of Radix rhapontici on erythrocyte immune function in rats. *African Journal of Traditional, Complementary and Alternative Medicines*, *10*(6), 538–541.

Zerbe, O., & Jurt, S. (2013). *Applied NMR spectroscopy for chemists and life scientists*. John Wiley & Sons.

Zhang, X., Zhang, J., Dong, M., Zhang, M., Huo, C., Shi, Q., & Gu, Y. (2010). Chemical constituents of plants from the genus Rhaponticum. *Chemistry & Biodiversity*, *7*(3), 594–609.

Zhang, Y.-H., & Wang, H.-Q. (2001). Ecdysteroids from Rhaponticum uniflorum. *Die Pharmazie*, *56*(10), 828–829.

Zhang, Y., Cheng, J., Yang, L., & Cheng, D. (2002). Triterpenoids from Rhaponticum uniflorum. *Journal of the Chinese Chemical Society*, *49*(1), 117–124.

Zhang, Y. H., Wu, Y., Yang, L., Liu, Z. L., & Cheng, D. L. (2009). Two new triterpenoid saponins from Rhaponticum uniflorum. *Chinese Chemical Letters*, *20*(6), 690–693.

Zhu, L., Lu, Y., & Chen, D. (1991). Composition of essential oil from inflorescences of Rhaponticum uniflorum (L.) DC. *Zhongguo Zhong Yao Za Zhi= Zhongguo Zhongyao Zazhi= China Journal of Chinese Materia Medica*, *16*(12), 739–740.

Zughdani, M., Yusufoğlu, H. S., Ekiz, G., Linden, A., & Çalış, İ. (2020). Ecdysteroids from the underground parts of Rhaponticum acaule (L.) DC. *Phytochemistry*, *180*. https://doi.org/10.1016/j.phytochem.2020.112530